CHAPTER 4

Kinetics and Mechanisms of Chemical Reactions at the Soil Mineral/Water Interface

Donald L. Sparks

CONTENTS

0-87371-883-6/99/$0.00+$.50

I. INTRODUCTION

Without question, one of the important paradigms in our society is preservation of the environment. Worldwide, concerns have been voiced about numerous soil and water contaminants. These include plant nutrients (e.g., nitrate and phosphate), heavy metals, radionuclides, pesticides, and other organic chemicals.

The reactions that these contaminants undergo with natural particles, such as sediments and soils, involving sorption, desorption, precipitation, complexation, redox, and dissolution phenomena, are critical in determining their fate and mobility in the subsurface environment.

Much of the research on migration and retention of contaminants on natural materials has been studied from a macroscopic, equilibrium approach. The focus of many of these investigations has been on the determination of distribution coefficients (determined primarily on a 24-hour basis), and the use of equilibrium-based models such as the Freundlich, Langmuir, and the various surface complexation models, e.g., constant-capacitance and triple-layer, to determine numerous sorption parameters, information on the physical description of the electric double layer, and data conformance over a wide range of experimental conditions such as varying pH and ionic strength. While the surface complexation models are predicated on molecular descriptions of the electric double layer, equilibrium-derived data are employed and, thus, no direct molecular information is provided.

The above criticism of equilibrium approaches is not meant to imply that they are not useful, since they provide important data on the final state of a reaction. However, they provide no information on reaction rates or mechanisms. Moreover, such equilibrium studies are usually not relevant to field settings, since reactions involving subsurface materials are seldom, if ever, at equilibrium. To understand the rates of chemical reactions on particle surfaces, one must study the kinetics of the reactions. Kinetic studies can assist in revealing reaction mechanisms. Of course, to determine mechanisms directly, one must use microscopic and spectroscopic surface techniques. Ideally, one should follow reaction rates microscopically and/or spectroscopically and couple these with macroscopically observed processes. Such approaches will be discussed later. In short, time-dependent reactions are important factors in controlling the fate and transport of contaminants in the subsurface environment.

Early studies by Way[1] on ion exchange in soils showed that reaction rates were often instantaneous. Similar conclusions were reached by Gedroiz[2] and Hissink.[3] The finding that ion-exchange kinetics were diffusion-controlled was discovered by Boyd et al.[4] In their seminal paper they also elucidated rate-limiting steps for ion exchange. Kelley[5] correctly hypothesized that rates of ion exchange should be highly dependent on the adsorbent. For example, reaction rates on kaolinite, which has only external surface sites, should be higher than on vermiculite, which has planar and edge external as well as internal sites. Reactions on internal sites, depending on their geometry, could be quite slow. Unfortunately, Kelley's[5] astute observations went unnoticed and little research on reaction rates on soils and soil components appeared over the next three decades. There were notable contributions by Helfferich[6] on ion-exchange kinetics and by Mortland and coworkers[7,8] and Scott and coworkers[9] on the kinetics of potassium release from vermiculites and mica.

In the late 1970s, and certainly in the 1980s and 1990s, the kinetics of environmentally important reactions at the soil mineral/water interface has become a major leitmotif in the soil and environmental sciences and in environmental engineering. This intense interest is in large part due to the recognition that reactions in natural settings are usually time dependent and thus, to predict accurately the fate of contaminants in the subsurface environment, a knowledge of the reaction kinetics is imperative. While major advances have been made in understanding time-dependent reactions on natural materials such as soils and sediments, there are still many unknowns and needs that are complicated by the complex, heterogeneous nature of natural materials. Research needs include models that accurately describe both chemical kinetics and transport processes in multiple-site, heterogeneous systems; better kinetic methods; more extensive studies on the effect of residence time ("aging") on contaminant retention/release; and mechanistic studies that employ time-resolved *in situ* microscopic and spectroscopic techniques.

In this chapter, I shall discuss the application of chemical kinetics to heterogeneous systems such as soils and soil components (clay minerals, organic matter, and humic substances), with emphasis on sorption/release processes. A critical review of kinetic models that can be used to describe reaction rates on heterogeneous surfaces will be covered. The chapter will also cover the kinetics of important inorganic and organic sorption/desorption and dissolution reactions at the soil mineral/water interface. Additionally, there are discussions on the use of *in situ* spectroscopic and microscopic techniques to confirm reaction mechanisms at the soil mineral/water interface. For additional details on these topics and other aspects of kinetics of soil chemical and geochemical processes the reader should consult a number of recent books.[10-14]

II. TIME SCALES OF SOIL CHEMICAL PROCESSES

A variety of chemical reactions occur in soils and often in combination with one another. Reaction time scales can vary from microseconds for many ion association reactions to microseconds and milliseconds for some ion exchange and sorption reactions, to years for many mineral-solution and mineral crystallization phenomena and for some sorption/desorption reactions (Figure 1). Ion association reactions include ion pairing, inner- and outer-sphere complexation, and chelation in solution. Gas-water reactions involve gaseous exchange across the air-liquid interface. Ion exchange reactions occur when cations and anions are adsorbed and desorbed from soil surfaces via electrostatic attractive forces. Ion exchange reactions are reversible and stoichiometric. Sorption reactions can involve physical sorption, outer-sphere complexation, inner-sphere complexation, and surface precipitation. Mineral-solution reactions include precipitation/dissolution of minerals, and coprecipitation reactions, whereby small constituents become a part of mineral structures.[10,11]

The type of soil component can drastically affect the reaction rate. For example, sorption reactions are often more rapid on clay minerals such as kaolinite and smectites than on vermiculitic and micaceous minerals. This is in large part due to the availability of sites for sorption. For example, kaolinite has readily available planar external sites and smectites have primarily internal sites that are also quite available for retention of sorptives. Thus, sorption reactions on these soil constituents are often quite rapid, even occurring on time scales of seconds and milliseconds.[10]

Metal and metalloid sorption reactions on oxides, hydroxides, and humic substances depend on the type of surface and metal being studied, but the chemical reaction rate appears to be rapid. For example, chemical reaction rates of molybdate, sulfate, selenate, and selenite on goethite occurred on millisecond time scales.[15-17] Half-times for divalent Pb, Cu, Zn sorption on peat ranged from 5 to 15 s.[18] Some studies have shown that heavy metal sorption on oxides[19-20] and clay minerals[20] increases with longer equilibration times. The mechanism for these lower reaction rates is not well understood and has been ascribed to diffusion phenomena, sites of lower reactivity, and surface nucleation/precipitation.[19-21] Recent findings on slow metal retention mechanisms at the mineral/water interface will be discussed later.

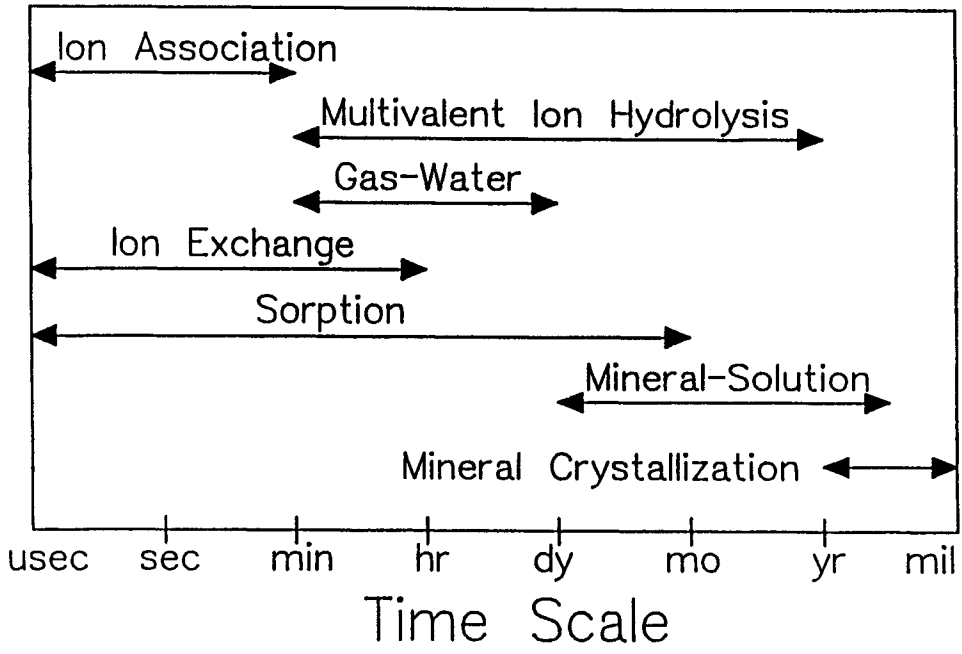

Figure 1 Time ranges required to attain equilibrium by different types of reactions in soil environments. (From Amacher, M. C., in *Rates of Soil Chemical Processes*, SSSA Spec. Publ. No. 27, Sparks, D. L. and Suarez, D. L., Eds., Soil Science Society of America, Madison, WI, 1991, 19. With permission.)

On the other hand, vermiculite and micas have multiple sites for retention of metals and organics, including planar, edge, and interlayer sites, with some of the latter sites being partially to totally collapsed. Consequently, sorption and desorption reactions on these sites can be slow, tortuous, mass transfer-controlled. Often, an apparent equilibrium may not be reached even after several days or weeks. Thus, with vermiculite and mica, sorption can involve two to three different reaction rates — high rates on external sites, intermediate rates on edge sites, and low rates on interlayer sites.[22-24]

Sorption/desorption of metals and organic chemicals on soils is often very slow, which has been attributed to diffusion into micropores of inorganic minerals and into humic substances, retention on sites of lower reactivity, and surface nucleation/precipitation. These reactions will be discussed in more detail later.

III. APPLICATION OF CHEMICAL KINETICS TO HETEROGENEOUS SURFACES

The study of chemical kinetics, even in homogeneous systems, is complex and often arduous. When one attempts to study the kinetics of reactions in heterogeneous systems such as soils, sediments, and even of soil components such as clay minerals, hydrous oxides, and humic substances, the difficulties are greatly magnified. This is largely due to the complexity of soils, which are made up of a mixture of inorganic and organic components. These components often interact with each other and display different types of sites with various reactivities for inorganic and organic sorptives. Moreover, the variety of particle sizes and porosities in soils and sediments further adds to their heterogeneity. In most cases, both *chemical kinetics* and multiple transport processes are occurring simultaneously. Thus, the determination of *chemical kinetics*, which can be defined as "the investigation of rates of chemical reactions and of the molecular processes by which reactions

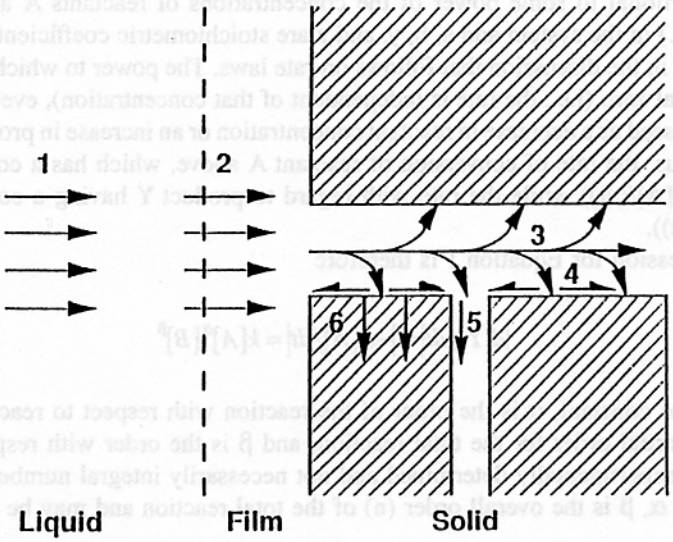

Figure 2 Transport processes in solid-liquid soil reactions. Nonactivated processes: **1**, transport in the soil solution; **2**, transport across a liquid film at the solid-liquid interface; **3**, transport in a liquid-filled macropore. Activated processes: **4**, diffusion of a sorbate at the surface of the solid; **5**, diffusion of a sorbate occluded in a micropore; **6**, diffusion in the bulk of the solid. (From Aharoni, C. and Sparks, D. L., in *Rates of Soil Chemical Precesses*, SSSA Spec. Publ. No. 27, Sparks, D. L. and Suarez, D. L., Eds., Soil Science Society of America, Madison, WI, 1991, 1. With permission.)

occur where transport is not limiting,"[25] is extremely difficult, if not impossible, in heterogeneous systems. In these systems, one is studying *kinetics*, which is a generic term referring to time-dependent or nonequilibrium processes. Thus, apparent and not mechanistic rate laws and rate parameters are determined.[10,26]

A. Rate-Limiting Steps

Both transport and chemical reaction processes can affect the reaction rates in the subsurface environment. Transport processes include:[27] transport in the solution phase, transport across a liquid film at the particle/liquid interface (film diffusion, FD), transport in liquid-filled macropores, all of which are nonactivated diffusion processes and occur in mobile regions, and particle diffusion (PD) processes, which include diffusion of sorbate occluded in micropores (pore diffusion) and along pore-wall surfaces (surface diffusion) and diffusion processes in the bulk of the solid, all of which are activated diffusion processes (Figure 2). Pore and surface diffusion within the immediate region can be referred to as intra-aggregate (intraparticle) diffusion and diffusion in the solid can be called interparticle diffusion. The actual chemical reaction (CR) at the surface, e.g., adsorption, is usually instantaneous. The slowest of the CR and transport processes is ratelimiting.

B. Rate Laws

There are two important reasons for investigating the rates of soil chemical processes:[10,28] (1) to determine how rapidly reactions attain equilibrium, and (2) to infer information on reaction mechanisms. One of the most important aspects of chemical kinetics is the establishment of a rate equation or law. By definition, a rate law is a differential equation. For the following reaction:[28,29]

$$aA + bB \rightarrow yY + zZ \tag{1}$$

the rate is proportional to some power of the concentrations of reactants A and B and/or other species (C, D, etc.) in the system and a, b, y, and z are stoichiometric coefficients and are assumed to be equal to one in the discussion that follows on rate laws. The power to which the concentration is raised may equal zero (i.e., the rate is independent of that concentration), even for reactant A or B. Rates are expressed as a decrease in reactant concentration or an increase in product concentration per unit time. Thus, the rate of conversion of reactant A above, which has a concentration [A] at any time t, is (–d[A]/(dt)) while the rate with regard to product Y having a concentration [Y] at time t is (d[Y]/(dt)).

The rate expression for Equation 1 is therefore

$$|d[Y]/dt| = |-d[A]/dt| = k[A]^{\alpha}[B]^{\beta} \tag{2}$$

where k is the rate constant, α is the order of the reaction with respect to reactant A and can be referred to as a partial order for the total reaction, and β is the order with respect to reactant B. These orders are experimentally determined and not necessarily integral numbers. The sum of all the partial orders, α, β is the overall order (n) of the total reaction and may be expressed as

$$n = \alpha + \beta + \ldots \tag{3}$$

Once the values of α, β, etc. are determined experimentally, the rate law is defined. Reaction order provides only information about the manner in which rate depends on concentration. Order does not mean the same as "molecularity," which concerns the number of reactant particles (atoms, molecules, free radicals, or ions) entering into an elementary reaction. One can define an elementary reaction as one in which no reaction intermediates have been detected or need to be postulated to describe the chemical reaction on a molecular scale. An elementary reaction is assumed to occur in a single step and to pass through a single transition state.[29]

To demonstrate that a reaction is elementary, one can use experimental conditions that are different from those employed in determining the reaction rate law. For example, if one conducted kinetic studies using a flow technique with set steady-state flow rates, one could see if reaction rate and rate constants changed with flow rate. If they did, one would not be determining mechanistic rate laws (see definition below).

Rate laws serve three purposes: they assist one in predicting the reaction rate, mechanisms can be proposed, and reaction orders can be ascertained. There are four types of rate laws that can be determined for soil chemical processes:[26] mechanistic, apparent, transport with apparent, and transport with mechanistic. Mechanistic rate laws assume that only chemical kinetics are operational and transport phenomena are not occurring. Consequently, it is difficult to determine mechanistic rate laws for most soil chemical systems due to the heterogeneity of the system caused by different particle sizes, porosities, and types of retention sites. There is evidence that with some kinetic studies, using chemical relaxation techniques and pure systems (e.g., clay minerals, oxides), that mechanistic rate laws are determined or closely approximated, since the agreement between equilibrium constants calculated from both kinetic and equilibrium studies is comparable.[30,31]

The heterogeneity of natural materials would indicate that in most cases transport processes affect the reaction rate. Thus, soil structure, stirring, mixing, and flow rate all would affect the kinetics. Transport with apparent rate laws emphasize transport-limited phenomena. One often assumes first-order or zero-order reactions (see discussion below on reaction order). In determining transport with mechanistic rate laws, one attempts to describe *simultaneously* transport-controlled and chemical kinetics phenomena. One is thus trying to explain accurately both the chemistry and physics of the system.

C. Determination of Reaction Order and Rate Constants/Coefficients

There are three basic ways to determine rate laws and rate constants/coefficients:[10,26,28,29] (1) initial rates, (2) directly using integrated equations and graphing the data, and (3) using non-linear least square analysis.

Let us assume the following elementary reaction between species A, B, and Y:

$$A + B \underset{k_{-1}}{\overset{k_1}{\rightleftharpoons}} Y \tag{4}$$

A forward reaction rate law can be written as

$$d[A]/dt = -k_1[A][B] \tag{5}$$

where k_1 is the forward rate constant and α and β (see Equation 2) are each assumed to be 1.

The reverse reaction rate law for Equation 4 is

$$d[A]/dt = +k_{-1}[Y] \tag{6}$$

where k_{-1} is the reverse rate constant.

Equations 5 and 6 are only applicable far from equilibrium where back or reverse reactions are insignificant. If both forward and reverse reactions are occurring, Equations 5 and 6 must be combined, such that

$$d[A]/dt = -k_1[A][B] + k_{-1}[Y] \tag{7}$$

Equation 7 applies the principle that the net reaction rate is the difference between the sum of all reverse reaction rates and the sum of all forward reaction rates.

One way to ensure that back reactions are not important is to measure initial rates. The initial rate is the limit of the reaction rate as time reaches zero. With an initial rate method, one plots the concentration of a reactant or product over a short reaction time period during which the concentrations of the reactants change so little that the instantaneous rate is hardly affected. Thus, by measuring initial rates, one could assume that only the forward reaction in Equation 4 predominates. This would simplify the rate law to that given in Equation 5, which, as written, would be a second-order reaction, first-order in reactant A and first-order in reactant B. Equation 5 under these conditions would represent a second-order irreversible elementary reaction. To measure initial rates, one must have available a technique that can measure rapid reactions such as a chemical relaxation method and an accurate analytical detection system to determine product concentrations.

Integrated rate equations can also be used to determine rate constants/coefficients. If one assumes that reactant B in Equation 5 is in large excess of reactant A, which is an example of the "method of isolation" to analyze kinetic data, and $Y_o = 0$, where Y_o is the initial concentration of product Y, Equation 5 can be simplified to:

$$d[A]/dt = -k_1'[A] \tag{8}$$

where $k_1' = k_1[B]$.

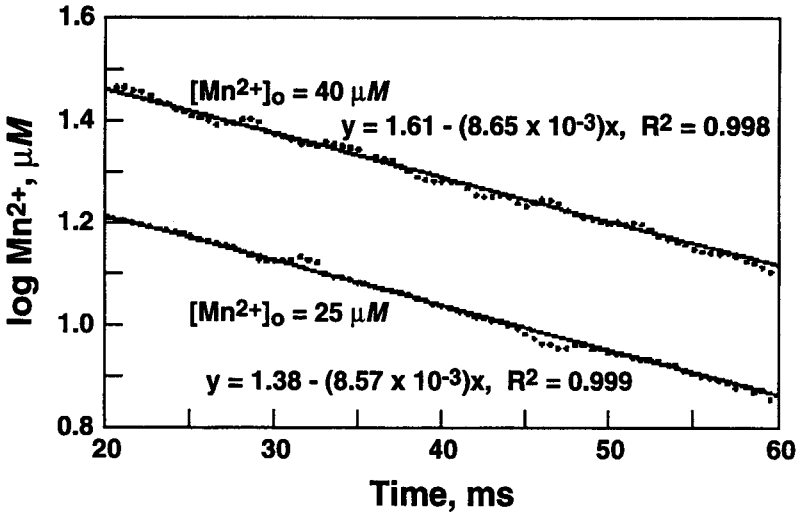

Figure 3 Initial reaction rates depicting the first-order dependence of Mn^{2+} sorption as a function of time for initial Mn^{2+} concentrations ($[Mn^{2+}]_0$) of 25 and 40 μ*M*. (From Fendorf, S. E. et al., *Soil Sci. Soc. Am. J.*, 57, 57, 1993. With permission.)

The first-order dependence of [A] can be evaluated using the integrated form of Equation 8, using the initial conditions at t = 0, A = A_0,

$$\log[A]_t = \log[A]_o - \frac{k_1' t}{2.303} \tag{9}$$

The half time ($t_{1/2}$) for the above reaction is equal to $0.693/k_1'$ and is the time required for half of reactant A to be consumed.

If a reaction is first-order a plot of log $[A]_t$ vs. t should result in a straight line with a slope = $-k_1'/2.303$ and an intercept of log $[A]_0$. An example of first-order plots for Mn^{2+} sorption on δ-MnO_2 at two initial Mn^{2+} concentrations, $[Mn^{2+}]_0$, 25 and 40 μ*M*, is shown in Figure 3. One sees that the plots are linear at both concentrations, which would indicate that the sorption process is first order. The $[Mn^{2+}]_0$ values, obtained from the intercept of Figure 3, were 24 and 41 μ*M*, which are in good agreement with the two $[Mn^{2+}]_0$ values. The rate constants were 3.73×10^{-3} and 3.75×10^{-3} s^{-1} at $[Mn^{2+}]_0$ of 25 and 40 μ*M*, respectively. The findings that the rate constants are not significantly changed with concentration is a good indication that the reaction in Equation 8 is first order under the experimental conditions that were imposed.

It is dangerous to conclude that a particular reaction order is correct, based simply on the conformity of data to an integrated equation. As illustrated above, multiple initial concentrations that vary considerably should be employed to see if the rate is independent of concentration. One should also test multiple integrated equations. It may also be useful to show that reaction rate is not affected by a species whose concentration does not change considerably during an experiment; they may be substances not consumed in the reaction (i.e., catalysts) or present in large excess.[10,23,29]

Least squares analysis can also be used to determine rate constants/coefficients. With this method, one fits the best straight line to a set of points that are linearly related as y = mx + b, where y is the ordinate and x is the abscissa datum point, respectively. The slope, m, and the intercept, b, can be calculated by least squares analysis.

Curvature may result when kinetic data are plotted. This may be due to an incorrect assumption of reaction order. If first-order kinetics is assumed and the reaction is really second-order, downward

curvature is observed. If second-order kinetics is assumed but the reaction is first order, upward curvature is observed. Curvature can also be due to fractional, third, higher, or mixed reaction order. Nonattainment of equilibrium often results in downward curvature. Temperature changes during the study can also cause curvature; thus, it is important that temperature be accurately controlled during a kinetic experiment.

IV. KINETIC MODELS

A. Ordered Models

First-order kinetics models often describe reactions at the particle/solution interface. Both single first-order and multiple first-order reactions have been described by many investigators (for example, see References 10, 23, 28, and 33).

It is not uncommon to observe biphasic kinetics, i.e., a rapid reaction rate followed by a much slower reaction rate. Such data can often be described by two first-order reactions. Some investigators have interpreted such biphasic kinetics to mean reactions on two types of sites, e.g., external, readily accessible sites (slope 1) and internal, difficultly accessible sites (slope 2).[22,24]

However, it is unsound to conclude anything about mechanisms based solely on multiple rate constants that are calculated from multiple slopes of kinetic plots. There are other ways to ascertain reaction mechanisms more definitively, such as calculating energies of activation, elucidating rate-limiting steps through stopped-flow and interruption approaches, using independent or direct methods to determine mechanisms such as spectroscopic techniques, and employing blocking agents that are specific for certain reaction sites. An example of the latter approach is found in the research of Jardine and Sparks,[22] who studied potassium-calcium exchange on a Delaware (U.S.) soil at three temperatures and observed two apparent simultaneous first-order reactions at 283 and 298 K (Figure 4). They hypothesized that the first, more rapid reaction, was predominantly due to adsorption on external planar sites of the organic matter and kaolinite in the soil. The slower reaction was ascribed to vermiculitic clay sites that promoted slow pore and surface diffusion. These hypotheses were seemingly validated by using a large organic polymer, cetyltrimethylammonium bromide (CTAB), which because of its size, is sterically hindered from internal sites. Thus, CTAB should only block external planar sites. When CTAB was applied to the soil, the first slope was eliminated, while the second slope was still present, indicating multireactive sites.

While first-order models have been used widely to describe the kinetics of chemical reactions on natural materials, a number of other simple kinetic models also have been employed. These include various ordered equations, such as zero-order, second-order, and fractional-order, and Elovich, power function or fractional power, and parabolic diffusion models. A brief discussion of some of these will be given; the final forms of the equations are given in Table 1. For more complete details and applications of these models one may consult Sparks.[10,28]

B. Elovich Equation

The Elovich equation was originally developed to describe the kinetics of heterogeneous chemisorption of gases on solid surfaces.[34] It seems to describe a number of reaction mechanisms, including bulk and surface diffusion and activation and deactivation of catalytic surfaces.

In soil chemistry, the Elovich equation has been used to describe the kinetics of sorption and desorption of various inorganic materials on soils.[10,28] It can be expressed as:[35]

$$q = (1/\beta)\ln(\alpha\beta) + (1/\beta)lnt \qquad (10)$$

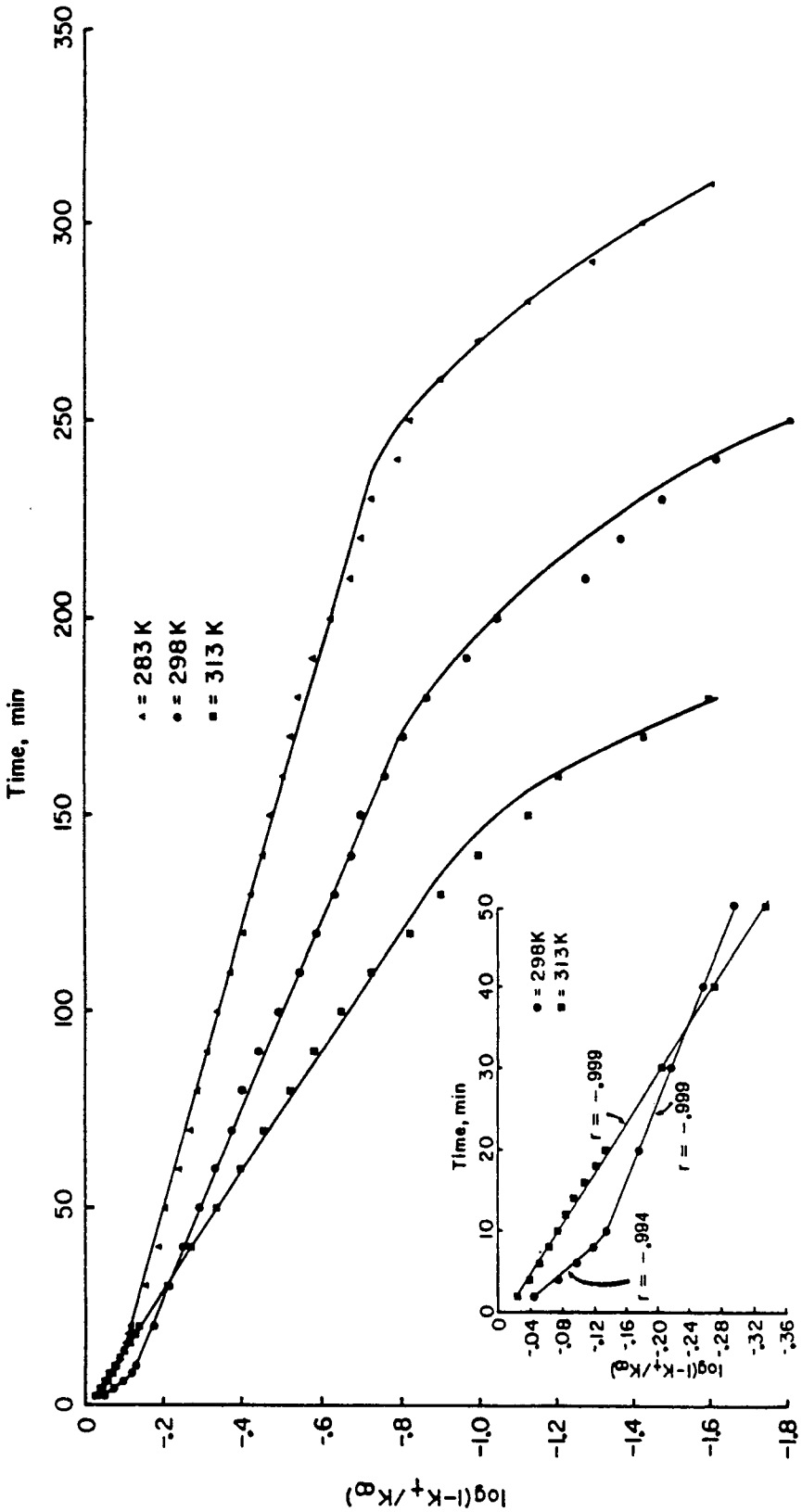

Figure 4 First-order kinetics for potassium adsorption at three temperatures on Evesboro soil with inset showing the initial 50 min of the first-order plots at 298 and 313 K. (From Jardine, P. M. and Sparks, D. L., *Soil Sci. Soc. Am. J.*, 48, 39, 1984. With permission.)

Table 1 Linear Forms of Kinetic Equations Commonly Used in Environmental Soil Chemistry[a]

Zero-order[b]
$[A]_t = [A]_0 - k_1't$
First-order[b]
$\log [A]_t = \log[A]_0 - \frac{k_1't}{2.303^c}$
Second-order[b]
$\frac{1}{[A]_t} = \frac{1}{[A]_0} + k$
Elovich
$q = (1/\beta) \ln (\alpha\beta) + (1/\beta) \ln t$
Parabolic diffusion
$\left(\frac{1}{t}\right)\left(\frac{Q_t}{Q_\infty}\right) = \frac{4}{\pi^{1/2}}\left(\frac{D}{r^2}\right)^{1/2} \frac{1}{t^{1/2}} - \frac{D}{r^2}$
Power function
$\ln q_t = \ln k + v \ln t$

[a] From Sparks;[28] terms in equations are defined in the text of the chapter.
[b] Describing the reaction A → Y.
[c] ln x = 2.303 log x is the conversion from natural logarithms (ln) to base 10 logarithms (log).

From Sparks, D. L., *Environmental Soil Chemistry*, Academic Press, San Diego, 1995. With permission.

where q is the amount of sorbate per unit mass of sorbent at time t and α and β are constants during any one experiment. A plot of q vs. ln t should give a linear relationship if the Elovich equation is applicable with a slope of (1/β) and an intercept of (1/β) ln (αβ). An application of Equation 10 to phosphate sorption on soils is shown in Figure 5.

Some investigators have used the α and β parameters from the Elovich equation to estimate reaction rates. For example, it has been suggested that a decrease in β and/or an increase in α would increase reaction rate. However, this is questionable. The slope of plots using Equation 10 changes with the concentration of the adsorptive and with the solution-to-soil ratio.[36] Therefore, the slopes are not always characteristic of the soil but may depend on various experimental conditions.

Some researchers also have suggested that "breaks" or multiple linear segments in Elovich plots could indicate a changeover from one type of binding site to another.[37] However, such mechanistic suggestions may not be correct.[10,28]

C. Parabolic Diffusion Equation

The parabolic diffusion equation is often used to indicate that diffusion-controlled phenomena are rate limiting. It was originally derived based on radial diffusion in a cylinder where the ion concentration on the cylindrical surface is constant, and initially the ion concentration throughout the cylinder is uniform. It is also assumed that ion diffusion through the upper and lower faces of the cylinder is negligible. Following Crank,[38] the parabolic diffusion equation, as applied to soils, can be expressed as:

$$(Q_t/Q_\infty) = \frac{4}{\pi^{1/2}}\left(\frac{Dt}{r^2}\right)^{1/2} - \frac{Dt}{r^2} - \frac{1}{3\pi^{1/2}}\left(\frac{Dt}{r^2}\right)^{3/2} \qquad (11)$$

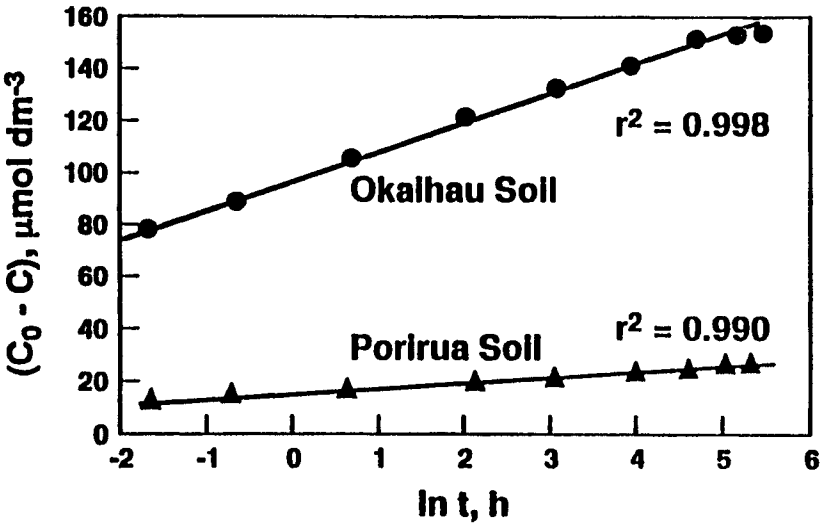

Figure 5 Plot of Elovich equation for phosphate sorption on two soils where C_0 is the initial phosphorus concentration added at time 0 and C is the phosphorus concentration in the soil solution at time t. The quantity (C_0 – C) can be equated to q, the amount sorbed at time t. (From Chien, S. H. and Clayton, W. R., *Soil Sci. Soc. Am. J.*, 44, 265, 1980. With permission.)

where r is the radius of the cylinder, Q_t is the quantity of diffusing substance that has left the cylinder at time t, Q_∞ is the corresponding quantity after infinite time, and D is an "apparent" diffusion coefficient.

For the relatively short times in most experiments, the third and subsequent terms may be ignored, and thus

$$\frac{Q_t}{Q_\infty} = \frac{4}{\pi^{1/2}}\left(\frac{Dt}{r^2}\right)^{1/2} - \frac{Dt}{r^2}$$

or

$$\frac{1}{t}\left(\frac{Q_t}{Q_\infty}\right) = \frac{4}{\pi^{1/2}}\left(\frac{D}{r^2}\right)^{1/2}\frac{1}{t^{1/2}} - \frac{D}{r^2} \tag{12}$$

and thus a plot of $\frac{(Q_t/Q_\infty)}{t}$ vs. $1/t^{1/2}$ should give a straight line with a slope

$$\frac{4}{\pi^{1/2}}\left(\frac{D}{r^2}\right)^{1/2}$$

and intercept ($-D/r^2$). Thus, if r is known, D may be calculated from both the slope and intercept.

The parabolic diffusion equation has successfully described metal reactions on soils and soil constituents,[22,39] feldspar weathering,[40] and pesticide reactions.[41]

D. Fractional-Power or Power-Function Equation

This equation can be expressed as

$$q = kt^v \tag{13}$$

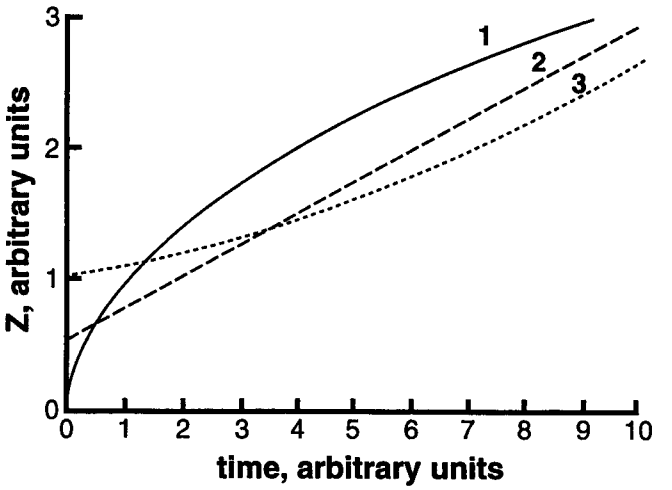

Figure 6 Plot of Z vs. time implied by (1) the power-function model, (2) the Elovich model, and (3) the first-order model. The equations for the models were differentiated and expressed as explicit functions of the reciprocal of the rate, Z. (From Aharoni, C. and Sparks, D. L., *Rates of Soil Chemical Processes*, SSSA Spec. Publ. No. 27, Sparks, D. L. and Suarez, D. L., Eds., Soil Science Society of America, Madison, WI, 1991, 1. With permission.)

where q is amount of sorbate per unit mass of sorbent at time t, k and v are constants, and v is positive and <1. Equation 13 is empirical, except for the case where v = 0.5, when it is similar to the parabolic diffusion equation.

Equation 13 and various modified forms have been used by a number of researchers to describe the kinetics of reactions on natural materials.[42,43]

E. Z(t) and Diffusion Models

In a number of studies it has been shown that several simple kinetic models, as described previously, describe rate data well, based on correlation coefficients and standard errors of the estimate.[35,44,45] Despite this, there is often not a consistent relation between the equation that gives the best fit and the physicochemical and mineralogical properties of the adsorbent(s) being studied. Another problem with some of the kinetic models is that they are empirical and no meaningful rate parameters can be obtained.

Aharoni and Ungarish[46] and Aharoni[47] noted that some simple kinetic models are approximations to which more general expressions reduce in certain limited time ranges. They suggested a generalized empirical equation by examining the applicability of power-function, Elovich, and first-order equations to experimental data. By writing these as the explicit functions of the reciprocal of the rate, Z, which is $(dq/dt)^{-1}$, one can show that a plot of Z vs. t should be convex if the power-function equation is operational (1 in Figure 6), linear if the Elovich equation is appropriate (2 in Figure 6), and concave if the first-order equation is appropriate (3 in Figure 6). However, Z vs. t plots for soil systems (Figure 7) are usually S-shaped, convex at small t, concave at large t, and linear at some intermediate t. These findings suggest that the reaction rate can best be described by the power-function equation at small t, by the Elovich equation at an intermediate t, and by a first-order equation at large t. Thus, the S-shaped curve indicates that the above equations may be applicable, each at some limited time range.

One of the reasons a particular kinetic model appears to be applicable may be that the study is conducted during the time range when the model is most appropriate. While sorption, for example, decreases over many orders of magnitude before equilibrium is approached, with most methods and experiments, only a portion of the entire reaction is measured and over this time range the

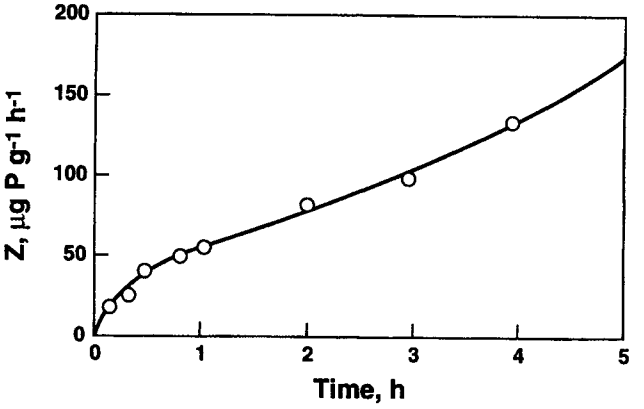

Figure 7 Sorption of phosphate by a typic Dystrochrept soil plotted as Z vs. time. The circles represent the experimental data of Polyzopoulos et al.[48] The solid line is a curve calculated according to a homogeneous diffusion model. (From Aharoni, C. and Sparks, D. L., in *Rates of Soil Chemical Processes*, SSSA Spec. Publ. No. 27, Sparks, D. L. and Suarez, D. L., Eds., Soil Science Society of America, Madison, WI, 1991, 1. With permission.)

assumptions associated with a simple kinetic model (power-function, Elovich, and first-order) are valid. Aharoni and Suzin[49,50] showed that the S-shaped curves could be well described using homogeneous and heterogeneous diffusion models. In homogeneous diffusion situations, the final and initial portions of the S-shaped curves (conforming to the power-function and first-order equations, respectively) predominated, whereas, in instances where the heterogeneous diffusion model was operational, the linear portion of the S-shaped curve, that conformed to the Elovich equation, predominated. Derivations of homogeneous and heterogeneous diffusion models can be found in Aharoni and Sparks.[27]

F. Implications of Diffusion Models

The finding that slower reactions at the soil particle/liquid interface can be described by diffusional models indicates that the kinetics of chemical processes cannot be considered separately from physically limited transport phenomena. Thus, such a combination of processes cannot be treated using first-order or other-order chemical kinetics equations. When one states that a reaction between the molecular species A and B is of first order with respect to A, one assumes that the molecules of A have equal chances of participating in the reaction and therefore the rate is proportional to the concentration, C_A. This reasoning can be extended to a reaction between an adsorbing surface and an adsorptive solute. The concentration C_A, in this case, refers to the number of reactive sites per unit area, which corresponds to the number of unoccupied sites per unit area $(1 - \theta_A)$. However, by using first-order kinetics (or other-order kinetics) one tacitly assumes that all of the surface sites are potential reactants at any time, and they have an opportunity of participating in the sorption process. If one assumes that there are sites that cannot be reached directly from the fluid phase, but can be reached after the sorbate has undergone sorption and desorption at other sites, one cannot separate chemical kinetics from diffusion-limited kinetics. The overall kinetic process obeys a diffusion equation since diffusion is the rate-limiting process. However, the diffusion coefficient, which reflects the rate at which the sorbate jumps from one site to another, is determined by the rate of the chemical reactions by which the sorbent-sorbate bonds are created and destroyed. Additionally, the activation energy for diffusion is equivalent to the activation energy of the chemical reaction.

G. Multiple-Site Models

Based on the previous discussion, it is evident that simple chemical kinetics models, such as ordered reaction models and the power-function and Elovich models, may not be appropriate to describe reactions in heterogeneous systems such as soils, sediments, and soil components. In these systems where there is a range of particle sizes and multiple retention sites, both chemical kinetics and transport phenomena are occurring simultaneously, and a fast reaction is often followed by a slower reaction(s). In such systems, nonequilibrium models that describe both chemical and physical nonequilibrium and that consider multiple components and sites are more appropriate. Physical nonequilibrium is ascribed to some rate-limiting transport mechanism such as FD or PD while chemical nonequilibrium is due to a rate-limiting mechanism at the particle surface (CR). Nonequilibrium models include two-site, multiple-site, radial diffusion (pore diffusion), surface diffusion, and multiprocess models (Table 2). Emphasis in this chapter will be on use of these models to describe sorption phenomena.

The term "sites" can have a number of meanings:[57] (1) specific, molecular scale reaction sites; (2) sites of differing degrees of accessibility (external, internal); (3) sites of differing sorbent type (organic matter and inorganic mineral surfaces); and (4) sites with different sorption mechanisms. With chemical nonequilibrium sorption processes, the sorbate may undergo two or more types of sorption reactions, one of which is rate limiting. For example, a metal cation may sorb to organic matter by one mechanism and to mineral surfaces by another mechanism, with one of the mechanisms being time dependent.

1. Chemical Nonequilibrium Models

Chemical nonequilibrium models describe time-dependent reactions at sorbent surfaces. The one-site model is a first-order approach that assumes that the reaction rate is limited by only one process or mechanism on a single class of sorbing site and that all sites are of the time-dependent type. In many cases this model appears to describe soil chemical reactions quite well. However, often it does not. This model would seem not appropriate for most heterogeneous systems, since multiple sorption sites exist.

The two-site (two compartment, two box) or bicontinuum model has been widely used to describe chemical nonequilibrium[52,58-62] and physical nonequilibrium[63-65] (Table 2). This model assumes that there are two reactions occurring, one that is fast and reaches equilibrium quickly and a slower reaction that can continue for long time periods. The reactions can occur either in series or in parallel.[57]

In describing chemical nonequilibrium with the two-site model it is assumed that the sorbent has two types of sites. One site involves an instantaneous equilibrium reaction and the other site involves the time-dependent reaction. The instantaneous equilibrium reaction is described by an equilibrium isotherm equation, while a first-order equation is usually employed to describe the time-dependent reaction.

Jardine et al.[66] modeled the transport of Al through Ca-saturated kaolinite columns using a two-site nonequilibrium transport process (Figure 8a). They assumed and showed that type 1 sites were in local equilibrium with the solution phase and involved an instantaneous Ca-Al exchange mechanism. Type 2 sites involved a time-dependent Al polymerization reaction mechanism and were described by first-order kinetics.

The polymerization mechanism was indirectly confirmed by investigating the effect of influent pH on Al transport. When influent pH was lowered, the slower kinetic reaction was eliminated and the Al breakthrough curve was described with a one-site equilibrium model (Figure 8b).

With the two-site model there are two adjustable or fitting parameters, the fraction of sites at local equilibrium (X_1) and the rate constant (k). A distribution (K_d) or partition coefficient (K_p) is determined independently from a sorption/desorption isotherm.

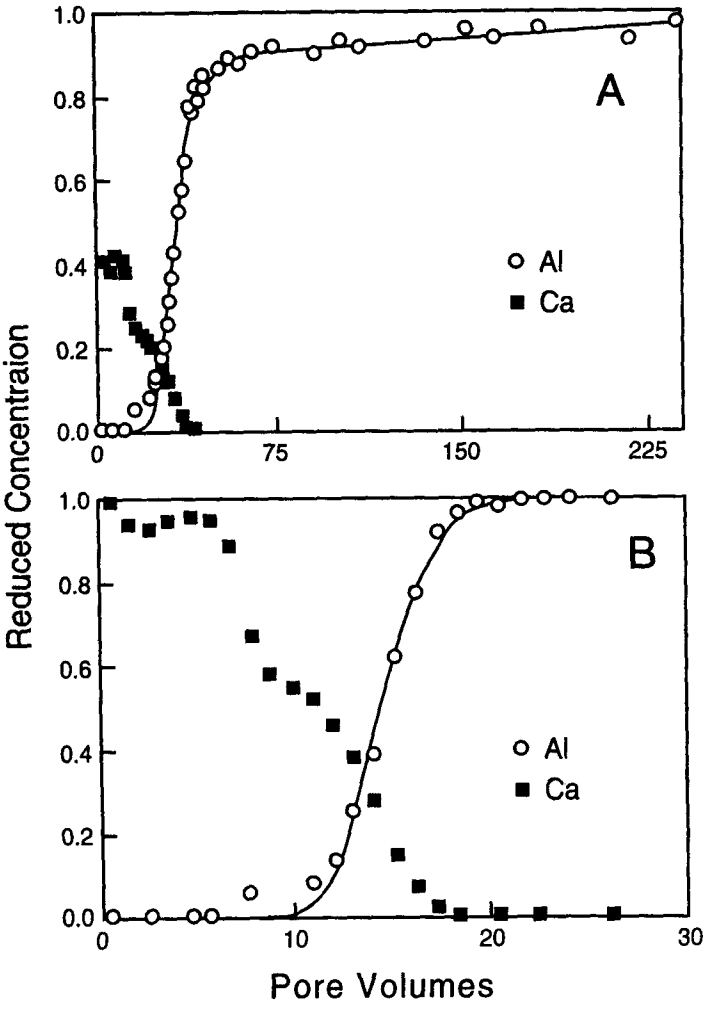

Figure 8 (a) Breakthrough curve for 0.73 mg l^{-1} Al at pH 4.29 on kaolinite with corresponding desorbed Ca. Solid line is the fitted curve from a two-site, nonequilibrium model. (b) Breakthrough curve for 1.50 mg l^{-1} Al at pH 3.97 on kaolinite with corresponding desorbed Ca. Solid line is the fitted curve from the one-site, equilibrium model. (From Jardine, P. M. et al., *Soil Sci. Soc. Am. J.*, 49, 867, 1985. With permission.)

Connaughton et al.[51] used a two-site model to describe naphthalene desorption from contaminated soil (Figure 9a). The model did not describe the data well and fitted and estimated desorption rate coefficients (k_d) did not agree, with the estimated k_d values being higher than the values obtained from fitting. The estimated k_d values were based on the relation $\log k_d = 0.301 - 0.688 \log K_p$.[57]

Connaughton et al.[51] related this discrepancy to the greater desorption times of their experiments and to the use of the two-site model to describe the entire desorption process. The two-site model, that the $K_p - k_d$ relationship was based on, assumes that the initial desorption is instantaneous, which is not the case for naphthalene desorption. One major disadvantage in using the two-site model to describe heterogeneous systems such as soil is the assumption that only two sorptive sites are present. Thus, the fitting parameters in the two-site model probably do not conform to actual reaction rates on multiple sites in soils. Moreover, it is difficult to relate the fitting parameters to known properties of the sorbent. For example, Wu and Gschwend[53] found two different sets of fitting parameters described tetrachlorobenzene sorption on a Charles River sediment if different

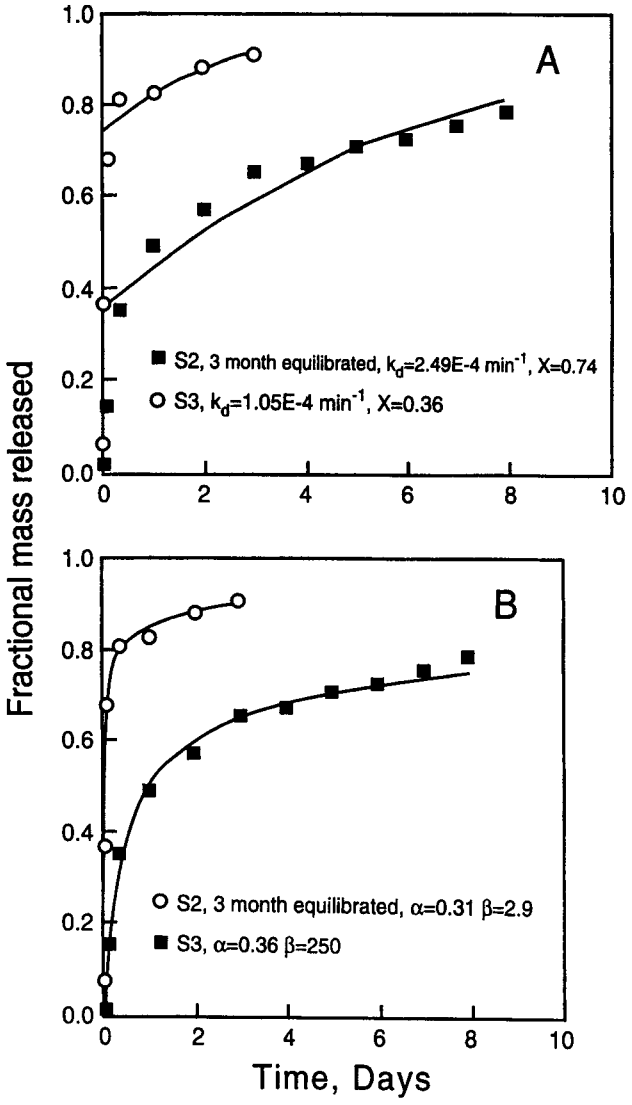

Figure 9 (a) Fitted two-site model with release profiles of naphthalene from two soils, S2 and S3 (S2 is a freshly contaminated soil, reacted with naphthalene for 3 months, and S3 is a field [aged] contaminated soil); R^2 = 0.88, 0.91 for S2 and S3 (regression fits, respectively, where X is the fraction of sites that reach an equilibrium in release instantaneously and k_d is the desorption rate coefficient). (b) Mass fractional release of naphthalene from S2 and S3 soils fitted with a multisite continuum compartment (Γ) model. (From Connaughton, D. F. et al., *Environ. Sci. Technol.*, 27, 2397, 1993. With permission.)

sediment mean aggregate sizes were used. Consequently, the parameters had to be experimentally determined for each sediment size.

To account for the multiple sites that may exist in heterogeneous systems Connaughton et al.[51] developed a multisite compartment model (Γ) that incorporates a continuum of sites or compartments with a distribution of rate coefficients that can be described by a gamma density function. A fraction of the sorbed mass in each compartment is at equilibrium and there is a desorption rate coefficient or distribution coefficient for each compartment or site (Table 2). The multisite model has two fitting parameters, α, a shape parameter, and 1/β, which is a scale parameter that determines the mean standard deviation of the rate coefficients. Figure 9b shows application of the Γ model

to desorption of naphthalene from contaminated soils. The entire desorption process was described well with this model.

2. Physical Nonequilibrium Models

There are a number of models that can be used to describe physical nonequilibrium reactions. Since transport processes in the mobile phase are not usually rate limiting, physical nonequilibrium models focus on diffusion in the immobile phase or intra-aggregate-diffusion processes (e.g., pore and/or surface diffusion). The transport between mobile and immobile regions is accounted for in physical nonequilibrium models in three ways:[57] (1) explicitly with Fick's law to describe the physical mechanism of diffusive transfer; (2) explicitly by using an empirical first-order mass-transfer expression to approximate solute transfer; and (3) implicitly by using an effective or lumped dispersion coefficient that includes the effects of sink/source differences and hydrodynamic dispersion and axial diffusion.

A pore diffusion model (Table 2) has been used by a number of investigators to study sorption processes using batch systems.[53,67-70] Wu and Gschwend[53] successfully used the pore diffusion model to describe chlorobenzene congener sorption/desorption on soils and sediments. Figure 10 shows experimental and model fits for tetrachlorobenzene and pentachlorobenzene sorption on soils. The sole fitting parameter in this model is the effective diffusion coefficient (D_e). This parameter may be estimated *a priori* from chemical and colloidal properties. However, this estimation is only valid if the sorbent material has a narrow particle size distribution such that an accurate, average particle size can be defined. Moreover, in the pore diffusion model it is assumed that there is an average representative D_e, which means there is a continuum in properties across an entire pore size spectrum. This is not a valid assumption for micropores (<2.0 nm), since there are higher adsorption energies of sorbates in micropores, which causes increased sorption. The increased sorption causes reduced diffusive transport rates and nonlinear isotherms for sorbents with pores < several sorbate diameters in size. Other factors can cause reduced transport rates in micropores including steric hindrance which increases as the pore size approaches the solute size and greatly increased surface area to pore volume ratios (which occurs as pore size decreases).

Another problem with the pore diffusion model is that sorption and desorption kinetics may have been measured over a narrow concentration range. This is a problem since a sorption/desorption mechanism in micropores at one concentration may be insignificant at another concentration.

Fuller et al.[55] used a pore space diffusion model (Table 2) to describe arsenate adsorption on ferrihydrite that included a subset of sites whereby sorption was at equilibrium. A Freundlich model was used to describe sorption on these sites. Diffusion into the particle was described by Fick's second law of diffusion; homogeneous, spherical aggregates and diffusion only in the aqueous phase were assumed.

Figure 11 shows the fit of the model when sorption at all sites was controlled by intra-aggregate diffusion. The fit was better when sites that had attained sorption equilibrium were included (Figure 11). The latter model assumed that there was an initial rapid sorption on external surface sites before intra-aggregate diffusion.

Pedit and Miller[56] have developed a general multiple-particle class pore diffusion model that accounts for differences in physical and sorptive properties for each particle class (Table 2). The model includes both instantaneous equilibrium sorption and time-dependent pore diffusion for each particle class. The pore diffusion portion of the model assumes that solute transfer between the intraparticle fluid and the solid phases is fast vis-à-vis intraparticle pore diffusion processes.

Surface diffusion models, assuming a constant surface diffusion coefficient, have been used by a number of researchers.[54,71] The dual resistance model (Table 2) combines both pore and surface diffusion.

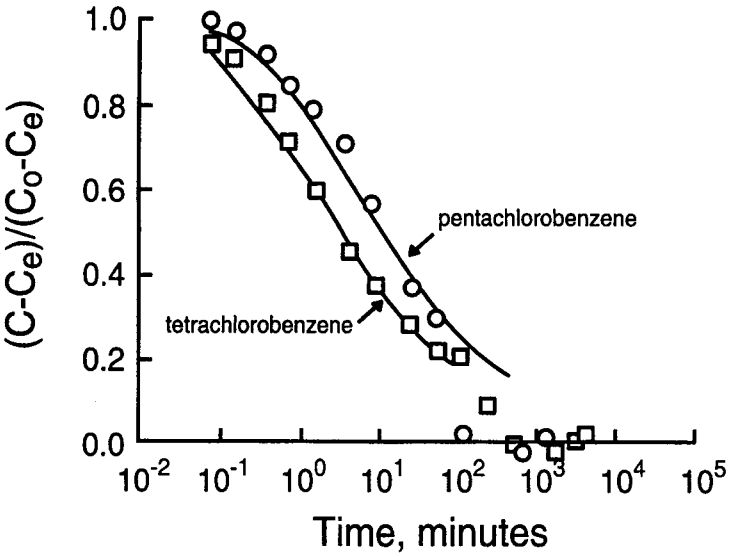

Figure 10 Experimental and model-fitting results for pentachlorobenzene and tetrachlorobenzene sorption on Iowa soils where C is the dissolved concentration of organic chemical in the bulk solution, C_0 is the initial concentration, and C_e is the equilibrium concentration. The points represent experimental data and the solid lines represent fit of the data to the radial diffusion (pore diffusion) model. (From Wu, S. and Gschwend, P. M., *Environ. Sci. Technol.*, 20, 717, 1986. With permission.)

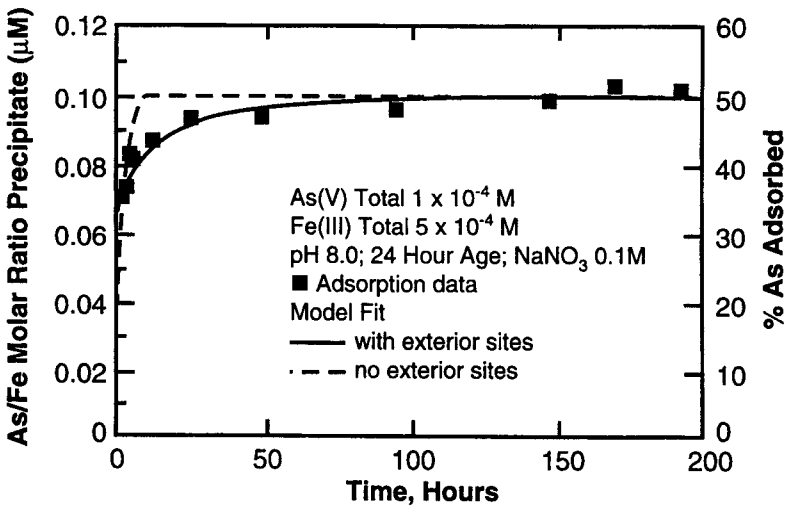

Figure 11 Comparison of pore space diffusion model fits of As(V) sorption with experimental data (dashed curve represents sorption where all surface sites are diffusion-limited and the solid curve represents sorption on equilibrium sites plus diffusion-limited sites). From Fuller, C. C. et al., *Geochim. Cosmochim. Acta*, 57, 2271, 1993. With permission.)

V. KINETIC METHODOLOGIES

A number of methodologies can be used to study the rates of soil chemical processes. These can be broadly classified as methods for slower reactions (>15 s), which include batch and flow techniques, and rapid techniques that can measure reactions on millisecond and microsecond time scales. It should be recognized that none of these methods is a panacea for kinetic analyses. They

Table 2 Comparison of Sorption Kinetic Models

Conceptual model	Fitting parameter(s)	Model limitations
One-site model $S \xrightarrow{k_d} C$	k_d	Cannot describe biphasic sorption/desorption
Two-site model $S_1 \leftrightarrow C \xleftarrow{X_1K_p\,k_d} S_2$	k_d,* K_p, X_1	May not describe the "bleeding" or slow, reversible, nonequilibrium desorption for residual sorbed compounds[52]
Radial diffusion penetration retardation (pore diffusion) model[53] $S' \xleftrightarrow{K_p} C' \xrightarrow{D_{eff}} C$	**$D_{eff} = f(n,t)D_m n/(1-n)\rho_s K_p$	Cannot describe instantaneous uptake without additional correction factor; did not describe kinetic data for times greater than 10^3 min[53]
Dual-resistance surface diffusion model[54] $S' \xrightarrow{D_s} C'_s \xrightarrow{k_b} C$	D_s, k_b	Model calibrated with sorption data predicted more desorption than occurred in the desorption experiments[54]
Multisite continuum compartment model[51] $F(t) = 1 - \frac{M(t)}{M} = 1 - \left(\frac{\beta}{\beta + t}\right)^{\alpha}$	α, β	Assumption of homogeneous, spherical particles and diffusion only in aqueous phase
Pore space diffusion model[55] $\left(\epsilon + \frac{S_a}{n} K_s C(r)^{(1-1/n)}\right)\frac{\partial C(r)}{\partial t} = D_e\left(\frac{\partial^2 C(r)}{\partial r^2} + \frac{2\partial C(r)}{r\partial r}\right)$	D_e, ϵ, K_s, 1/n, F_{eq}	
Multiple particle class pore diffusion model[56] $\left(\frac{\theta_p^i + \rho_a^i}{\partial C_p^i}\right)\frac{\partial q_r^i(r,t)}{(r,t)}\frac{\partial C_p^i(r,t)}{\partial t} = \frac{\theta_p^i D_p^i}{r^2}\frac{\partial}{\partial_r}\left(\frac{r^2 \partial C_p^i(r,t)}{\partial r}\right)$ $-\theta_p^i \lambda_p^i C_p^i(r,t) - \rho_a^i \lambda_r^i q_r^i(r,t)$	θ_p^i, ρ_a^i, D_p^i, λ_p^i, λ_r^i	Multiple fitting parameters; variations in sorption equilibrium and rates that might occur within a particle class or an individual particle grain are not addressed

Partially adapted from Connaughton et al.[51]

Abbreviations used are as follows: S, concentration of the bulk sorbed contaminant (g g^{-1}); C, concentration of the bulk aqueous-phase contaminant (g ml^{-1}); k_d, first-order desorption rate coefficient (min^{-1}); S_2, concentration of the sorbed contaminant that is rate limited (g g^{-1}); S_1, concentration of the contaminant that is in equilibrium with the bulk aqueous concentration (g g^{-1}); X_1, fraction of the bulk sorbed contaminant that is in equilibrium with the aqueous concentration; K_p, sorption equilibrium partition coefficient (ml g^{-1}); D_{eff}, effective diffusivity of sorbate molecules or ions in the particles (cm^2 s^{-1}); S′, concentration of contaminant in immobile bound state (mol g^{-1}); C′, concentration of contaminant free in the pore fluid (mol cm^{-3}); n, porosity of the sorbent (cm^3 of fluid cm^{-3}); D_m, pore fluid diffusivity of the sorbate (cm^2 s^{-1}); ρ_s, specific gravity of the sorbent (g cm^{-3}); f (n,t), pore geometry factor; k_b, boundary layer mass transfer coefficient (m s^{-1}); r, radius of the spherical solid particle, assumed constant (m); ρ, macroscopic particle density of the solid phase (g m^{-3}); C'_s, solution-phase solute concentration corresponding to an equilibrium with the solid-phase solute concentration at the exterior of the particle (g l^{-1}); D_s, surface diffusion coefficient (m s^{-1}).

*K_p can be determined independently.

**K_p, D_m, and ρ_s can be determined independently; F(t), fraction of mass released through time t; M(t), mass remaining after time t; M, total initial mass; β, scale parameter necessary for determination of mean and standard deviation of k_s; α, shape parameter; ϵ, internal porosity of sorbent; C(r), concentration of sorptive in the aqueous phase in the pore fluid at radial distance r; S_a is the surface of sorbent per unit volume of solid; 1/n, the adsorption isotherm slope; K_s, adsorption isotherm intercept; D_e, effective diffusion coefficient; a, radius of the aggregate; F_{eq}, equilibrium fraction of adsorption sites; θ_p^i, intraparticle porosity of particle class i; ρ_a^i, apparent particle density of particle class i; r, radial distance; C_p^i (r, t), intraparticle fluid-phase solute concentration of the particle class i; D_p^i, pure diffusion coefficient for particle class i; λ_p^i, intraparticle fluid-phase first-order reaction rate coefficient for particle class i; λ_r^i, intraparticle solid-phase first-order reaction rate coefficient for particle class i; q_r^i (r, t), intraparticle solid-phase solute concentration of particle class i.

all have advantages and disadvantages. For comprehensive discussions on kinetic methodologies one should consult Sparks,[10] Amacher,[11] Sparks and Zhang,[72] and Sparks et al.[73]

A. Batch Methods

Batch methods have been the most widely used kinetic techniques. In the simplest traditional batch technique, an adsorbent is placed in a series of vessels such as centrifuge tubes with a particular volume of adsorptive. The tubes are then mixed by shaking or stirring. At various times a tube is sacrificed for analysis, i.e., the suspension is either centrifuged or filtered to obtain a clear supernatant for analysis. A number of variations of batch methods exist and these are discussed in Amacher.[11]

There are a number of disadvantages to traditional batch methods. Often the reaction is complete before a measurement can be made, particularly if centrifugation is necessary, and the solid:solution ratio may be altered as the experiment proceeds. Too much mixing may cause abrasion of the adsorbent, altering the surface area, while too little mixing may enhance mass transfer and transport processes. Another major problem with all batch techniques, unless a resin or chelate material such as Na-tetraphenylboron is used, is that products are not removed. This can cause inhibition in further adsorbate release and promotion of secondary precipitation in dissolution studies. Moreover, reverse reactions are not controlled, which makes the calculation of rate coefficients difficult and perhaps inaccurate.

Many of the disadvantages listed above for traditional batch techniques can be eliminated by using a method like that of Zasoski and Burau,[74] shown in Figure 12. In this method an absorbent is placed in a vessel containing the adsorptive, pH and suspension volume are adjusted, and the suspension is vigorously mixed with a magnetic stirrer. At various times, suspension aliquots are withdrawn using a syringe containing N_2 gas. The N_2 gas prevents CO_2 and O_2 from entering the reaction vessel. The suspension is rapidly filtered and the filtrates are then weighed and analyzed. With this apparatus a constant pH can be maintained, reactions can be measured at 15-s intervals, excellent mixing occurs, and a constant solid-to-solution ratio is maintained.

B. Flow Methods

Flow methods can range from continuous flow techniques (Figure 13), which are similar to liquid-phase chromatography, to stirred-flow methods (Figure 14) that combine aspects of both batch and flow methods. Important attributes of flow techniques are that one can conduct studies at realistic soil-to-solution ratios that better simulate field conditions, the adsorbent is exposed to a greater mass of ions than in a static batch system, and the flowing solution removes desorbed and detached species.

With continuous flow methods, samples can be injected as suspensions or spread dry on a membrane filter. The filter is attached to its holder by securely capping it, and the filter holder is connected to a fraction collector and peristaltic pump, the latter maintaining a constant flow rate. Influent solution then passes through the filter, reacts with the adsorbent, and at various times, effluents are collected for analysis. Depending on flow rate and the amount of effluent needed for analysis, samples can be collected about every 30 to 60 s. One of the major problems with this method is that the colloidal particles may not be dispersed, i.e., the time necessary for an adsorptive to travel through a thin layer of colloidal particles is not equal at all locations of the layer. This plus minimal mixing promotes significant transport effects. Thus, apparent rate laws and rate coefficients are measured, with the rate coefficients changing with flow rate. There can also be dilution of the incoming adsorptive solution by the liquid used to load the adsorbent on the filter, particularly if the adsorbent is placed on the filter as a suspension, or if there is washing out of remaining adsorptive solution during desorption. This can cause concentration changes not due to adsorption or desorption.

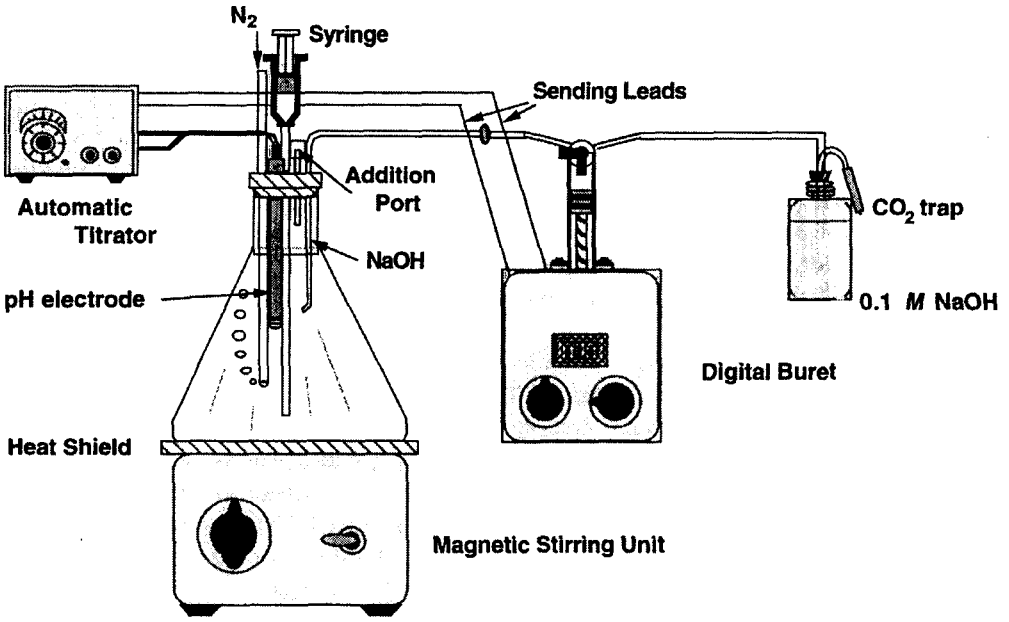

Figure 12 Schematic diagram of equipment used in batch technique of Zasoski and Burau.[74] (From Zasoski, R. G. and Burau, R. G., *Soil Sci. Soc. Am. J.*, 47, 372, 1978. With permission.)

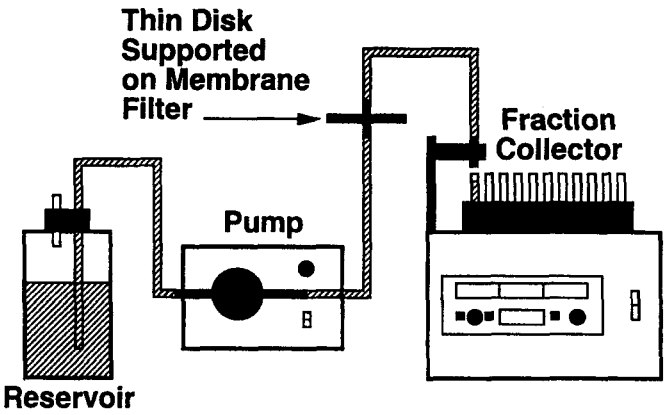

Figure 13 Continuous flow method experimental setup. Background solution and solute are pumped from the reservoir through the thin disk and are collected as aliquots by the fraction collector. (From Amacher, M. C., in *Rates of Soil Chemical Processes*, SSSA Spec. Publ. No. 27, Sparks, D. L. and Suarez, D. L., Eds., Soil Science Society of America, Madison, WI, 1991, 19. With permission.)

A more preferred method for measuring soil chemical reaction rates is the stirred-flow method. The experimental setup is similar to the continuous flow method (Figure 13), except there is a stirred-flow reaction chamber rather than a membrane filter. A schematic of this method is shown in Figure 14. The sorbent is placed into the reaction chamber, where a magnetic stir bar or an overhead stirrer (Figure 14) keeps it suspended during the experiment. There is a filter placed in the top of the chamber which keeps the solids in the reaction chamber. A peristaltic pump maintains a constant flow rate and a fraction collector is used to collect the leachates. The stirrer effects perfect mixing, i.e., the concentration of the adsorptive in the chamber is equal to the effluent concentration.

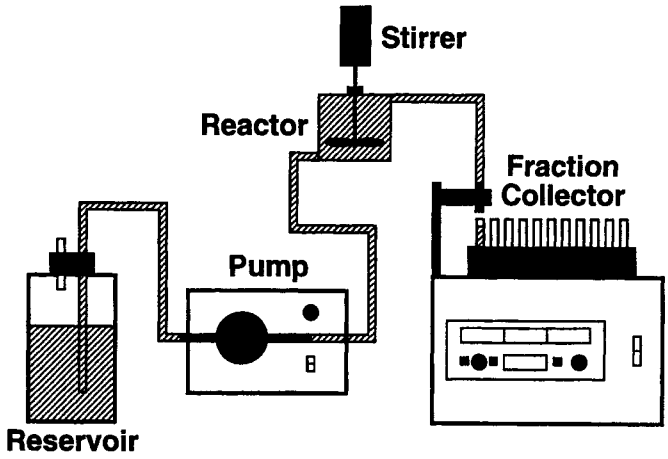

Figure 14 Stirred-flow reactor experimental setup. Background solution and solute are pumped from the reservoir through the stirred reactor containing the solid phase and are collected as aliquots by the fraction collector. Separation of solid and liquid phases is accomplished by a membrane filter at the outlet end of the stirred reactor. (From Amacher,[11] (From Amacher, M. C., in *Rates of Soil Chemical Processes*, SSSA Spec. Publ. No. 27, Sparks, D. L. and Suarez, D. L., Eds., Soil Science Society of America, Madison, WI, 1991, 19. With permission.)

This method has several advantages over the continuous flow technique and other kinetic methods. Reaction rates are independent of the physical properties of the porous media, the same apparatus can be used for adsorption and desorption experiments, desorbed species are removed, continuous measurements allow for monitoring reaction progress, experimental factors such as flow rate and adsorbent mass can be easily altered, a variety of solids can be used (however, sometimes fine particles can clog the filter, causing a buildup in pressure which results in a nonconstant flow rate) with the technique, the adsorbent is dispersed, and dilution errors can be measured. With this method, one can also use stopped-flow tests and vary influent concentrations and flow rates to elucidate possible reaction mechanisms.[75]

C. Relaxation Techniques

As noted earlier, many soil chemical reactions are very rapid, occurring on millisecond and microsecond time scales. These include metal and organic sorption-desorption reactions, ion exchange processes, and ion association reactions. Batch and flow techniques, which measure reaction rates of >15 s, cannot be employed to measure these reactions. Chemical relaxation methods must be used to measure very rapid reactions. These include pressure-jump (p-jump), electric field pulse, temperature-jump (t-jump), and concentration jump (c-jump) methods. These methods are fully outlined and described in other sources.[10,72] Only a brief discussion of the theory of chemical relaxation and a description of p-jump methods, which have been the most widely used chemical relaxation method to describe reaction rates at the mineral/water interface, will be given here. The theory of chemical relaxation can be found in a number of sources.[76-78] It should be noted that relaxation techniques are best used with soil components such as oxides and clay minerals and not with soils. Soils are heterogeneous, which complicates the analyses of the relaxation data.

All chemical relaxation methods are based on the theory that the equilibrium of a system can be rapidly perturbed by some external factor such as pressure, temperature, or electric field strength. Rate information can then be obtained by measuring the approach from the perturbed equilibrium to the final equilibrium by measuring the relaxation time, τ (the time that it takes for the system to relax from one equilibrium state to another, after the perturbation pulse) by using a detection system such as conductivity. The relaxation time is related to the specific rates of the elementary

reactions involved. Since the perturbation is small, all rate expressions reduce to first-order equations regardless of reaction order or molecularity.[78] The rate equations are then linearized such that:

$$\tau^{-1} = k_1(C_A + C_B) + k_{-1} \tag{14}$$

where k_1 and k_{-1} are the forward and backward rate constants and C_A and C_B are the concentrations of reactants A and B at equilibrium. From a linear plot of τ^{-1} vs. (C_A + C_B) one could calculate k_1 and k_{-1} from the slope and intercept, respectively. Pressure-jump relaxation is based on the principle that chemical equilibria depend on pressure, as shown below:[78]

$$\left(\frac{\partial \ln K^\circ}{\partial \ln p}\right)_T = -\Delta V/RT \tag{15}$$

where K° is the equilibrium constant, ΔV is the standard molar volume change of the reaction, p is pressure, and R and T were defined earlier. For a small perturbation,

$$\frac{\Delta K^\circ}{K^\circ} = \frac{-\Delta V \Delta p}{RT} \tag{16}$$

Details on the experimental protocol for a p-jump study can be found in several sources.[10,15,79]

Fendorf et al.[32] used an electron paramagnetic resonance stopped-flow (EPR-SF) method (an example of a c-jump method) to study reactions in colloidal suspensions *in situ* on millisecond time scales. If one is studying an EPR active species (paramagnetic) such as Mn, this technique has several advantages over other chemical relaxation methods. With many relaxation methods, the reactions must be reversible and reactant species are not directly measured. Moreover, in some relaxation studies, the rate constants are calculated from linearized rate equations that are dependent on equilibrium parameters. Thus, the rate parameters are not directly measured.

With the EPR-SF method of Fendorf et al.[32] the mixing can be done in <10 msec and EPR digitized within a few microseconds. A diagram of the EPR-SF instrument is shown in Figure 15. Dual 2-ml in-port syringes feed a mixing cell that is located in the EPR spectrometer. This allows for EPR detection of the cell contents. A single outflow port is fitted with a 2-ml effluent collection syringe equipped with a triggering switch. The switch activates the data acquisition system. Each run consists of filling the in-port syringes with the desired reactants, flushing the system with the reactants several times, and initiating and monitoring the reaction. Fendorf et al.[32] used this system to study the kinetics of Mn^{2+} sorption on γ-MnO_2 (see Figure 3). The sorption reaction was complete in 200 msec. Data were taken every 50 μsec and 100 points were averaged to give the time-dependent sorption of Mn(II).

D. Choice of Kinetic Method

The method that one chooses to study the kinetics of soil chemical reactions depends on several factors. The reaction rate will certainly dictate the choice of method. With batch and flow methods, the most rapid measurements one can make require about 15 s. For more rapid reactions, one must use relaxation techniques where millisecond and microsecond time scales can be measured.

Another factor in deciding on a kinetic method is the objective of one's experiment(s). If one wishes to measure the chemical kinetics of a reaction where transport is minimal, most batch and flow techniques are unsuitable and a relaxation technique should be employed. On the other hand, if one wants to simulate time-dependent reactions in the field, perhaps a flow technique would be more realistic than a batch method.

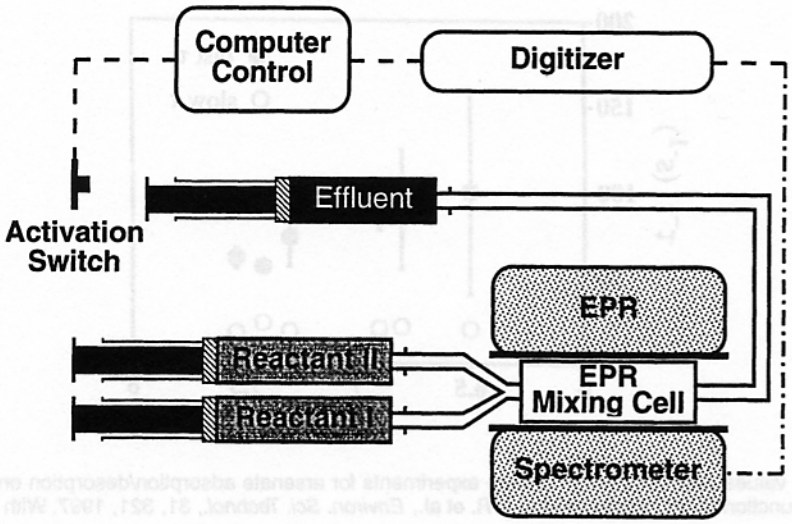

Figure 15 Schematic diagram of the electron paramagnetic resonance monitored stopped-flow kinetic apparatus. (From Fendorf, S. E. et al., *Soil Sci. Soc. Am. J.*, 57, 57, 1993. With permission.)

VI. KINETICS OF IMPORTANT REACTIONS ON NATURAL PARTICLES

In the past two decades numerous studies have been conducted on the kinetics of metal, radionuclide, plant nutrient, and organic chemical reactions on natural materials.

In this section emphasis will be placed on the kinetics of sorption-desorption and precipitation/dissolution reactions on soils and soil constituents.

A. Sorption/Desorption Reaction Rates

1. *Heavy Metals and Metalloids*

The chemical reaction of heavy metals on soil components is rapid, occurring on millisecond time scales. For such rapid reactions, chemical relaxation techniques, i.e., pressure-jump relaxation must be employed.[10,72,79,80]

The use of p-jump relaxation to measure the kinetics of ion sorption/desorption on metal oxide surfaces was pioneered by several Japanese chemists. Their research includes some of the following adsorption/desorption kinetic studies: divalent metal ion,[30] phosphate,[81] chromate,[82] and uranyl[83] adsorption reactions on γ-Al_2O_3. Hayes and Leckie[80] were the first to use p-jump relaxation to study adsorption/desorption kinetics of a metal ion contaminant (Pb^{2+}) on goethite (α-FeOOH). Other successive studies monitored the rapid adsorption/desorption kinetics of molybdate,[15] sulfate,[16] selenate and selenite,[17] Cu^{2+},[84] and arsenate and chromate[85] on goethite. Additionally, studies have investigated borate adsorption/desorption kinetics on pyrophyllite[86] and on γ-Al_2O_3.[87]

Details of many of these studies are summarized in Hayes and Leckie,[80] Sparks,[10] and Sparks and Zhang[72] and will not be detailed here. A recent study of Grossl et al.[85] will be summarized to illustrate rapid chemical reaction rates of chromate and arsenate on goethite. A double relaxation was observed for both arsenate and chromate adsorption/desorption over a pH range of 6.5 to 7.5 for arsenate and 5.5 to 6.5 for chromate, respectively (Figures 16 and 17). Based on the double relaxations, a two-step process, resulting in the formation of an inner-sphere bidentate surface complex (Figure 18), was proposed. The first step involves an initial ligand exchange reaction of the aqueous oxyanion ($H_2AsO_4^-$ or $HCrO_4^-$) with goethite, forming an inner-sphere monodentate

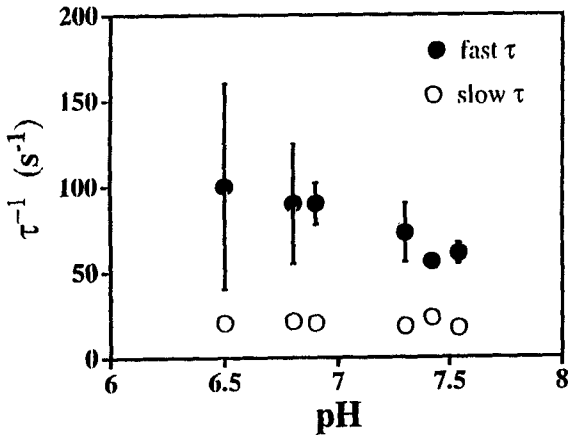

Figure 16 τ^{-1} values determined from p-jump experiments for arsenate adsorption/desorption on goethite, as a function of pH. (From Grossl, P. R. et al., *Environ. Sci. Technol.*, 31, 321, 1997. With permission.)

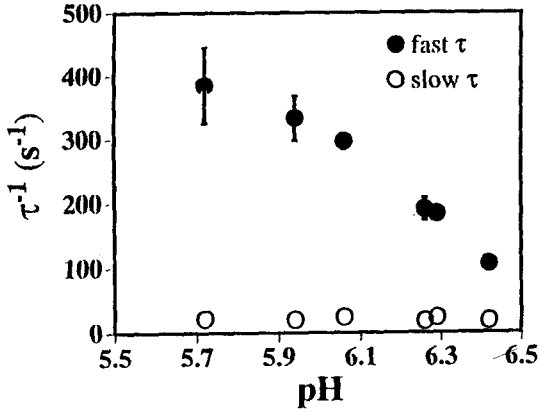

Figure 17 τ^{-1} values determined from p-jump experiments for chromate adsorption/desorption on goethite, as a function of pH. (From Grossl, P. R., et al., *Environ. Sci. Technol.*, 31, 321, 1997. With permission.)

surface complex. This first step produces the signals associated with the fast τ values. The succeeding step involves a second ligand exchange reaction, resulting in the formation of an inner-sphere bidentate surface complex. This step produces the signal associated with the slow τ values.

To determine if the mechanism displayed in Figure 18 was plausible and consistent with the kinetic data, the following linearized rate equations relating reciprocal relaxation time values (τ^{-1}) to the concentrations of reactive species were used:

$$\tau_{fast}^{-1} + \tau_{slow}^{-1} = k_1\left([XOH] + [ion\ species]\right) + k_{-1} + k_2 + k_{-2} \tag{17}$$

$$\tau_{fast}^{-1} \cdot \tau_{slow}^{-1} = k_1\left[k_2 + k_{-2}\right]\left([XOH] + [ion\ species]\right) + k_{-1}k_{-2} \tag{18}$$

where the ion species are $H_2AsO_4^-$ or $HCrO_4^-$. The derivation of these equations was obtained from Bernasconi[78] and is based on the two-step reaction system (A + B ↔ C ↔ D). If the mechanism portrayed in Figure 18 is accurate then a plot of $\tau_{fast}^{1} + \tau_{slow}^{-1}$ and $\tau_{fast}^{-1} \cdot \tau_{slow}^{-1}$ as a function of the concentration term ([XOH] + [ion species]) should be linear. Plots of Equations 17 and 18 were

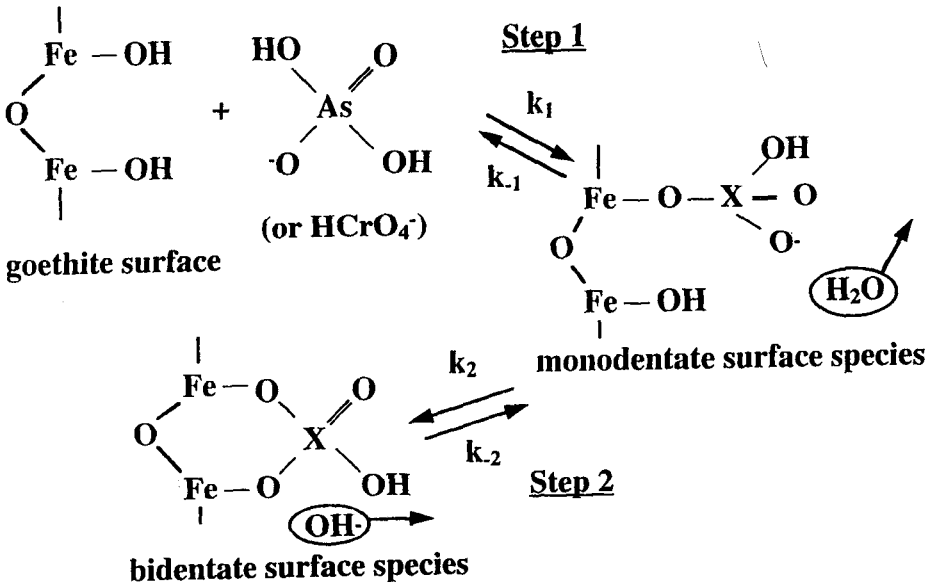

Figure 18 Proposed mechanism for oxyanion adsorption/desorption on goethite. The X represents either As(V) or Cr(VI). (From Grossl, P. R. et al., *Environ. Sci. Technol.*, 31, 321, 1997. With permission.)

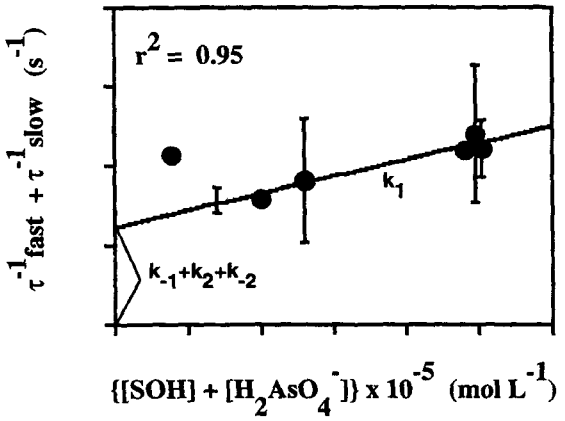

Figure 19 Evaluation of the linearized rate Equation 17 for the mechanism displayed in Figure 18 for arsenate. (From Grossl, P. R. et al., *Environ. Sci. Technol.*, 31, 321, 1997. With permission.)

linear for both arsenate and chromate, suggesting that the proposed mechanism was plausible. Figures 19 and 20 show the linear relationships for Equations 17 and 18, respectively, for arsenate.

From the plots in Figures 19 and 20 forward and reverse rate constants were obtained for the adsorption and desorption reactions of both the monodentate and bidentate steps, where k_1 = slope (Figure 19); k_{-1} = intercept (Figure 19) – slope (Figure 20)/slope (Figure 19); k_2 = intercept (Figure 19) – k_{-1} – k_{-2}; and k_{-2} = intercept (Figure 20)/k_{-1} . The calculated rate constants for both chromate and arsenate adsorption/desorption on goethite are listed in Table 3.

For both oxyanions, the rate constants for the reverse reactions (associated with the breaking of arsenate or chromate/goethite bonds) were lower than the rate constants for the forward reactions (formation of the inner-sphere oxyanion/goethite surface complexes). Therefore, the rate-limiting steps were the reverse reactions. The equilibrium constants listed in Table 3 were calculated using

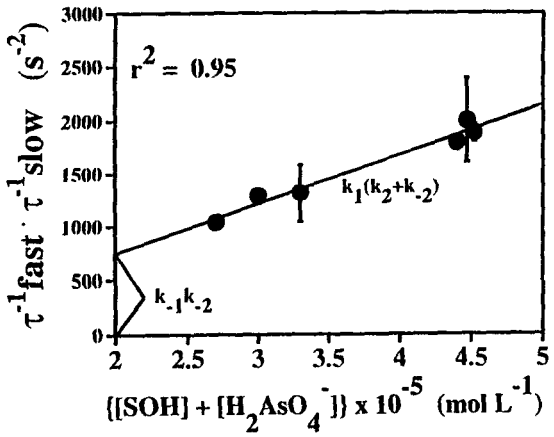

Figure 20 Evaluation of the linearized rate Equation 18 for the mechanism displayed in Figure 18 for arsenate. (From Grossl, P. R. et al., *Environ. Sci. Technol.*, 31, 321, 1997. With permission.)

Table 3 Calculated Rate Constants for Chromate and Arsenate Adsorption/Desorption on Goethite

	Step I	Step II
Arsenate	$k_1 = 10^{6.3}$ l/mol s	$k_2 = 15\ s^{-1}$
	$k_{-1} = 8\ s^{-1}$	$k_{-2} = 8\ s^{-1}$
	$K_{eq} = 10^{5.35}$ l/mol s	$K_{eq} = 10^{0.26}$
Chromate	$k_1 = 10^{5.8}$ l/mol s	$k_2 = 16\ s^{-1}$
	$k^{-1} = 129\ s^{-1}$	$k_{-2} = 38\ s^{-1}$
	$K_{eq} = 10^{3.7}$ l/mol s	$K_{eq} = 10^{-0.4}$

From Grossl, P.R. et al, *Environ. Sci. Technol.*, 31, 321, 1997. With permission.

the rate constants for each reaction step in our proposed mechanism (Figure 18) from the following relationship:

$$K_{eq} = k_f / k_r \tag{19}$$

The calculated equilibrium constant for step 1 for arsenate was $10^{5.35}$ and for step 2 was $10^{0.26}$, while the calculated K_{eq} for step 1 for chromate was $10^{3.7}$ and for step 2 was $10^{-0.4}$. The adsorption of both oxyanions and subsequent formation of inner-sphere surface complexes are thermodynamically favorable, with the exception of the equilibrium constant for the second step associated with chromate adsorption (slightly less than 1). Thus, the bidentate chromate/goethite surface complex is less likely to form than the monodentate surface complex. This is in agreement with spectroscopic data obtained from X-ray absorption fine structure (XAFS) analyses which indicate a mixture of both monodentate and bidentate chromate surface complexes, but at low surface coverage a greater proportion of chromate is associated with the monodentate complex than the bidentate complex. The results from both kinetic and XAFS experiments suggest that arsenate is more likely to form an inner-sphere surface complex with goethite than chromate.

While the initial sorption of heavy metals is rapid, with the chemical reaction step occurring on millisecond time scales, further sorption is usually quite slow (Figure 21) occurring over time scales of days and longer. This slow sorption has been ascribed to interparticle or intraparticle diffusion in pores, sites of low reactivity, and surface precipitation.[88-90] Examples from the literature of each hypothesis will be discussed. However, these hypotheses have primarily been based on

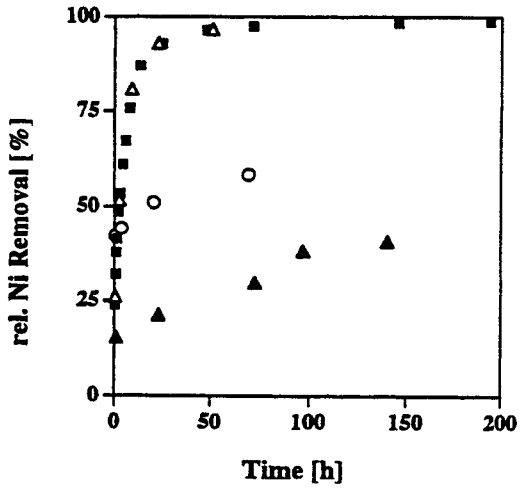

Figure 21 Kinetics of Ni sorption (%) on pyrophyllite (■), kaolinite (△), gibbsite (▲), and montmorillonite (○) from a 3 m*M* Ni solution at pH = 7.5 and an ionic strength I = 0.1 *M* ($NaNO_3$). (From Scheidegger, A. M. et al., *J. Colloid Interface Sci.*, 186, 118, 1997. With permission.)

macroscopic observations. To confirm the mechanism(s), *in situ* surface spectroscopic/microscopic techniques should be employed. These will be discussed later.

Obviously, an important factor affecting the degree of slow sorption of metals (and for that matter also of organic chemicals) is the time period the sorbate has been in contact with the sorbent (residence time). Bruemmer et al.[19] studied Ni^{2+}, Zn^{2+}, and Cd^{2+} adsorption on goethite, a porous Fe-oxide that has defect structures in which metals can be incorporated to satisfy charge imbalances. Bruemmer et al.[19] found at pH 6 that as reaction time increased from 2 h to 42 d (at 293 K), adsorbed Ni^{2+} increased from 12% to 70% of total adsorption, and total increases in Zn^{2+} and Cd^{2+} adsorption over this time increased 33% and 21%, respectively. The kinetic reactions could be well described using a Fickian diffusion model. Metal uptake was hypothesized to occur via a three-step mechanism: (1) adsorption of metals on external surfaces; (2) solid-state diffusion of metals from external to internal sites; and (3) metal binding and fixation at positions inside the goethite particle.

Fuller et al.[55] combined kinetic sorption and desorption experiments with spectroscopic observations[90] to study As sorption on ferrihydrite. Using X-ray absorption fine structure (XAFS) spectroscopy, they found that As was sorbed predominantly as inner-sphere bidentate complexes, regardless of whether the As was adsorbed postmineralization of the ferrihydrite, or it was present during precipitation. No As surface precipitates were observed. Slow As sorption and desorption were explained as slow diffusion of the As to or from interior surface complexation sites that exist within disordered aggregates of crystallites. The kinetic reactions could be described using a Fickian diffusion model.

Slow metal sorption has also been ascribed to conversion of the metal sorbate from a high-energy state to a low-energy state. For example, Lehmann and Harter[91] measured the kinetics of chelate-promoted Cu^{2+} release from a soil to assess the strength of the bond formed. Sorption/desorption was biphasic, which was attributed to high- and low-energy bonding sites. With increased residence time from 30 min to 24 h, Lehmann and Harter[91] speculated that there was a transition of Cu from low-energy sites to higher-energy sites (as evaluated by release kinetics). Incubations for up to 4 d showed a continued uptake of Cu and a decrease in the fraction released within the first 3 min, which was referred to as the low-energy adsorbed fraction.

Ainsworth et al.[92] studied the adsorption/desorption of Co^{2+}, Cd^{2+}, and Pb^{2b+} on hydrous ferric oxide (HFO) as a function of oxide aging and metal-oxide residence time. Oxide aging did not cause hysteresis of metal cation sorption-desorption. Aging the oxide with the metal cations resulted

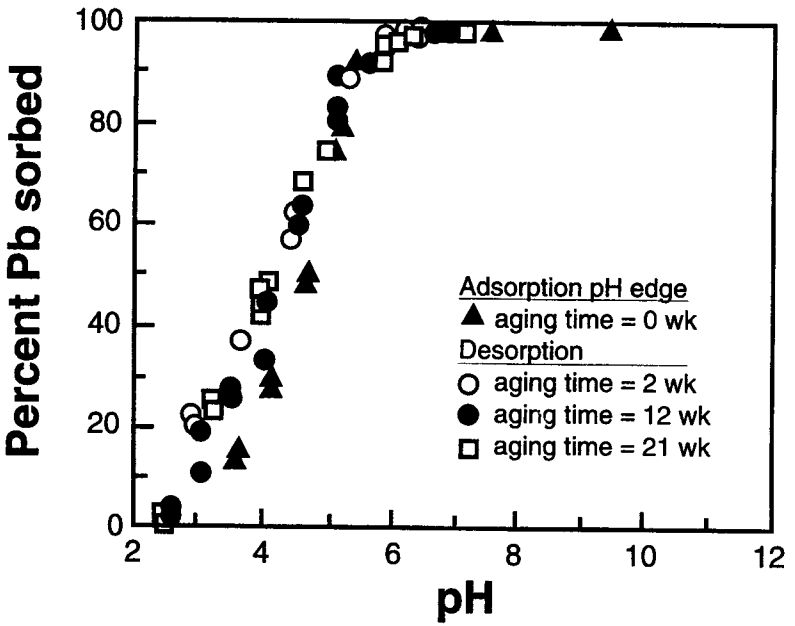

Figure 22 Fractional sorption-desorption of Pb^{2+} to hydrous Fe-oxide (HFO) as a function of pH and HFO-Pb^{2+} aging time. (From Ainsworth, C. C. et al., *Soil Sci. Soc. Am. J.*, 58, 1615, 1994. With permission.)

in hysteresis with Cd^{2+} and Co^{2+} but little hysteresis was observed with Pb^{2+}. With Pb^{2+}, between pH 3 and 5.5 there was slight hysteresis over a 21 week aging process (hysteresis varied from <2% difference between sorption and desorption to ≈10%). At pH 2.5 Pb^{2+} desorption was complete within a 16 h desorption period and was not affected by aging time (Figure 22). However, with Cd^{2+} and Co^{2+}, extensive hysteresis was observed over a 16 week aging period and the hysteresis increased with aging time (Figures 23 and 24). After 16 weeks of aging 20% of the Cd^{2+} and 53% of the Co^{2+} was not desorbed, and even at pH 2.5, hysteresis was observed. The extent of reversibility with aging for Co^{2+}, Cd^{2+}, and Pb^{2+} was inversely proportional to the ionic radius of the ions, i.e., $Co^{2+} < Cd^{2+} < Pb^{2+}$. Ainsworth et al.[92] attributed the hysteresis to Co and Cd incorporation into a recrystallizing solid (probably goethite) via isomorphic substitution and not to micropore diffusion.

Scheidegger et al.[93] investigated Ni sorption on pyrophyllite, kaolinite, gibbsite, and montmorillonite. Nickel sorption was characterized by a rapid reaction in which 15% to 40% of the initial Ni was removed within the first hour. Following the rapid reaction, the rate of sorption decreased significantly. Using XAFS, the slow sorption was directly ascribed to the formation of mixed Ni-Al hydroxides on the sorbents. The "surface" precipitates had a structure similar to a Ni-bearing mineral, tacovite ($Ni_6Al_2(OH)_{16}\,CO_3{\cdot}H_2O$). Scheidegger et al.,[93] hypothesized that the release of Al from the sorbents into solution was the rate-determining step for the formation of the mixed Ni/Al hydroxide-like phases.

2. *Organic Contaminants*

There have been a number of studies on the kinetics of organic chemical sorption/desorption with soils and soil components. Many of these investigations have shown that sorption/desorption is characterized by a rapid, reversible stage followed by a much slower, nonreversible stage[60,94-95] or biphasic kinetics. The rapid phase has been ascribed to retention of the organic chemical in a labile form that is easily desorbed. However, the much slower reaction phase involves the entrapment of the chemical in a nonlabile form that is difficult to desorb. This slower sorption/desorption

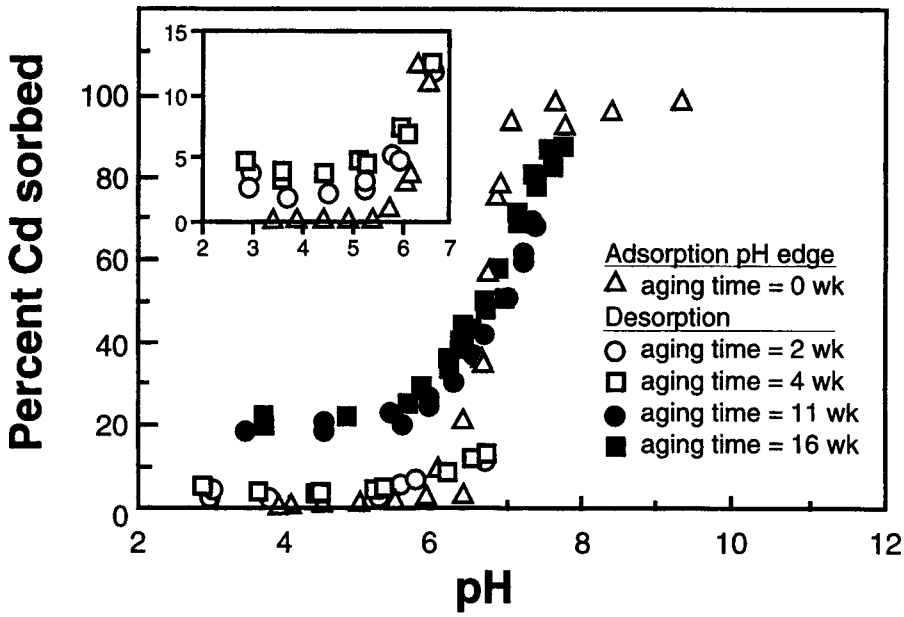

Figure 23 Fractional sorption-desorption of Cd^{2+} to hydrous Fe-oxide (HFO) as a function of pH and HFO-Cd^{2+} aging time; insert shows adsorption-desorption of Cd^{2+} to HFO at 2- and 4-week aging times. (From Ainsworth, C. C. et al., *Soil Sci. Soc. Am. J.*, 58, 1615, 1994. With permission.)

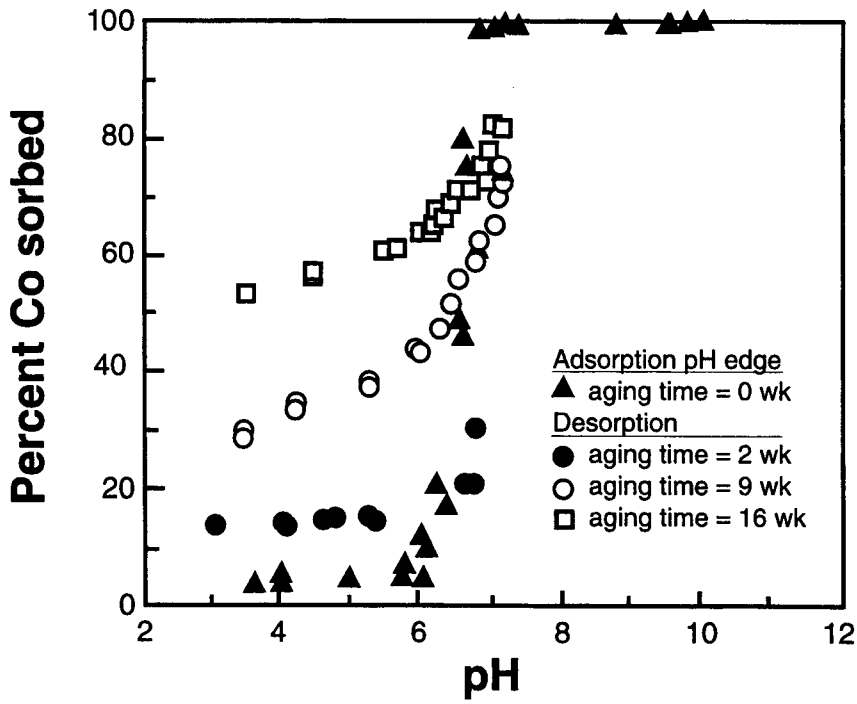

Figure 24 Fractional adsorption of Co^{2+} to hydrous Fe-oxide (HFO) as a function of pH and HFO-Co^{2+} aging time. (From Ainsworth, C. C. et al., *Soil Sci. Soc. Am. J.*, 58, 1615, 1994. With permission.)

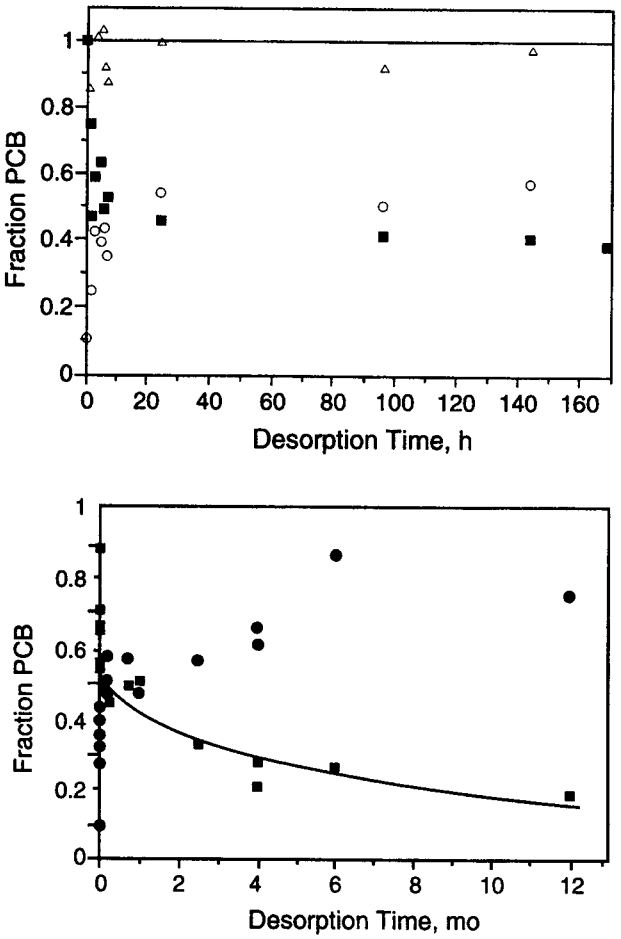

Figure 25 (a) Short-term polychlorinated biphenyl (PCB) desorption in hours (h) from Hudson River sediment contaminated with 25 mg kg^{-1} PCB. Distribution of the PCB between the sediment (■) and XAD-4 resin (○) is shown, as well as the overall mass balance (△). The resin acts as a sink to retain the PCB that is desorbed. (b) Long-term PCB desorption in months (mo) from Hudson River sediment contaminated with 25 mg kg^{-1} PCB. Distribution of the PCB between the sediment (■) and XAD-4 resin (●) is shown. The line represents a nonlinear regression of the data by a two-site model. (From Carroll, K. M. et al., *Environ. Sci. Technol.*, 28, 253, 1994. With permission.)

reaction has been ascribed to diffusion of the chemical into micropores of organic matter and inorganic soil components.[53,67-68] The labile form of the chemical is available for microbial attack while the nonlabile portion is resistant to biodegradation.

An example of the biphasic kinetics that is observed for many organic chemical reactions in soils/sediments is shown in Figure 25. In this study 55% of the labile polychlorinated biphenyls (PCBs) were desorbed from sediments in a 24-h period, while little of the remaining 45% nonlabile fraction was desorbed in 170 h (Figure 25a). Over another 1-year period about 50% of the remaining nonlabile fraction desorbed (Figure 25b).

In another study with volatile organic compounds (VOCs), Pavlostathis and Mathavan[97] observed a biphasic desorption process for field soils contaminated with trichloroethylene (TCE), tetrachloroethylene (PCE), toluene (TOL), and xylene (XYL). A fast desorption reaction occurred in 24 h, followed by a much slower desorption reaction beyond 24 h. In 24 h, 9% to 29%, 14% to 48%, 9% to 40%, and 4% to 37% of the TCE, PCE, TOL, and XYL, respectively, were released.

Table 4 Sorption Distribution Coefficients for Herbicides in "Freshly Aged" and "Aged" Soils

Herbicide	Soil	K_d[a]	K_{app}[b]
Metolachlor	CVa	2.96	39
	CVb	1.46	27
	W1	1.28	49
	W2	0.77	33
Atrazine	CVa	2.17	28
	CVb	1.32	29
	W3	1.75	4

[a] Sorption distribution coefficient (l kg^{-1}) of "freshly aged" soil based on a 24 h equilibration period.

[b] Apparent sorption distribution coefficient (l kg^{-1}) in contaminated soil ("aged" soil) determined using a 24 h equilibration period.

Adapted from Pignatello and Huang.[99]

A number of studies have also shown that with "aging" the nonlabile portion of the organic chemical in the soil/sediment becomes more resistant to release.[61,67,97-99] However, Connaughton et al.[51] did not observe the nonlabile fraction increasing with age for naphthalene contaminated soils.

One way to gauge the effect of time on organic contaminant retention in soils is to compare K_d (sorption distribution coefficient) values for "freshly aged" and "aged" soil samples. In most studies, K_d values are measured based on a 24-h equilibration between the soil and the organic chemical. When these values are compared to K_d values for field soils previously reacted with the organic chemical ("aged" samples) the latter have much higher K_d values, indicating that much more of the organic chemical is in a sorbed state. For example, Pignatello and Huang[99] measured K_d values in "freshly aged" (K_a) and "aged" soils (K_{app}, apparent sorption distribution coefficient) reacted with atrazine and metolachlor, two widely used herbicides. The "aged" soils had been treated with the herbicides 15 to 62 months before sampling. The K_{app} values ranged from 2.3 to 42 times higher than the K_d values (Table 4).

Scribner et al.,[98] studying simazine (a widely used triazine herbicide for broadleaf and grass control in crops) desorption and bioavailability in aged soils, found that K_{app} values were 15 times higher than K_d values. Scribner et al.[98] also showed that 48% of the simazine added to the freshly aged soils was biodegradable over a 34-d incubation period while none of the simazine in the aged soil was biodegraded.

One of the implications of these results is that while many transport and degradation models for organic contaminants in soils and waters assume that the sorption process is an equilibrium process, the above studies clearly show that kinetic reactions must be considered when making predictions about the mobility and fate of organic chemicals. Moreover, calculation of K_d values based on a 24-h equilibration period, which is commonly used in fate and risk assessment models, can be inaccurate, since 24-h K_d values often overestimate the amount of organic chemical in the solution phase.

The finding that many organic chemicals are quite persistent in the soil environment has both good and bad features. The beneficial aspect is that the organic chemicals are less mobile and may not be readily transported in groundwater supplies. The negative aspect is that their persistence and inaccessibility to microbes may make decontamination more difficult, particularly if *in situ* remediation techniques such as biodegradation are employed.

B. Kinetics of Mineral Dissolution

1. *Rate-Limiting Steps*

Dissolution of minerals involves several steps (Stumm and Wollast[100]): (1) mass transfer of dissolved reactants from the bulk solution to the mineral surface, (2) adsorption of solutes, (3) interlattice transfer

of reaction species, (4) surface chemical reactions (CR), (5) removal of reactants from the surface, and (6) mass transfer of products into the bulk solution. Under field conditions mineral dissolution is slow and mass transfer of reactants or products in the aqueous phase (steps 1 and 6) are not rate-limiting. Thus, the rate-limiting steps are either transport of reactants and products in the solid phase (step 3) or surface chemical reactions (step 4) and removal of reactants from the surface (step 5).

Transport-controlled dissolution reactions or those controlled by mass transfer or diffusion can be described using a parabolic rate law given below:[100]

$$r = \frac{dC}{dt} = kt^{-1/2} \tag{20}$$

where r is the reaction rate, C is the concentration in solution, t is time, and k is the reaction rate constant. Integrating, C increases with $t^{1/2}$,

$$C = C_0 + 2kt^{1/2} \tag{21}$$

where C_0 is the initial concentration in solution.

If the surface reactions are slow compared to the transport reactions, dissolution is surface-controlled which is the case for most dissolution reactions of silicates and oxides. In surface-controlled reactions the concentrations of solutes next to the surface are equal to the bulk solution concentrations and the dissolution kinetics are zero-order if steady-state conditions are operational on the surface. Thus, the dissolution rate, r is

$$r = \frac{dC}{dt} = kA \tag{22}$$

and r is proportional to the surface area, A, of the mineral. Thus, for a surface-controlled reaction the relationship between time and C should be linear. Figure 26 compares transport- and surface-controlled dissolution mechanisms.

Intense arguments have ensued over the years concerning the mechanism for mineral dissolution. Those who supported a transport-controlled mechanism believed that a leached layer formed as mineral dissolution proceeded and that subsequent dissolution took place via diffusion through the leached layer.[101] Advocates of this theory found that dissolution was described by the parabolic rate law (Equation 20). However, the "apparent" transport-controlled kinetics may be an artifact caused by dissolution of hyperfine particles, formed on the mineral surfaces after grinding that are highly reactive sites, or by use of batch methods that cause reaction products to accumulate causing precipitation of secondary minerals. These experimental artifacts can cause incongruent reactions and pseudoparabolic kinetics. Recent studies employing surface spectroscopies, such as X-ray photoelectron spectroscopy (XPS) and nuclear resonance profiling,[102,103] have demonstrated that although some incongruency may occur in the initial dissolution process, which may be diffusion-controlled, the overall reaction is surface-controlled. An illustration of the surface-controlled dissolution of γ-Al_2O_3 resulting in a linear release of Al^{3+} with time is shown in Figure 27. The dissolution rate, r, can be obtained from the slope of Figure 27.

2. Surface-Controlled Dissolution Mechanisms

Dissolution of oxide minerals via a surface-controlled reaction by ligand-promoted and proton-promoted processes has been described by Stumm and coworkers[104-106] using a surface coordination

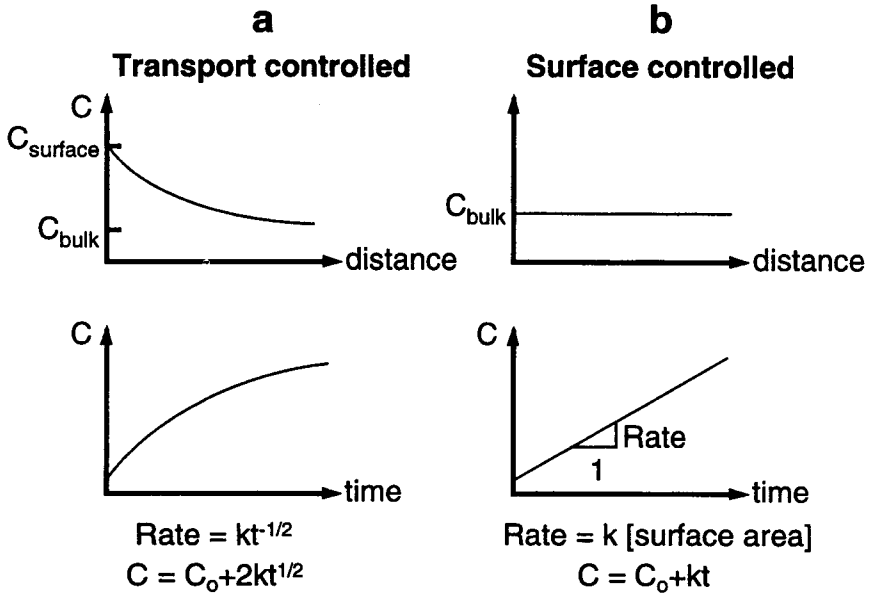

Figure 26 Transport vs. surface-controlled dissolution. Schematic representation of concentration in solution, C, as a function of distance from the surface of the dissolving mineral. In the lower part of the figure, the change in concentration is given as a function of time. From Stumm, W., *Chemistry of the Solid-Water Interface*, John Wiley & Sons, New York, 1992. With permission.)

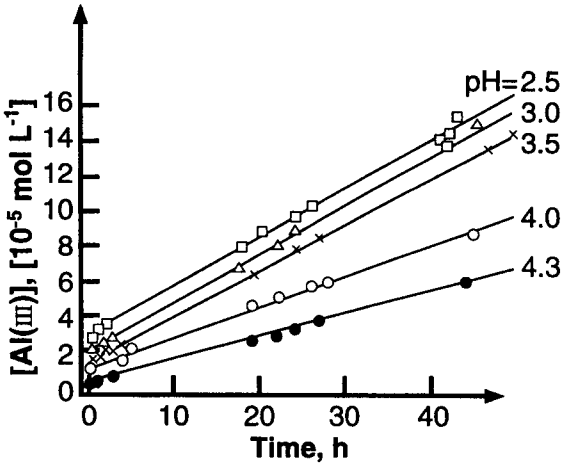

Figure 27 Linear dissolution kinetics observed for the dissolution of γ-Al_2O_3. Representative of processes whose rates are controlled by a surface reaction and not by transport. (From Furrer, G. and Stumm, W., *Geochim. Cosmochim. Acta*, 50, 1847, 1986. With permission.)

approach. The important reactants in these processes are H_2O, H^+, OH^-, ligands, and reductants and oxidants. The reaction mechanism occurs in two steps:[100]

$$\text{Surface sites} + \text{Reactants } (H^+, OH^-, \text{ or ligands}) \xrightarrow{\text{Fast}} \text{Surface species} \qquad (23)$$

$$\text{Surface sites} \xrightarrow[\text{detachment of metal (M)}]{\text{slow}} \text{M(aq)} \tag{24}$$

Thus, the attachment of the reactants to the surface sites is fast and detachment of metal species from the surface into solution is slow and rate-limiting.

3. Ligand-Promoted Dissolution

Figure 28 shows how the surface chemistry of the mineral affects dissolution. One sees that surface protonation of the surface ligand increases dissolution by polarizing interatomic bonds close to the central surface ions that promotes the release of a cation surface group into solution. Hydroxyls that bind to surface groups at higher pHs can ease the release of an anionic surface group into the solution phase.

Ligands that form surface complexes via ligand exchange with a surface hydroxyl add negative charge to the Lewis acid center coordination sphere, and lower the Lewis acid acidity. This polarizes the M-oxygen bonds causing detachment of the metal cation into the solution phase. Thus, inner-sphere surface complexation plays an important role in mineral dissolution. Ligands such as oxalate, salicylate, F^-, EDTA, and NTA increase dissolution but others, e.g., SO_4^{2-}, CrO_4^{2-} and benzoate inhibit dissolution. Phosphate and arsenate enhance dissolution at low pH and dissolution is inhibited at pH>4.[12]

The reason for these differences may be that bidentate species that are mononuclear promote dissolution while binuclear bidentate species inhibit dissolution. With binuclear bidentate complexes, more energy may be needed to remove two central atoms from the crystal structure. With phosphate and arsenate, at low pH mononuclear species are formed while at higher pH (around pH = 7) binuclear or trinuclear surface complexes form. Mononuclear bidentate complexes are formed with oxalate while binuclear bidentate complexes form with CrO_4^{2-}. Additionally, the electron donor properties of CrO_4^{2-} and oxalate are also different. With CrO_4^{2-} a high redox potential is maintained at the oxide surface which restricts reductive dissolution.[12,100]

Dissolution can also be inhibited by cations such as VO^{2+}, Cr(III), and Al(III) that block surface functional groups.

One can express the rate of the ligand-promoted dissolution, R_L, as

$$R_L = k_L'(\equiv ML) = k_L' \, C_L^s \tag{25}$$

where k_L' is the rate constant for ligand-promoted dissolution ($time^{-1}$), ≡ML is the metal-ligand complex, and C_L^s is the surface concentration of the ligand (mol m^{-2}). Figure 29 shows that Equation 25 adequately described ligand promoted dissolution of γ-Al_2O_3.

4. Proton-Promoted Dissolution

Under acid conditions, protons can promote mineral dissolution by binding to surface oxide ions, causing bonds to weaken. This is followed by detachment of metal species into solution. The proton-promoted dissolution rate, R_H, can be expressed as:[12]

$$R_H = k_H'\left(\equiv MOH_2^+\right)^j = k_H'\left(C_H^s\right)^j \tag{26}$$

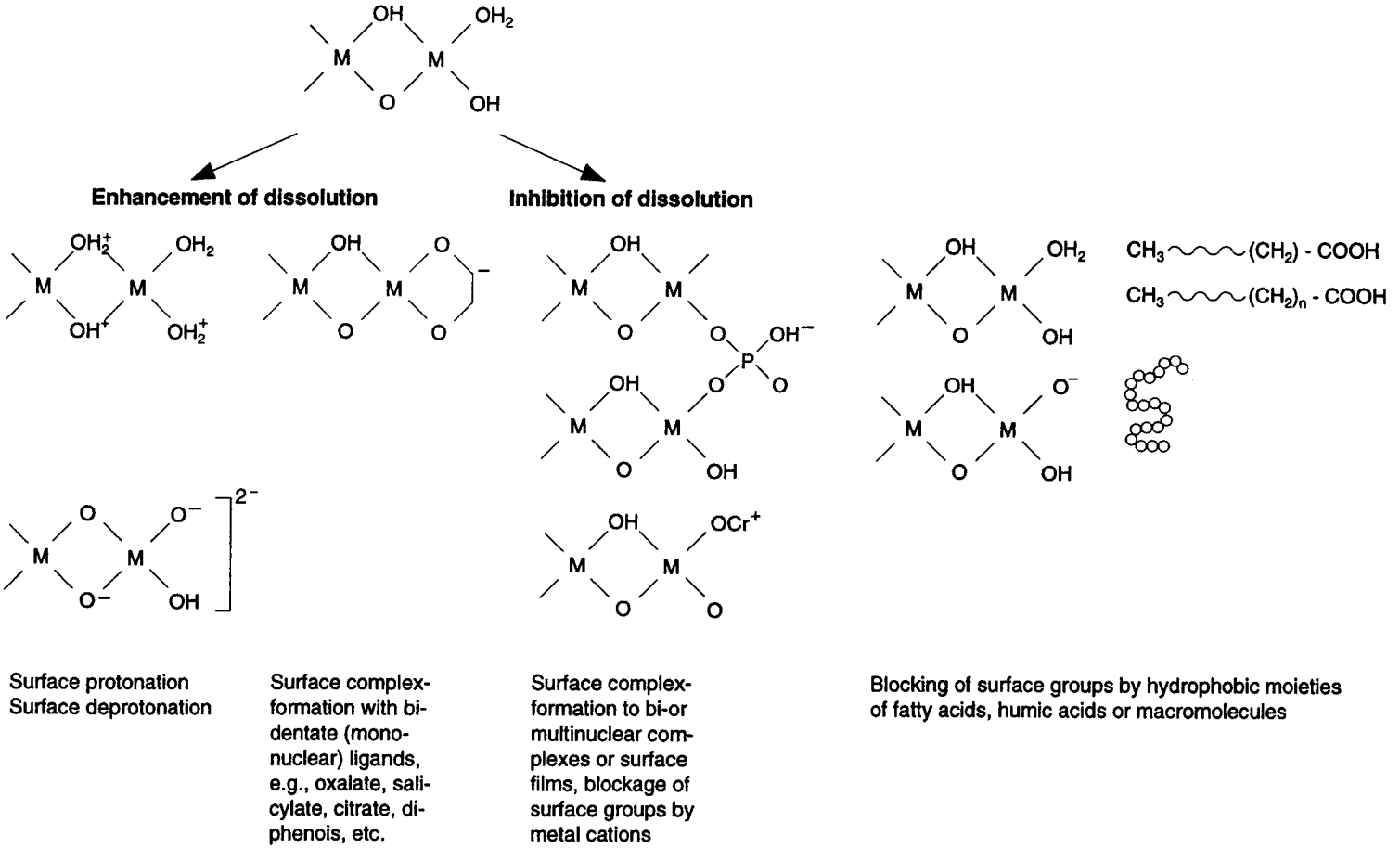

Figure 28 The dependence of surface reactivity and of kinetic mechanisms on the coordinative environment of the surface groups. (From Stumm, W. and Wollast, R., *Rev. Geophys.*, 28, 53, 1990. With permission.)

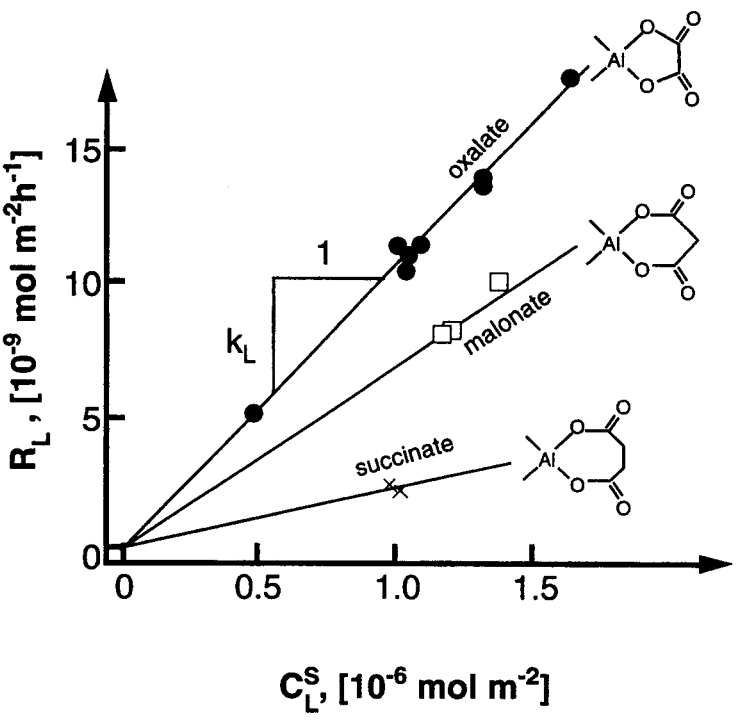

Figure 29 The rate of ligand-catalyzed dissolution of γ-Al_2O_3 by the aliphatic ligands oxalate, malonate, and succinate, R_L (nmol m^{-2} h^{-1}), can be interpreted as a linear dependence on the surface concentrations of the ligand complexes, C_L^S. In each case the individual values for C_L^S were determined experimentally. (From Furrer, G. and Stumm, W., *Geochim. Cosmochim. Acta*, 50, 1847, 1986. With permission.)

where k'_H is the rate constant for proton-promoted dissolution, $\equiv MOH_2^+$ is the metal-proton complex, C_H^s is the concentration of the surface adsorbed proton complex (mol^{-2}), and j corresponds to the oxidation state of the central metal ion in the oxide structure (i.e., j = 3 for Al(III) and Fe(III) in simples cases). If dissolution occurs by only one mechanism j is an integer. Figure 30 shows an application of Equation 26 for the proton-promoted dissolution of γ-Al_2O_3.

5. Overall Dissolution Mechanisms

The rate of mineral dissolution, which is the sum of the ligand-promoted, proton-promoted, and deprotonation-promoted (or bonding of OH^- ligands) dissociation ($R_{OH} = k_{OH}' (C_{OH}^s)^i$) rates along with the pH-independent portion of the dissolution rate (k'_{H_2O}) which is due to hydration, can be expressed as:[12]

$$R = +k'_L\left(C_L^s\right) + k'_H\left(C_H^s\right)^j + k'_{OH}\left(C_{OH}^s\right)^i + k'_{H_2O} \tag{27}$$

Equation 27 is valid if dissolution occurs in parallel at varying metal centers.[104]

6. Dissolution Kinetics of Polynuclear Surface Species

Recent studies using surface spectroscopic and microscopic techniques such as XAFS, electron paramagnetic resonance spectroscopy (EPR), X-ray photoelectron spectroscopy (XPS), auger electron

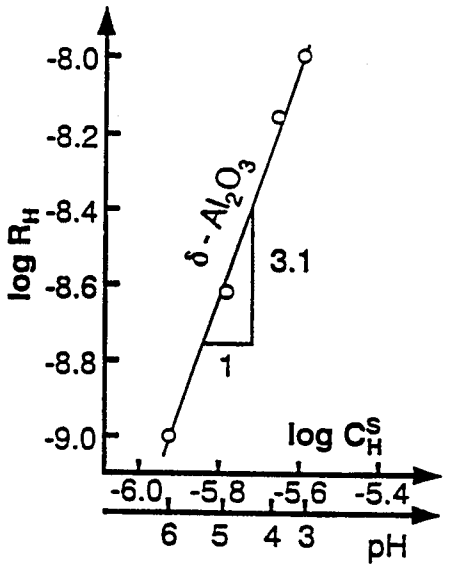

Figure 30 The dependence of the rate of proton-promoted dissolution of γ-Al_2O_3, R_H (mol m^{-2} h^{-1}), on the surface concentration of the proton complexes, C_H^s (mol m^{-2}). (From Furrer, G. and Stumm, W., *Geochim. Cosmochim. Acta*, 50, 1847, 1986. With permission.)

spectroscopy (AES), scanning electron microscopy (SEM), and atomic force microscopy (AFM) have shown that the formation of polynuclear surface species (e.g., surface precipitates) on natural materials is an important phenomenon.[107-111]

Multinuclear metal hydroxides of Pb, Ni, Co, Cu, and Cr(III) on oxides and aluminosilicates have been discerned.[93,108,110,112-121] Such surface precipitates have been observed at metal surface loadings far below a theoretical monolayer coverage, and in a pH range well below the pH where the formation of metal hydroxide precipitates would be expected according to the thermodynamic solubility product.

While metal surface precipitates could have important ramifications with respect to environmental quality (bioavailability, mobility, and fate of metals in soils and waters) via dissolution, little information is available in the literature on the dissolution kinetics of surface precipitates. Scheidegger and Sparks.[21] studied the dissolution of mixed Ni-Al polynuclear surface precipitates from pyrophyllite. Nickel detachment was slow and depended strongly on the pH and the experimental method (Figure 31). Under steady-state conditions, a constant Ni detachment rate was observed which was much slower than the dissolution of a crystalline $Ni(OH)_2$ reference compound.

The mixed Ni/Al hydroxide-like phases explain the finding of Scheidegger et al.[93] that the dissolution rates (Si-release) are strongly enhanced (relative to the dissolution rates of the clays alone) as long as Ni sorption is pronounced. This suggests that the surface complexes of Ni destabilize surface metal ions (Al and Si) relative to the bulk solution, and therefore lead to an enhanced dissolution of the clay. The association of Ni with Al could explain why the enhanced dissolution rate is only observable where Ni sorption is pronounced (Figure 32).

The structure of the mixed Ni-Al polynuclear surface precipitates is also not changed after extensive dissolution. EXAFS analysis shows that a tacovite-like structure remains after dissolution that is identical to the precipitate before commencement of dissolution.[21,93] It is obvious that metal surface precipitates must be carefully considered in metal surface complexation modeling, metal speciation, and risk assessments for the migration of contaminants in polluted sites.

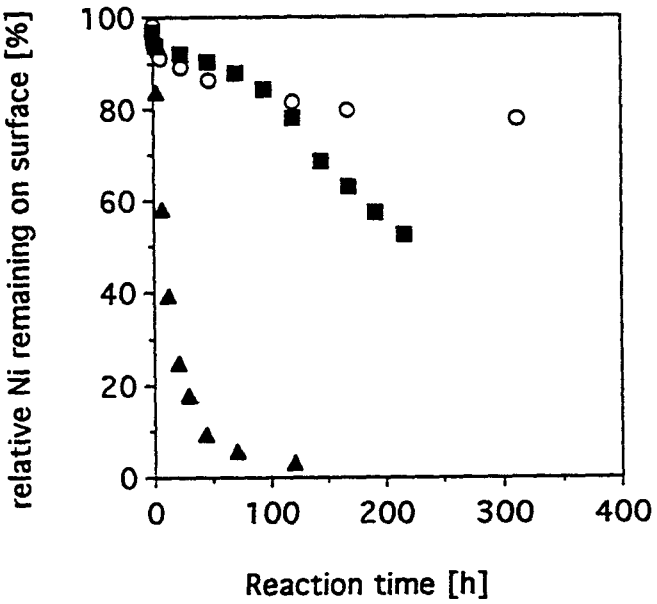

Figure 31 Kinetics of Ni detachment from surface precipitates at pH = 4. Relative Ni remaining on the surface (%) is shown for the *conventional method* (○) and the *replenishment method* (■) as a function of the reaction time; 98% of the initial Ni was sorbed in the beginning of the detachment experiment. The dissolution of an equivalent amount of crystalline $Ni(OH)_2$ (in mol) at pH = 4 is given for comparison (▲). (From Scheidegger, A. M. and Sparks, D. L., *Chem. Geol.*, 132, 157, 1996. With permission.)

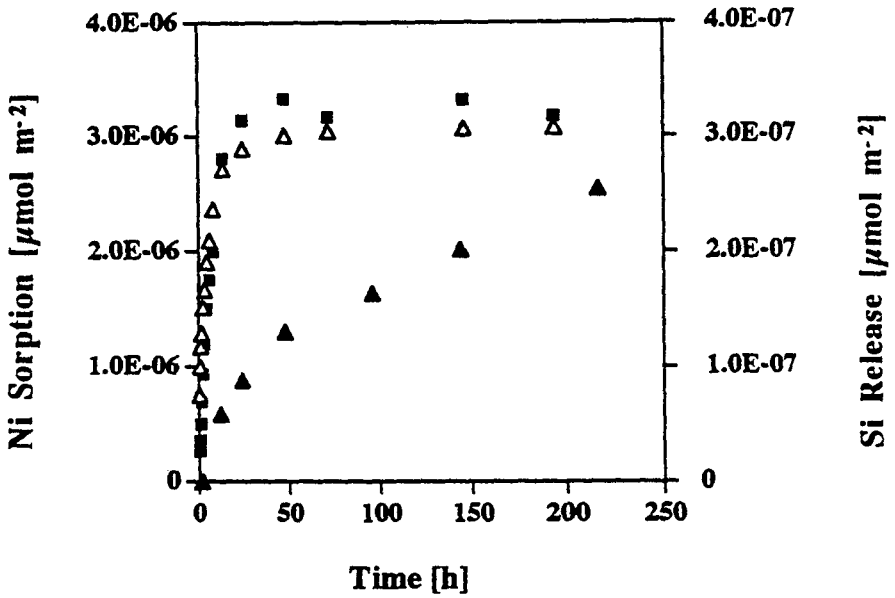

Figure 32 The kinetics of Ni sorption on pyrophyllite from a 3×10^{-3} *M* Ni solution at pH = 7.5. (■) denotes the amount of sorbed Ni (μmol m^{-2}) and (△) the amount of simultaneous dissolved Si (μmol m^{-2}). The dissolution of untreated pyrophyllite at pH = 7.5 is shown for comparison (▲). (From Scheidegger, A. M. et al., *J. Colloid Interface Sci.*, 186, 118, 1997. With permission.)

VII. CONFIRMATION OF REACTION MECHANISMS USING SPECTROSCOPIC AND MICROSCOPIC TECHNIQUES

In spite of many decades of intensive efforts by soil chemists to understand sorption processes, our understanding of the mechanisms of chemical reactions at the solid/liquid interface is still not definitive. One of the main reasons for this is that studies of the reactions between environmental particle surfaces and aqueous solutions have been limited to macroscopic studies, until quite recently. While macroscopic equilibrium studies and models reveal some important information about sorption/desorption phenomena, no mechanistic or molecular information is revealed. Kinetic studies can reveal something about reaction mechanisms at the soil particle/solution interface, particularly if energies of activation are calculated and stopped-flow or interruption techniques are employed. However, molecular and/or atomic resolution surface techniques should be employed to corroborate the proposed mechanism hypothesized from equilibrium and kinetic studies. These techniques can be used either separately or, preferably, simultaneously with kinetic investigations. While the latter approach is preferable, only limited studies have been reported in the literature. Examples of both approaches will be cited in the following discussions. Additionally, an overview will be presented of contemporary spectroscopic and microscopic techniques that are important for studying sorption processes on soils and soil minerals. Without question, the application of molecular and atomic resolution techniques to elucidation of sorption mechanisms should be a major research thrust in soil and environmental chemistry for decades to come.

There are two principal subdivisions in molecular spectroscopy: *in situ* and non-*in situ* methods.[23,122] The principal invasive non-*in situ* techniques used for soil and aquatic systems are XPS, AES, and secondary mass spectroscopy (SIMS). Each of these techniques yields detailed information about the structure and bonding of minerals, and the chemical species present on the mineral surfaces. The disadvantage of invasive techniques is that they often must be performed under adverse experimental conditions, e.g., desiccation, high vacuum, heating, or particle bombardment. Such conditions may yield data that are misleading as a result of experimental artifacts.[123,124] XPS is the most widely used non-*in situ* surface-sensitive technique. It has been used to study sorption mechanisms of inorganic cations and anions such as Cu^{2+}, Co^{2+}, Ni^{2+}, Cd^{2+}, Cr^{3+}, Fe^{3+}, selenite, and uranyl in soil and aquatic systems.[109,111,125-132]

In situ methods require little or no alteration of the sample from its natural state.[129] They can be applied to aqueous solutions or suspensions; most involve the input and detection of photons. Examples of *in situ* techniques are EPR, Fourier-transform infrared (FTIR), nuclear magnetic resonance (NMR), X-ray absorption (XAS), and Mössbauer spectroscopies. However, many other techniques are available.[23,133]

EPR spectroscopy is a technique for detecting paramagnetism. Electron paramagnetism occurs in all atoms, ions, organic free radicals and molecules with an odd number of electrons. EPR is based upon the resonant absorption of microwaves by paramagnetic substances and describes the interaction between an electronic spin subjected to the influence of a crystal field and an external magnetic field.[23,134] The method is applicable to transition metals of Fe^{3+}, Cu^{2+}, Mn^{2+}, V^{4+}, and molybdenum (V) and has been widely used to study metal ion sorption on soil mineral components[135-138] and soil organic matter.[139-144] Several review articles on EPR are available.[134,145-146]

The Mössbauer effect is based on the recoil-free emission and resonant absorption of γ rays by specific atomic nuclei in a solid. γ rays are used as a probe of nuclear energy levels which, in turn, are sensitive to the details of both local electron configuration and the electric and magnetic fields of the solid.[147] In natural systems, Mössbauer effects specifically relate to iron.[145] Mössbauer spectroscopy is able to distinguish between high spin Fe^{2+} and Fe^{3+} without interference from any other element.[23] It also provides information on the chemical nature of chemical entities bound to the iron. Application of Mössbauer spectroscopy in soil science is not common.[141,148-151] There are some review articles available on application of Mössbauer spectroscopy to soil materials.[145,147,152]

Application of infrared (IR) spectroscopy to the study of sorbed species has a long history. The introduction of Fourier transform techniques has made a significant contribution to the development of new investigation techniques such as diffuse reflectance infrared Fourier transform (DRIFT) and attenuated total reflectance (ATR) spectroscopy. IR spectroscopy now extends far beyond classical chemical analysis and is successfully applied to study sorption processes of inorganic and organic soil components. These techniques, and other vibrational spectroscopies such as Raman, are the subject of numerous reviews.[123,153-156]

The use of NMR spectroscopy to study surfaces has a shorter history, and fewer applications than vibrational spectroscopies. The primary reason is that the sensitivity of NMR is much lower than IR. Properties that might be exploited are the chemical shift, NMR relaxation times, and magnetic couplings to nuclei that are characteristic of a surface.[157] Most NMR studies in the field of soil science concentrate on the characterization of soil organic matter and soil humification processes and therefore involve ^{1}H, ^{13}C, and ^{15}N NMR. Reviews on these and related topics are available.[122,157-159] In the past few years ^{3}Li, ^{3}Na, ^{39}K, ^{111}Cd, and ^{133}Cs NMR spectroscopy have been increasingly used as tools to elucidate cation exchange sites on clay mineral surfaces.[160-163] Since it is virtually impossible to obtain any useful molecular information by observing the nucleus of a paramagnetic metal directly, studies of cation exchange have focused on diamagnetic metals, such as Cd^{2+}, which have a spin of 1/2 and an acceptable natural abundance (e.g., 12% and 13%, respectively, for the two NMR-active isotopes, ^{113}Cd and ^{111}Cd). NMR is essentially a bulk spectroscopic technique.[23] The advent of high-resolution, solid-state NMR techniques, such as magic angle sample spinning (MAS) and cross-polarization (CP), along with more sensitive, high-magnetic-field, user-friendly, pulsed NMR spectrometers, has brought increased applications to heterogeneous aqueous systems.[23,122] In particular, ^{27}Al and ^{29}Si NMR in zeolites and other minerals have proven valuable for the structural elucidation of samples whose disorder has prevented diffraction techniques from being very useful.[164-166]

One of the most powerful noninvasive surface sensitive techniques is XAS. XAS is a powerful, element-specific, *in situ* technique that can be used to determine the local structure (bond distance, number and type of nearest neighbors) around a sorbing element, even when the element is at low concentration levels (depending on element and matrix as low as 0.03% to 0.05% per weight[107]). XAS can be used to probe most types of phases (crystalline or amorphous solids, liquids, gases) and at structural sites ranging from those in crystals and glasses to those at interfaces, such as the mineral/water interface. Like other spectroscopic methods, XAS is not without limitations. It requires intense X-rays, and these are generated by electrons/positrons that circulate in a storage ring of a synchrotron facility at energies of 1 to 6 GeV in paths curved by a magnetic field. Synchrotron facilities are not readily accessible. In addition, in most cases studies are primarily limited to elements heavier than Sc.[23] There are several reviews on XAS that the reader can consult. Particularly relevant to soil science are those by Brown et al.,[167] Brown,[133] Charlet and Manceau,[107] Fendorf et al.,[124] and Schulze and Bertsch.[168]

By convention, XAS spectra (one scans near the X-ray absorption edge K, L, M of the element of concern) can be divided into two energy regions: (1) the X-ray absorption near edge structure (XANES) region and (2) the extended edge X-ray absorption structure (EXAFS) region. The XANES region runs to about 50 eV above the absorption edge.[168] It is usually characterized by intense resonance features arising from electron transitions to unoccupied bound state and continuum levels, and from multiple scattering of the emitted photoelectrons by atoms surrounding the absorber. For many first row transition elements the pre-edge resonances provide information on the site geometry of the absorber, which is commonly related to the oxidation state.[23] For example, Cr oxidation states can be deduced from the presence or absence of a predominant pre-edge feature that is characteristic of Cr(VI), which is tetrahedrally coordinated, but is nearly absent for Cr(III), which is octahedrally coordinated.[167-169] XANES was also used to determine oxidation states of Mn,[170-172] Se,[173] Ce,[174] Ti,[169] Tl,[175] and U[176] in natural environments. Although interatomic distances

can be deduced from the XANES region,[177-179] the main application of XANES is "fingerprinting". By comparison of known spectra with unknown samples important qualitative information on bonding environments can be deduced. This method has proven to be beneficial for investigating unknown heterogeneous samples such as soils.[180]

The EXAFS region which follows the XANES region in the XAS spectra runs up to about 800 eV beyond the edge.[107] The frequency oscillations in this region arise from constructive and destructive interference patterns between the outgoing and the returning photoelectronic wave that has been backscattered from first and sometimes second shell neighboring atoms. The frequency of the oscillations is inversely related to the bond distance between the absorber and neighboring atoms. The amplitude of these oscillations is related to both the identity and number of atoms surrounding the central absorber.[168] EXAFS has been applied to problems in physics, chemistry, biochemistry, and materials science for quite some time.[181] It is also well established in research on earth and marine material.[177,182,183] One of the earliest uses of EXAFS to determine sorption mechanisms of ions on natural surfaces was in the research of Hayes et al.[184] who studied selenate and selenite adsorption on goethite. They showed that selenate was absorbed as an outer-sphere complex and selenite was adsorbed as an inner-sphere complex.[184] This interpretation was later questioned by Manceau and Charlet,[185] who found that selenate ions form binuclear bidentate surface complexes on goethite. Recently, numerous studies have demonstrated the usefulness of EXAFS for providing specific chemical speciation information on contaminants associated with sorptive phases, including soils.[23]

While XAS provides local chemical information, it provides no information on spatial resolution of surface species. Such information can only be obtained by microscopic methods. Scanning electron microscopy (SEM) and transmission electron microscopy (TEM or HRTEM, high-resolution TEM) are well-established methods for acquiring both chemical and micromorphological data on soils and soil materials. TEM can provide spatial resolution of surface alterations and the amorphous nature or degree of crystallinity of sorbed species (ordering). It can also be combined with electron spectroscopies to determine elemental analysis.[23] In the last two decades several books and review articles on microcharacterization of soils using electron microscopy have been published. A partial list of these includes the books edited by Smart and Tovey,[186] Bullock and Murphy,[187] and Douglas,[188] as well as review articles by Whalley,[189] Bisdom et al.,[190] Tovey et al.,[191] and Chen.[192]

From the very inception of the scanning tunneling microscope (STM) in 1981 it was apparent that the technique would revolutionize the study of mineral surfaces and surface-related phenomena. Indeed, by the end of the 1980s, applications of STM were beginning to appear in the earth sciences literature.[193,194] However, the major event for the environmental science community came with the development of scanning force microscopy (SFM; also known as atomic force microscopy, AFM). SFM allows imaging of mineral surfaces in air or immersed in solution, and at subnanometer scale resolution.[195] Applications to date include determining the molecular to atomic scale structure of mineral surfaces,[196,197] probing forces at the mineral/water interface,[198,199] visualizing sorption of hemimicelles and macromolecular organic substances such as humic and fulvic acid,[195,200] determining clay particle thicknesses and morphology of clay-sized particles,[201-205] imaging soil bacteria,[206] and measuring directly the kinetics of growth, dissolution, heterogeneous nucleation, and redox processes (see later discussion).

Nevertheless, one must realize that SFM imaging of soil samples presents a challenge for the microscopist because natural samples tend to be heterogeneous. SFM does not provide chemical data; hence, minerals must be identified primarily based on morphology. Yet, morphology alone can lead to ambiguous results. Even atomic-scale imaging may not be conclusive because the crystal structures of many soil minerals are similar.[23] To work with soil samples, Maurice[195] suggested the following approach: (1) it is essential to compile as many images as possible of well-characterized minerals to use as a catalog for particle identification, (2) the soil samples should be characterized as fully as possible by XRD and other chemical and physical analytical techniques, and (3)

techniques for isolating different components and fractions can greatly simplify image interpretation. Several review articles on SFM are available; particularly relevant to soil scientists are those by Hochella,[207] Vempati and Cocke,[208] and Maurice.[195]

VIII. USE OF KINETIC AND SPECTROSCOPIC APPROACHES TO ELUCIDATE SORPTION MECHANISMS

An ideal way to confirm sorption/desorption mechanisms is to combine kinetic investigations with surface spectroscopic/microscopic experiments. There are a few examples in the literature of studies where mechanisms of metal sorption reactions on soil components have been hypothesized via kinetic experiments and verified in separate spectroscopic investigations.[55,85,90,93,209] An example of this approach can be found in the recent research of Fuller et al.[55] and Waychunas et al.,[90] who studied the kinetics and mechanisms of As(V) sorption on ferrihydrite. Adsorption was investigated during coprecipitation, in which As(V) was present in solution during the hydrolysis and precipitation of Fe, and after coprecipitation (postsynthesis adsorption). In the postsynthesis adsorption studies, As(V) uptake was initially rapid and then slowly increased for up to 8 d. The rapid uptake was ascribed to adsorption on surface sites near the outside of aggregates, while the slower adsorption was attributed to diffusion of As(V) to adsorption sites on ferrihydrite surfaces within aggregates of colloidal particles. The latter were caused by coagulation and crystallite growth processes. These processes resulted in a decrease in the number of adsorption sites, and as aggregates formed, adsorption sites were buried in large clusters of the particles.[55] In the coprecipitation studies, initial As(V) uptake was much greater than observed for the postsynthesis adsorption studies, and the uptake rate was not diffusion controlled as As(V) was coordinated by surface sites before crystallite growth.

The mechanistic hypotheses, based on the kinetic studies, were verified with companion EXAFS studies.[90] Analyses of the EXAFS data provided no evidence for surface precipitation, one possible mechanism that has been proposed for slow metal sorption processes. Arsenate retention in both the coprecipitation and postsynthesis adsorption studies involved primarily inner-sphere bidentate and monodentate binding on sites initially adsorbing arsenate. Waychunas et al.[90] hypothesized that these defect sites probably adsorb As(V) as a bidentate complex first, and then sorb as a monodentate complex. Monodentate complexes accounted for about 30% of all As-Fe correlations and occurred at only low As loading levels.

Scheidegger et al.[210] studied the kinetics of Ni surface precipitate formation on clay minerals and gibbsite using XAFS. Reaction times of minutes to months were investigated. Figure 33 shows the formation of multinuclear Ni complexes on pyrophyllite (pH = 7.5) within minutes. There was a small peak at $R \approx 2.8$ Å in the radial structure function (RSF) of pyrophyllite treated with Ni for 15 min (Figure 33f). This peak represented the second Ni shell and reflected backscattering among multinuclear Ni complexes. The presence of multinuclear surface complexes after a sorption time of only 15 min (28% of the initial Ni sorbed) is a surprising finding. Traditionally, adsorption (strictly a two-dimensional process) is considered to be the predominant sorption mode responsible for metal uptake on mineral surfaces within the first few hours,[28] while surface precipitation is considered to be a much slower process occurring on time scales of hours to days.[211]

As reaction time progressed (15 min to 24 h) and relative Ni removal in solution increased from 28% to 97% the peak at $R \approx 2.8$ Å in the RSFs increased in intensity (Figure 33b, c, d, and e). As time increased from 15 min to 3 months, the number of Ni second-neighbor (N) atoms at a distance of 2.99 to 3.03 Å increased from N = 1.4 to 4.5. These findings indicate the formation of surface precipitates that increase in size with progressing reaction time. Moreover, adsorption and the onset of surface precipitation can occur simultaneously.

Ideally, one would prefer to study sorption reaction mechanisms by following reaction rates spectroscopically (time-resolved or real-time studies) using *in situ* approaches. Such studies are

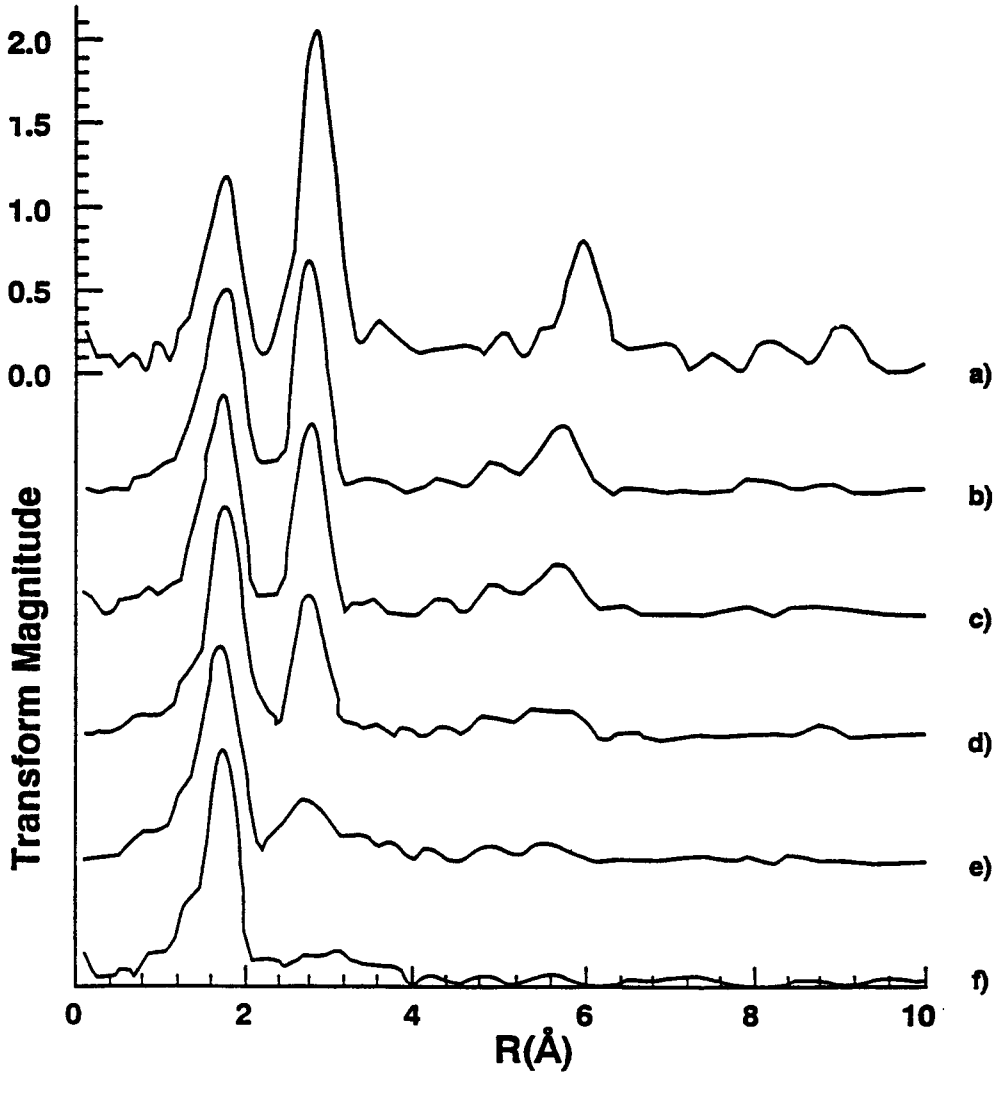

Figure 33 Radial structure functions (RSFs) of pyrophyllite samples reacted with Ni for (a) 3 months, (b) 24 h, (c) 12 h, (d) 3 h, (e) 75 min, and (f) 15 min. The spectra are uncorrected for phase shift. Note the appearance of a peak at R of about 2.8 Å with increasing reaction time. (From Scheidegger, A. M. et al., *J. Phys. IV,* 7, C2-773, 1997. With permission.)

scarce in the literature. The quick EXAFS technique, abbreviated (QEXAFS), depends on a constant monochromator scan rate and fast array defectors to obtain a full EXAFS spectrum in a fraction of a second, compared to tens of minutes in a traditional EXAFS method. Thus, milli- or micro-second time scales can be spectroscopically monitored.[168,212-214] Such studies would be very useful for many soil particle/solution reactions that are rapid. Energy dispersive EXAFS, abbreviated (DEXAS), can also be used to determine a full EXAFS spectrum in a fraction of a second.[215] However, detection can only be determined in the transmission mode.

A recent example of time-resolved *in situ* spectroscopic analyses is the research of Hunter and Bertsch.[216] They employed attenuated total reflectance Fourier transform infrared spectroscopy (ATR-FTIR) to quantitatively measure the degradation kinetics of tetraphenylboron (TPB) on clay minerals. The mechanisms of degradation were ascribed to surface-facilitated oxidation at Lewis acid and Brönsted acid sites. First-order models, based on these mechanisms, described the time-dependent data quite well.

Table 5 Studies on the Kinetics of Mineral Reactions Using Scanning Force Microscopy (SFM)

Dove et al.[222]	Calcite precipitation
Hellman et al.[223]	Albite dissolution
Hillner et al.[224,225]	Calcite growth and dissolution
Johnsson et al.[226]	Muscovite dissolution
Dove and Hochella[217]	Calcite precipitation mechanisms and inhibition by orthophosphate
Gratz and Hillner[218]	Step dynamics and spiral growth on calcite
Bosbach and Rammensee[219]	Gypsum growth and dissolution
Junta and Hochella[109]	Mn(II) oxidation on hematite, goethite, and albite
Stipp et al.[220]	Calcite surface structure
Maurice et al.[205]	Dissolution of hematite in organic acids
Fendorf et al.[221]	Precipitation kinetics of chromium hydroxide on goethite and silica

Note: Studies are listed in chronological order.

IX. USE OF KINETIC AND MICROSCOPIC APPROACHES

Scanning force microscopy (SFM) has been used increasingly as an *in situ* technique for imaging mineral surfaces immersed in aqueous solution, over the course of dissolution, precipitation, and heterogeneous nucleation reactions.[109,205,217-221] SFM permits a direct measure of surface-controlled growth and dissolution rates by providing three-dimensional data on changes in microtopography. *In situ* SFM has the perhaps unique ability to detect separate processes, such as dissolution and secondary phase formation, occurring simultaneously on a mineral surface.[195] Some of the studies in which SFM have been used to study the kinetics of mineral reactions are reported in Table 5.

Recently, Fendorf et al.[221] studied the kinetics of Cr(III) sorption reactions on single goethite and silica particles using a flow-cell mounted in a SFM. This procedure enabled one to study the reactions *in situ* and to react the surface while imaging (real-time measurements). Figure 34a shows an image of the unreacted silica in an aqueous environment. The surface is mostly flat and smooth with no island outcroppings. One hour after a 1 m*M* Cr(III) solution at pH 6 was introduced into the flow cell one sees that the surface morphology of silica has changed dramatically (Figure 34b). Surface clusters have formed on the surface and within 2 h (figure not shown) the clusters have expanded in width and girth. The precipitates form as discrete surface clusters on the silica surface rather than distributing across the surface.[221]

X. CONCLUSIONS AND FUTURE RESEARCH NEEDS

Research on the kinetics and mechanisms of sorption/release reactions at the soil particle-solution interface will be a common theme in soil and environmental sciences for decades to come. This research emphasis is in large part due to the need to more accurately control the long-term fate and transport of contaminants in the subsurface environment. Without such data, economically sound decisions about soil remediation cannot be made and risk assessment models are not complete. For further advancement to occur in the area of sorption/desorption the following research is needed: long-term sorption/desorption rate studies, a better understanding of residence time effects on nutrient, radionuclide, metal, and organic retention/release mechanisms on soils and other natural materials, and increased use of time-resolved, *in situ* spectroscopic and microscopic techniques to confirm sorption/desorption reaction mechanisms.

In just the last decade major advances in surface spectroscopic and microscopic techniques have greatly enhanced one's ability to study sorption phenomena at the solid/solution interface. One of the most important findings is the direct verification that the chemical properties of natural interfaces are highly heterogeneous.[23,227] The microtopography of the natural mineral/water interface is invariably complex (microtopography includes surface features on atomic and molecular scales

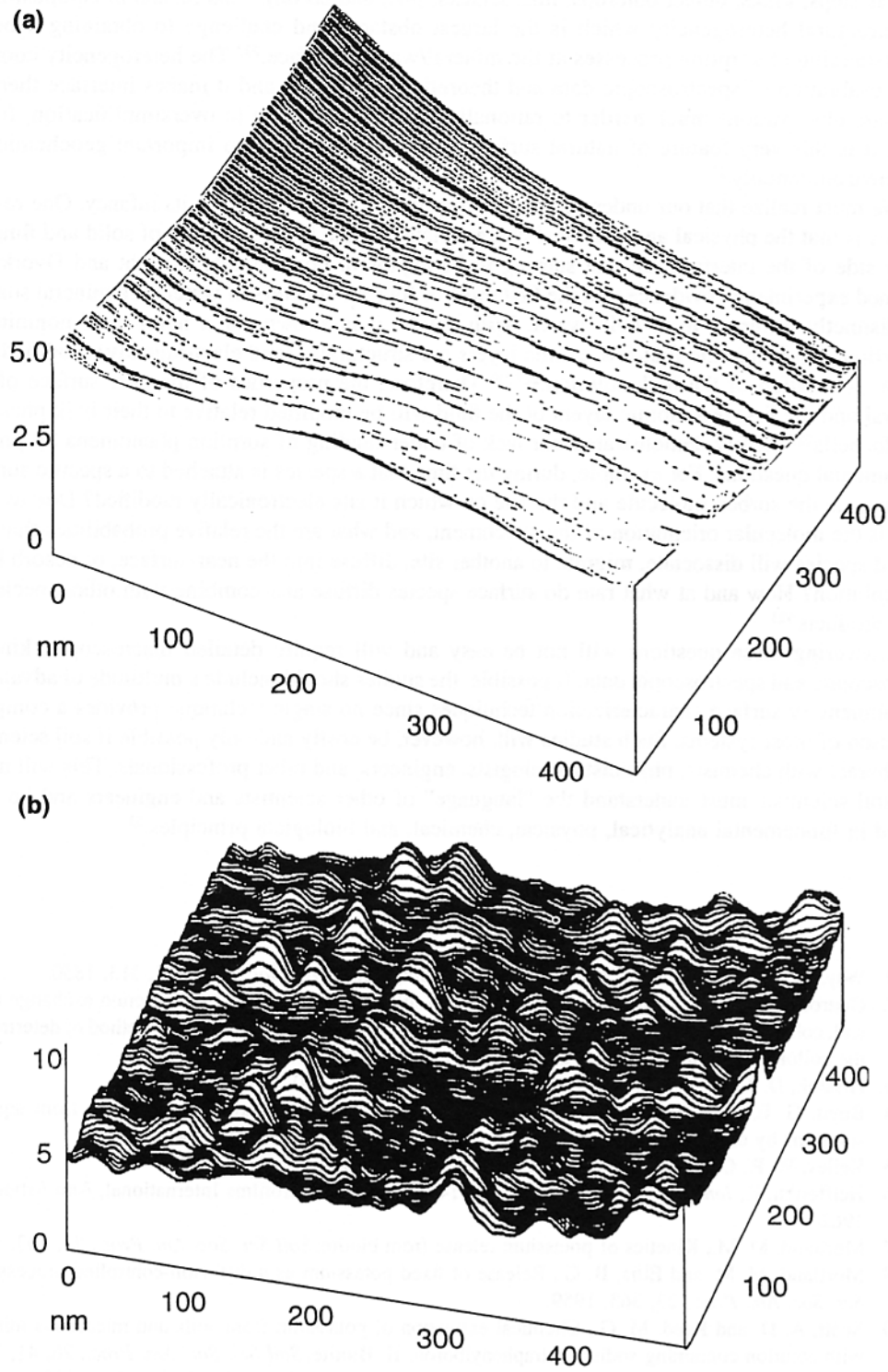

Figure 34 Using a flow cell, a single particle of silica was imaged in an aqueous environment. The unreacted silica (a) is relatively flat and smooth over the 500 × 500 nm scan region; no pronounced outcroppings from the surface are observed. After reacting with 1 m*M* Cr(III) for 1 h at pH 6.0 (b) a different surface morphology is apparent: distinct surface clusters have formed which protrude away from the silica surface. (From Fendorf, S. E. et al., *Soil Sci. Soc. Am. J.*, 60, 99, 1996. With permission.)

such as steps, kinks, defect outcrops, microcracks, pits, and so on). This results in compositional and structural heterogeneity which is the largest obstacle and challenge to obtaining a better understanding of sorption processes at the mineral/water interface.[227] The heterogeneity complicates evaluation of spectroscopic data and theoretical modeling, and it makes interface thermodynamic observations much harder to rationalize without resorting to oversimplification. Ironically, it is this very feature of natural surfaces which makes them so important geochemically and environmentally.[23]

We must realize that our understanding of sorption processes is still in its infancy. One reason for this is that the physical and chemical characteristics of the first few layers of solid and fluid on either side of the interface are just starting to be explored. For example, Knight and Dvorkin[228] obtained experimental evidence that the first three or four monolayers of water on a mineral surface are distinctly different from bulk water. With solids, it is known for a number of nonmineral crystalline solids that the first few atomic layers are structurally (and electronically) modified due to the termination of the bulk solution.[229,230] Therefore, the properties of the near surface of the mineral and the first few atomic layers of the fluid will be modified relative to their bulk phases.[23]

Hochella[227] clearly demonstrated our lack of understanding of sorption phenomena by posing fundamental questions. For example, during the time that a species is attached to a specific surface site, how is the sorbed molecule and the site on which it sits electronically modified? Due to this, what is the molecular orientation of the attachment, and what are the relative probabilities that this sorbed species will dissociate, migrate to another site, diffuse into the near-surface, or desorb back into solution? How and at what rate do surface species diffuse and combine with other species to form products?[23]

Answering these questions will not be easy and will require detailed macroscopic, kinetic, microscopic, and spectroscopic data. If possible, the studies should include a multitude of advanced, complimentary surface characterization techniques since no single technique provides a complete depiction of most systems. Such studies will, however, be costly and only possible if soil scientists collaborate with chemists, physicists, biologists, engineers, and other professionals. This will mean that soil scientists must understand the "language" of other scientists and engineers and be well versed in fundamental analytical, physical, chemical, and biological principles.[23]

REFERENCES

1. Way, J. T., On the power of soils to absorb manure, *J. R. Agric. Soc. Engl.*, 11, 313, 1850.
2. Gedroiz, K. K., Colloidal chemistry as related to soil science. II. Rapidity of reaction exchange in the soil, colloidal condition of the soil saturated with various bases and the indicator method of determining the colloidal content of the soil, *Zh. Opytn. Agron.*, 15, 181, 1914.
3. Hissink, D. J., Base exchange in soils, *Trans. Faraday Soc.*, 20, 551, 1924.
4. Boyd, G. E., Adamson, A. W., Meyers, L. S., Jr., The exchange adsorption of ions from aqueous solutions by organic zeolites. II. Kinetics. *J. Am. Chem. Soc.*, 69, 2836, 1947.
5. Kelley, W. P., Cation exchange in soils, in *ACS Monogr.* 1948.
6. Helfferich, F., *Ion Exchange,* Vol. No. 2003414, University Microfilms International, Ann Arbor, MI, 1962.
7. Mortland, M. M., Kinetics of potassium release from biotite, *Soil Sci. Soc. Am. Proc.*, 22, 503, 1958.
8. Mortland, M. M. and Ellis, B. G., Release of fixed potassium as a diffusion-controlled process, *Soil Sci. Soc. Am. Proc.*, 23, 363, 1959.
9. Scott, A. D. and Reed, M. G., Chemical extraction of potassium from soils and micaceous minerals with solution containing sodium tetraphenylboron. II. Biotite, *Soil Sci. Soc. Am. Proc.*, 26, 41, 1962.
10. Sparks, D. L., *Kinetics of Soil Chemical Processes*, Academic Press, San Diego, CA, 1989.
11. Amacher, M. C., Methods of obtaining and analyzing kinetic data, in *Rates of Soil Chemical Processes,* SSSA Spec. Publ. No. 27, Sparks, D. L. and Suarez, D. L., Eds., Soil Science Society of America, Madison, WI, 1991, 19.

12. Stumm, W., *Chemistry of the Solid-Water Interface*, John Wiley & Sons, New York, 1992.
13. Schwarzenbach, R. T., Gschwend, P. M., and Boden, D. M., *Environmental Organic Chemistry*, John Wiley & Sons, New York, 1993.
14. Sposito, G., *Chemical Equilibria and Kinetics in Soils*, John Wiley & Sons, New York, 1994.
15. Zhang, P. C. and Sparks, D. L., Kinetics and mechanisms of molybdate adsorption/desorption at the goethite/water interface using pressure-jump relaxation, *Soil Sci. Soc. Am. J.*, 53, 1028, 1989.
16. Zhang, P. C. and Sparks, D. L., Kinetics and mechanisms of sulfate adsorption/desorption on goethite using pressure-jump relaxation, *Soil Sci. Soc. Am. J.*, 54, 1266, 1990.
17. Zhang, P. C. and Sparks D. L., Kinetics of selenate and selenite adsorption/desorption at the goethite/water interface, *Environ. Sci. Technol.*, 24, 1848, 1990.
18. Bunzl, K., Schmidt, W., and Sansoni, B., Kinetics of ion exchange in soil organic matter. IV. Adsorption and desorption of Pb^{2+}, CU^{2+}, ZN^{2+}, and CA^{2+} by peat, *J. Soil Sci.*, 27, 32, 1976.
19. Bruemmer, G. W., Gerth, J., and Tiller, K. G., Reaction kinetics of the adsorption and desorption of nickel, zinc and cadmium by goethite. I. Adsorption and diffusion of metals, *J. Soil Sci.*, 39, 37, 1988.
20. Lövgren, L., Sjöberg, S., and Schindler, P. W., Acid/base reactions and Al(III) complexation at the surface of goethite, *Geochim. Cosmochim. Acta*, 54, 1301, 1990.
21. Scheidegger, A. M. and Sparks, D. L., Kinetics of the formation and the dissolution of nickel surface precipitates on pyrohyllite, *Chem. Geol.*, 132, 157, 1996.
22. Jardine, P. M. and Sparks, D. L., Potassium-calcium exchange in a multireactive soil system. I. Kinetics, *Soil Sci. Soc. Am. J.*, 48, 39, 1984.
23. Scheidegger, A. M., and Sparks, D. L., A critical assessment of sorption-desorption mechanisms at the soil mineral/water interface, *Soil Sci.*, 161, 813, 1996.
24. Comans, R. N. J. and Hockley, D. E., Kinetics of cesium sorption on illite, *Geochim. Cosmochim. Acta*, 56, 1157, 1992.
25. Gardiner, W. C., Jr., *Rates and Mechanisms of Chemical Reactions*, Benjamin, New York, 1969.
26. Skopp, J., Analysis of time dependent chemical processes in soils, *J. Environ. Qual.*, 15, 205, 1986.
27. Aharoni, C. and Sparks, D. L., Kinetics of soil chemical reactions: A theoretical treatment, in *Rates of Soil Chemical Processes*, SSSA Spec. Publ. No. 27, Sparks, D. L. and Suarez, D. L, Eds., Soil Science Society of America, Madison, WI, 1991, 1.
28. Sparks. D. L., *Environmental Soil Chemistry*, Academic Press, San Diego, 1995.
29. Bunnett, J. F., Kinetics in solution, in *Investigations of Rates and Mechanisms of Reactions*, Bernasconi, C. F., Ed., John Wiley & Sons, New York, 1986, 171.
30. Hachiya, K., Sasaki, M., Ikeda, I., Mikami, N., and Yasunaga, T., Static and kinetic studies of adsorption-desorption of metal ions on a γ-Al_2O_3 surface. II. Kinetic studies by means of pressure-jump technique, *J. Phys. Chem.*, 88, 27, 1984.
31. Tang, L. and Sparks, D L., Cation exchange kinetics on montmorillonite using pressure-jump relaxation, *Soil Sci. Soc. Am. J.*, 57, 42, 1993.
32. Fendorf, S. E., Sparks, D. L., Franz, J. A., and Camaioni, D. M., Electron paramagnetic resonance stopped-flow kinetic study of manganese (II) sorption-desorption on birnessite, *Soil Sci. Soc. Am. J.*, 57, 57, 1993.
33. Sparks, D. L., Fendorf, S. E., Zhang, P. C., and Tang, L., Kinetics and mechanisms of environmentally important reactions on soil colloidal surfaces, in *Migration and Fate of Pollutants in Soils and Subsoils*, Petruzzelli, D. and Helfferich, F. G., Eds., Springer-Verlag, Berlin, 1993, 141.
34. Low. M. J. D., Kinetics of chemisorption of gases on solids, *Chem. Rev.*, 60, 267, 1960.
35. Chien, S. H. and Clayton, W. R., Application of Elovich equation to the kinetics of phosphate release and sorption in soils, *Soil Sci. Soc. Am. J.*, 44, 265, 1980.
36. Sharpley, A. N., Effect of soil properties on the kinetics of phosphorus desorption, *Soil Sci. Soc. Am. J.*, 47, 462, 1983.
37. Atkinson, R. J., Hingston, F. J., Posner, A. M., and Quirk, J. P., Elovich equation for the kinetics of isotope exchange reactions at solid-liquid interfaces, *Nature (London)*, 226, 148, 1970.
38. Crank, J., *The Mathematics of Diffusion*, 2nd ed., Oxford University Press (Clarendon), London, 1976.
39. Chute, J. H. and Quirk, J. P., Diffusion of potassium from mica-like materials, *Nature (London)*, 213, 1156, 1967.
40. Wollast, R., Kinetics of the alteration of K-feldspar in buffered solutions at low temperature, *Geochim. Cosmochim. Acta*, 31, 635, 1967.

41. Weber, W. J., Jr. and Gould, J. P., Sorption of organic pesticides from aqueous solution, *Adv. Chem. Ser.*, 60, 280, 1966.
42. Kuo, S. and Lotse, E. G., Kinetics of phosphate adsorption and desorption by lake sediments, *Soil Sci. Soc. Am. Proc.*, 38, 50, 1974.
43. Havlin, J. L. and Westfall, D. G., Potassium release kinetics and plant response in calcareous soils, *Soil Sci. Soc. Am. J.*, 49, 366, 1985.
44. Onken, A. B. and Matheson, R. L., Dissolution rate of EDTA-extractable phosphate from soils, *Soil Sci. Soc. Am. J.*, 46, 276, 1982.
45. Sparks, D. L. and Jardine, P. M., Comparison of kinetic equations to describe K-Ca exchange in pure and in mixed systems, *Soil Sci.*, 138, 115, 1984.
46. Aharoni, C. and Ungarish, M., Kinetics of activated chemisorption. I. The non-Elovichian part of the isotherm, *J. Chem. Soc. Faraday Trans.*, 172, 400, 1976.
47. Aharoni, C., Kinetics of adsoprtion: the S-shaped Z(t) plot, *Adsorpt. Sci. Technol.*, 1, 1, 1984.
48. Polyzopoulos, N. A., Keramidas, V. Z., and Pavlatou, A., On the limitations of the simplified Elovich equation in describing the kinetics of phosphate sorption and release from soils, *J. Soil Sci.*, 37, 81, 1986.
49. Aharoni, C. and Suzin, Y., Application of the Elovich equation to the kinetics of occlusion. I. Homogenous microporosity, *J. Chem. Soc. Faraday Trans. 1*, 78, 2313, 1982.
50. Aharoni, C. and Suzin, Y., Application of the Elovich equation to the kinetics of occlusion. III. Heterogenous microporosity, *J. Chem. Soc. Faraday Trans. 1*, 78, 2329, 1982.
51. Connaughton, D. F., Stedinger, J. R., Lion, L. W., and Shuler, M. L., Description of time-varying desorption kinetics: release of naphthalene from contaminated soils, *Environ. Sci. Technol.*, 27, 2397, 1993.
52. Karickhoff, S. W., Sorption kinetics of hydrophobic pollutants in natural sediments, in *Contaminants and Sediments*, Vol. 2, Baker, R. A., Ed., Ann Arbor Science, Ann Arbor, MI, 1980, 193.
53. Wu, S. and Gschwend, P. M., Sorption kinetics of hydrophobic organic compounds to natural sediments and soils, *Environ. Sci. Technol.*, 20, 717, 1986.
54. Miller, C. T. and Pedit, J., Use of a reactive surface-diffusion model to describe apparent sorption-desorption hysteresis and abiotic degradation of lindane in a subsurface material, *Environ. Sci. Technol.*, 26, 1417, 1992.
55. Fuller, C. C., Davis, J. A., and Waychunas, G. A., Surface chemistry of ferrihydride. II. Kinetics of arsenate adsorption and coprecipitation, *Geochim. Cosmochim. Acta*, 57, 2271, 1993.
56. Pedit, J. A. and Miller, C. T., Heterogenous sorption processes in subsurface systems. II. Diffusion modeling approaches, *Environ. Sci. Technol.*, 29, 1766, 1995.
57. Brusseau, M. L. and Rao, P. S. C., Sorption nonideality during organic contaminant transport in porous media, *CRC Crit. Rev. Environ. Control*, 19, 33, 1989.
58. Leenheer, J. A. and Ahlrichs, J. L., A kinetic and equilibrium study of the adsorption of carbaryl and parathion upon soil organic matter surfaces, *Soil Sci. Soc. Am. Proc.*, 35, 700, 1971.
59. Hamaker, J. W. and Thompson, J. M., Adsorption, in *Organic Chemicals in the Environment*, Goring, C. A. I. and Hamaker, J. W., Eds., Marcel Dekker, New York, 1972, 39.
60. Karickhoff, S. W. and Morris, K. R., Sorption dynamics of hydrophobic pollutants in sediment suspensions, *Environ, Toxicol. Chem.*, 4, 469, 1985.
61. McCall, P. J. and Agin, G. L., Desorption kinetics of picloram as affected by residence time in the soil, *Environ. Toxicol. Chem.*, 4, 37, 1985.
62. Jardine, P. M., Dunnivant, F. M., Selim, H. M., and McCarthy, J. F., Comparison of models for describing the transport of dissolved organic carbon in aquifer columns, *Soil Sci. Soc. Am. J.*, 56, 393, 1992.
63. Nkedi-Kizza, P., Biggar, J. W., Selim, H. M., van Genuchten, M. T., Wierenga, P. J., Davison, J. M., and Nielsen, D. R., On the equivalence of two conceptual models for describing ion exchange during transport through an aggregated Oxisol, *Water Resour. Res.*, 20, 1123, 1984.
64. Lee, L. S., Rao, P. S. C., Brusseau, M. L., and Ogwada, R. A., Nonequilibrium sorption of organic contaminants during flow through columns of aquifer materials, *Environ. Toxicol. Chem.*, 7, 779, 1988.
65. van Genuchten, M. T. and Wagenet, R. J., Two-site/two-region models for pesticide transport and degradation: theoretical development and analytical solutions, *Soil Sci. Soc. Am. J.*, 53, 1303, 1989.
66. Jardine, P. M., Parker, J. C., and Zelazny, L. W., Kinetics and mechanisms of aluminum adsorption on kaolinite using a two-site nonequilibrium transport model, *Soil Sci. Soc. Am. J.*, 49, 867, 1985.

67. Steinberg, S. M., Pignatello, J. J., and Sawhney, B. L., Persistence of 1,2 dibromoethane in soils: entrapment in intra particle micropores, *Environ. Sci. Technol.*, 21, 1201, 1987.
68. Ball, W. P. and Roberts, P. V., Long-term sorption of halogenated organic chemiclas by aquifer materials. I. Equilibrium, *Environ. Sci. Technol.*, 25, 1223, 1991.
69. Harmon, T. C., Semprini, L., and Roberts, P. V., Simulating solute transport using laboratory-based sorption parameters, *J. Environ. Eng.*, 118, 666, 1992.
70. Pignatello, J. J., Ferrandino, F. J., and Huang, L. Q., Elution of aged and freshly added herbicides from a soil, *Environ. Sci. Technol.*, 27, 1563, 1993.
71. Weber, W. J., Jr. and Miller, C.T., Modeling the sorption of hydrophobic contaminants by aquifer materials. I. Rates and equilibria, *Water Res.*, 22, 457, 1988.
72. Sparks, D. L. and Zhang, P. C., Relaxation methods for studying kinetics of soil chemical phenomena, in *Rates of Soil Chemical Processes*, Soil Sci. Soc. Am. Spec. Publ. 27, Sparks, D. L. and Suarez, D. L., Eds., Soil Science Society of America, Madison, WI, 1991, 61.
73. Sparks, D L., Fendorf, S. E., Toner, C. V., IV, and Carski, T. H., Kinetic methods and measurements, in *Methods of Soil Analysis, Pt. 3: Chemical Methods*, Soil Sci. Soc. Am. Book Series No. 5., Sparks, D. L., Ed., Soil Science Society of America, Madison, WI, 1996, 1275.
74. Zasoski, R. G. and Burau, R. G., A technique for studying the kinetics of adsorption in suspensions, *Soil Sci. Soc. Am. J.*, 42, 372, 1978.
75. Bar-Tal, A., Sparks, D. L., Pesek, J. D., and Feigenbaum, S., Analysis of adsorption kinetics using a stirred-flow chamber. I. Theory and critical tests, *Soil Sci. Soc. Am. J.*, 54, 1273, 1990.
76. Eigen, M., Ionic reactions in aqueous solutions with half-times as short as 10^{-9} second. Applications to neutralization and hydrolysis reactions, *Discuss. Faraday Soc.*, 17, 194, 1954.
77. Takahashi, M. T., and Alberty, R. A., The pressure-jump methods, in *Methods in Enzymology*, Vol. 16, Kustin, K., Ed., Academic Press, New York, 1969, 31.
78. Bernasconi, C. F., *Relaxation Kinetics*, Academic Press, New York, 1976.
79. Grossl, P. R. and Sparks, D. L., Evaluation of contaminant ion adsorption/desorption on goethite using pressure-jump relaxation kinetics, *Geoderma*, 67, 87, 1995.
80. Hayes, K. F. and Leckie, J. O., Mechanism of lead ion adsorption at the goethite-water interface, *ACS Symp. Ser.*, 323, 114, 1986.
81. Mikami, N., Sasaki, M., Hachlya, K., Ikeda, R. D., and Yasunaga, T., Kinetics of the adsorption of PO_4 on the γ-Al_2O_3 surface using the pressure-jump technique, *J. Phys. Chem.*, 87, 1454, 1983.
82. Mikami, N., Sasaki, M., Kikuchi, T., and Yasunaga, T., Kinetics of the adsorption-desorption of chromate on γ-Al_2O_3 surfaces using the pressure-jump technique, *J. Phys. Chem.*, 87, 5245, 1983.
83. Mikami, N., Sasaki, M., Hachiya, K., and Yasunaga, T., Kinetic study of the adsorption-desorption of the uranyl ion on a γ-Al_2O_3 surface using the pressure-jump technique, *J. Phys. Chem.*, 87, 5478, 1983.
84. Grossl, P. R., Sparks, D. L., and Ainsworth, C. C., Rapid kinetics of Cu (II) adsorption/desorption on goethite, *Environ. Sci. Technol.*, 28, 1422, 1994.
85. Grossl, P. R, Eick, M. J., Sparks, D. L., Goldberg, S., and Ainsworth, C. C., Arsenate and chromate retention on goethite. II. Kinetic evaluation using a p-jump relaxation technique, *Environ. Sci. Technol.*, 31, 321, 1997.
86. Keren, R., Grossl, P. R., and Sparks, D. L., Equilibrium and kinetics of borate adsorption-desorption on pyrophyllite in aqueous suspensions, *Soil Sci. Soc. Am. J.*, 58, 1116, 1994.
87. Toner, C. V., IV, and Sparks, D. L., Chemical relaxation and double layer model analysis of boron adsorption on alumina, *Soil Sci. Soc. Am. J.*, 59, 395, 1995.
88. Sparks, D. L., Kinetics of sorption/release reactions on natural particles, in *Structure and Surface Reactions of Soil Particles*, Huang, P. M., Senesi, N., and Buffle, J., Eds., John Wiley & Sons, New York, 1998, 413.
89. Sparks, D. L., Kinetic processes at the soil particle-solution interface, SSSAJ Spec. Publ., Soil Science Society of America, Madison, WI, 1998, in press.
90. Waychunas, G. A., Rea, B. A., Fuller, C. C., and Davis, J. A., Surface chemistry of ferrihydrite. I. EXAFS studies of the geometry of coprecipitated and adsorbed arsenate, *Geochim. Cosmochim. Acta*, 57, 2251, 1993.
91. Lehmann, R. G., and Harter, R. D., Assessment of copper-soil bond strength by desorption kinetics, *Soil Sci. Soc. Am. J.*, 48, 769, 1984.

92. Ainsworth, C. C., Pilou, J. L., Gassman, P. L., and Sluys, W. G. V. D., Cobalt, cadmium, and lead sorption to hydrous iron oxide: residence time effect, *Soil Sci. Soc. Am. J.*, 58, 1615, 1994.
93. Scheidegger, A M., Lamble, G. M., and Sparks, D. L., Spectroscopic evidence for the formation of mixed-cation hydroxide phases upon metal sorption on clays and aluminum oxides, *J. Colloid Interface Sci.*, 186, 118, 1997.
94. Karickhoff, S. W., Brown, D. S., and Scott, T. A., Sorption of hydrophobic pollutants on natural sediments, *Water Res.*, 13, 241, 1979.
95. DiToro, D. M. and Horzempa, L. M., Reversible and resistant components of PCB adsorption-desorption: isotherms, *Environ. Sci. Technol.*, 16, 594, 1982.
96. Carroll, K. M., Harkness, M. R., Bracco, A. A., and Balcarcel, R. B., Application of a permeant/polymer diffusional model to the desorption of polychlorinated biphenyls from Hudson River sediments, *Environs. Sci. Technol.*, 28, 253, 1994.
97. Pavlostathis, S. G. and Mathavan, G. N., Desorption kinetics of selected volatile organic compounds from field contaminated soils, *Environ. Sci. Technol.*, 26, 532, 1992.
98. Scribner, S. L., Benzing, T. R., Sun, S., and Boyd, S. A., Desorption and bioavailability of aged simazine residues in soil from a continuous corn field, *J. Environ. Qual.*, 21, 115, 1992.
99. Pignatello, J. J. and Huang, L. Q., Sorptive reversibility of atrazine and metolachlor residues in field soil samples, *J. Environ. Qual.*, 20, 222, 1991.
100. Stumm, W. and Wollast, R., Coordination chemistry of weathering. Kinetics of the surface-controlled dissolution of oxide minerals, *Rev. Geophys.*, 28, 53, 1990.
101. Petrovic, R., Berner, R. A., and Goldhaber, M. B., Rate control in dissolution of alkali feldspars. I. Study of residual feldspar grains by x-ray photoelectron spectroscopy, *Geochim. Cosmochim, Acta*, 40, 537, 1976.
102. Schott, J. and Petit, J. C., New evidence for the mechanisms of dissolution of silicate minerals, in *Aquatic Surface Chemistry*, Stumm, W., Ed., Wiley Interscience, New York, 1987, 293.
103. Casey, W. H., Westrich, H. R., Arnold, G. W., and Banfield, J. F., The surface chemistry of dissolving labradorite feldspar, *Geochim. Cosmochim. Acta*, 53, 821, 1989.
104. Furrer, G. and Stumm, W., The coordination chemistry of weathering. I. Dissolution kinetics of γ-Al_2O_3 and BeO, *Geochim. Cosmochim. Acta*, 50, 1847, 1986.
105. Zinder, B., Furrer, G., and Stumm, W., The coordination chemistry of weathering. II. Dissolution of Fe(III) oxides, *Geochim. Cosmochim. Acta*, 50, 1861, 1986.
106. Stumm, W. and Furrer, G., The dissolution of oxides and aluminum silicates: examples of surface-coordination-controlled kinetics, in *Aquatic Surface Chemistry*, Stumm, W., Ed., Wiley Interscience, New York, 1987, 197.
107. Charlet, L. and Manceau, A., Structure, formation, and reactivity of hydrous oxide particles: insights from x-ray absorption spectroscopy, in *Environmental Particles*, Buffle, J. and van Leeuwen, H. P., Eds., Lewis Publishers, Boca Raton, Fl, 1993, 117.
108. Fendorf, S. E., Lamble, G. M., Stapelton, M. G., Kelley, M. J., and Sparks, D. L., Mechanisms of chromium (III) sorption on silica. I. Cr(III) surface structure derived by extended x-ray absorption fine structure spectroscopy, *Environ. Sci. Technol.*, 28, 284, 1994.
109. Junta, J. L. and Hochella, M. F., Jr., Manganese (II) oxidation at mineral surfaces: a microscopic and spectroscopic study, *Geochim. Cosmochim. Acta*, 58, 4985, 1994.
110. O'Day, P. A., Parks, G. A., and Brown, G. E., Jr., Molecular structure and binding sites of cobalt(II) surface complexes on kaolinite from X-ray absorption spectroscopy, *Clays Clay Miner.*, 42, 337, 1994.
111. Wersin, P., Hochella, M. F., Jr., Persson, P., Redden, G., Leckie, J. O., and Harris, D. W., Interaction between aqueous uranium (VI) and sulfide minerals: spectroscopic evidence for sorption and reduction, *Geochim. Cosmochim. Acta*, 58, 2829, 1994.
112. Chisholm-Brause, C. J., O'Day, P. A., Brown, G. E., Jr., and Parks, G. A., Evidence for multinuclear metal-ion complexes at solid/water interfaces from X-ray absorption spectroscopy, *Nature*, 348, 528, 1990.
113. Chisholm-Brause, C. J., Roe, A. L., Hayes, K. F., Brown, G. E., Jr., Parks, G. A., and Leckie, J. O., Spectroscopic investigation of Pb(II) complexes at the γ-Al_2O_3/water interface, *Geochim. Cosmochim. Acta*, 54, 1897, 1990b.
114. Roe, A. L., Hayes, K. F., Chisholm-Brause, C. J., Brown, G. E., Jr., Parks, G. A., Hodgson, K. O., and Leckie J. O., In situ X-ray absorption study of lead ion surface complexes at the goethite/water interface, *Langmuir*, 7, 367, 1991.

115. Charlet, L. and Manceau, A., X-ray absorption spectroscopic study of the sorption of Cr(III) at the oxide-water interface. II. Adsorption, co-precipitation and surface preciptitation on ferric hydrous oxides, *J. Colloid Interface Sci.*, 148, 443, 1992.
116. Fendorf, S. E. and Sparks, D. L., Mechanisms of chromium (III) sorption on silica. II. Effect of reaction conditions, *Environ. Sci. Technol.*, 28, 290, 1994.
117. O'Day, P. A., Brown, G. E., Jr., and Parks, G. A., X-ray absorption spectroscopy of cobalt (II) multinuclear surface complexes and surface precipitates on kaolinite, *J. Colloid Interface Sci.*, 165, 269, 1994.
118. Bargar, J. R., Brown, G. E., Jr., and Parks, G. A., XAFS study of lead (II) chemisorption at the α-Al_2O_3-water interface, in *209th American Chemical Society National Meeting*, Abstract, ENVR 152, 1995.
119. Papelis, C. and Hayes, K. F., Distinguishing between interlayer and external sorption sites of clay minerals using X-ray absorption spectroscopy, *Colloid Surfaces*, 107, 89, 1996.
120. Scheidegger, A. M., Lamble, G. M., and Sparks, D. L., Investigation of Ni sorption on pyrophyllite: an XAFS study, *Environ. Sci. Technol.*, 30, 548, 1996.
121. O'Day, P. A., Chisholm-Brause, C. J., Towle, S. N., Parks, G. A., and Brown, G. E., Jr., X-ray absorption spectroscopy of Co(II) sorption complexes on quartz (α-SiO_2) and rutile (TiO_2), *Geochim. Cosmochim. Acta*, 60, 2515, 1996.
122. Johnston, C. T., Sposito, G., and Earl, W. L., Surface spectroscopy of environmental particles by Fourier-transform infrared and nuclear magnetic resonance spectroscopy, in *Environmental Particles*, Buffle, J. and van Leeuwen, H. P., Eds., Lewis Publishers, Boca Raton, FL, 1993, 1.
123. Perry, D. L., Taylor, J. A., and Wagner, C. D., X-ray-induced photoelectron and Auger spectroscopy, in *Instrumental Surface Analysis of Geologic Materials*, Perry, D. L, Ed., VCH Publishers, New York, 1990, 45.
124. Fendorf, S. E., Sparks, D. L., Lamble, G. M., and Kelley, M. J., Applications of X-ray absorption fine structure spectroscopy to soils, *Soil Sci. Soc. Am.*, 58, 1583, 1994
125. Koppelmann, M. H., Emerson, A. B., and Dillard, J. G., Adsorbed Cr(III) on chlorite, illite, and kaolinite: an x-ray photoelectron spectroscopic study, *Clays Clay Miner.*, 28, 119, 1980.
126. Dillard, J. G. and Koppelman, M. H., X-ray photoelectron spectroscopic (XPS) surface characterization of cobalt on the surface of kaolinite, *J. Colloid Interface Sci.*, 95, 298, 1982.
127. Schenk, C. V. and Dillard, J. G., Surface analysis and the adsorption of Co(II) on goethite, *J. Colloid Interface Sci.*, 95, 398, 1983.
128. Hochella, M. F. and Carim, A. H., A reassessment of electron escape depths in silicon and thermally grown silicon dioxide thin films, *Surf. Sci.*, 197, 260, 1988.
129. Davison, N. and Whinnie, W. R., X-ray photoelectron spectroscopic study of cobalt(II) and nickel(II) on hectorite and montmorillonite, *Clays Clay Miner.*, 39, 22, 1991.
130. Stipp, S. L. and Hochella, M. F., Structure and bonding environments at the calcite surface as observed with X-ray photoelectron spectroscopy (XPS) and low energy electron diffraction (LEED), *Geochim. Cosmochim. Acta*, 55, 1723, 1991.
131. Scheidegger, A. M., Borkovec, M., and Sticher, H., Coating of silica sand with goethite: preparation and analytical identification, *Geoderma*, 58, 43, 1993.
132. Papelis, C., X-ray photoelectron spectroscopic studies of cadmium and selenite adsorption on aluminum oxide, *Environ. Sci. Technol.*, 29, 1526, 1995.
133. Brown, G. E., Jr., Spectroscopic studies of chemisorption reaction mechanisms at oxide-water interfaces, in *Mineral-Water Interface Geochemistry*, Hochella, M. F. and White, A. F., Eds., Mineralogical Society of America, Washington, D.C., 1990, 309.
134. Calas, G., Electron paramagnetic resonance, in *Reviews in Mineralogy*, Vol. 18, *Spectroscopic Methods in Mineralogy and Geology*, Hawthorne, F. C., Ed., Mineralogical Society of America, Washington, D.C., 1988, 513.
135. McBride, M. B., Cu^{2+} adsorption characteristics of aluminum hydroxide and oxyhydroxides, *Clays Clay Miner.*, 30, 21, 1982.
136. McBride, M. B., Fraser, A. R., and McHardy, W. J., Cu^{2+} interaction with microcrystalline gibbsite. Evidence for oriented chemisorbed copper ions, *Clays Clay Miner.*, 32, 12, 1984.
137. Bleam, W. F. and McBride, M.B., The chemistry of adsorbed Cu(II) and Mn(II) in aqueous titanium dioxide suspensions, *J. Colloid Interface Sci.*, 110, 335, 1986.
138. Wersin, P., Charlet, L., Karthein, R., and Stumm, W., From adsorption to precipitation: sorption of Mn^{2+} on $FeCO_3$(s), *Geochim. Cosmochim. Acta*, 53, 2787, 1989.

139. Senesi, N. and Sposito, G., Residual copper(II) complexes in purified soil and sewage sludge fulvic acids: an electron spin resonance study, *Soil Sci. Soc. Am. J.*, 48, 1247, 1984.
140. Senesi, N., Bocian, D. F., and Sposito, G., Electron spin resonance investigation of copper(II) complexation by soil fulvic acid, *Soil Sci. Soc. Am. J.*, 49, 114, 1985.
141. Goodman, B. A. and Cheshire, M. V., Characterization of iron-fulvic acid complexes using Mossbauer and EPR spectroscopy, *Sci. Total Environ.*, 62, 229, 1987.
142. Senesi, N. and Calderoni, G., Structural and chemical characterization of copper, iron and manganese complexes formed by paleosol humic acids, *Organic Geochem.*, 13, 1145, 1988.
143. Senesi, N., Garrison, S., Holtzclaw, K., and Bradford, G. R., Chemical properties of metal-humic fractions of a sewage sludge-amended aridisol, *J. Environ. Qual.*, 18, 186, 1989.
144. Neto, L. M., Nascimento, O. R., Talamoni, J., and Poppi, N. R., EPR of micronutrients — humic substances complexes extracted from a Brazil soil, *Soil Sci.*, 151, 363, 1991.
145. Cheshire, M. V., ESR and Mossbauer spectroscopy applied to soil matrices, in *15th World Congr. Soil Science*, ISSS, Acapulco, Mexico. Transactions, Vol. 3a, Commission II, 1994.
146. Senesi, N., Spectroscopic studies of metal ion — humic substance complexation in soil, in *15th World Congr. Soil Science,* ISSS, Acapulco, Mexico, Transactions, Vol. 3a, Commission II, 1994.
147. Hawthorne, F. C., Mossbauer spectroscopy, in *Reviews in Mineralogy, Vol. 18, Spectroscopic Methods in Mineralogy and Geology,* Hawthorne, F. C., Ed., Mineralogical Society of America, Washington, D.C., 1988, 573.
148. Goodman, B. A. and Cheshire, M. V., A Mossbauer spectroscopic study of the effect of pH on the reaction between iron and humic acid in aqueous media, *J. Soil Sci.*, 30, 85, 1979.
149. Kallianou, C. S. and Yassoglou, N. J., Bonding and oxidation state of iron-fulvic acid in humic complexes extracted from some Greek soils, *Geoderma*, 35, 209, 1985.
150. Kodama, H., Schnitzer, M., and Mirai, E., An investigation of iron(II)-fulvic acid reaction by Mossbauer spectroscopy and chemical methods, *Soil Sci. Soc. Am. J.*, 52, 994, 1988.
151. Goodman, B. A., Cheshire, M. V., and Chadwick, J., Characterization of the Fe(III)-fulvic acid reaction by Mossbauer spectroscopy, *J. Soil Sci.*, 42, 25, 1991.
152. Goodman, B. A., The use of Mossbauer spectroscopy in the study of soil colloidal materials, in *Soil Colloids and their Association in Aggregates*, Vol. 215, DeBoodt, M. F., Hayes, H. B., and Herbillon, A., Eds., Plenum Press, New York, 1990, 119.
153. Hair, M. I., *Infrared Spectroscopy in Surface Chemistry*, Marcel Dekker, New York, 1967.
154. Bell, A. T., Applications of fourier transform infrared spectroscopy to studies of adsorbed species, in *ACS Symp. Ser. No. 137*, American Chemical Society, Washington, D.C., 1980.
155. McMillan, P. F. and Hofmeister, A. M., Infrared and Raman Spectroscopy, in *Reviews in Mineralogy, Vol. 18, Spectroscopic Methods in Mineralogy and Geology*, Hawthorne, F. C., Ed., Mineralogical Society of America, Washington, D.C., 1988, 573.
156. Piccolo, A., Advanced infrared techniques (FT-IR, DRIFT, and ATR) applied to organic and inorganic soil materials, in *15th World Congr. Soil Science*, ISSS, Acapulco, Mexico, Transactions, Vol. 3a, Commission II, 1994.
157. Wilson, M. A., *NMR Techniques and Applications in Geochemistry and Soil Chemistry*, Pergamon Press, Oxford, 1987.
158. Wershaw, R. L. and Mikita, M. A., *NMR of Humic Substances and Coal*, Lewis Publishers, Chelsea, MI, 1987.
159. Hatcher, P. G., Bortiatynski, J. M., and Knicker, H., NMR techniques (C, H, and N) in soil chemistry, in *15th World Congr. Soil Science*, ISSS, Acapulco, Mexico, Transactions, Vol. 3a, Commission II, 1994.
160. Bank, S., Bank, J. F., and Ellis, P. D., Solid-state ^{113}Cd nuclear magnetic resonance study of exchanged montorillonites, *J. Phys. Chem.*, 93, 4847, 1989.
161. Luca, V., Cardile, C. M., and Meingold, R. H., High-resolution multinuclear NMR study of cation migration in montmorrillonite, *Clay Miner.*, 24, 115, 1989.
162. Laperche, V., Lambert, J. F., Prost, R., and Fripiat, J. J., High resolution solid-state NMR of exchangeable cations in the interlayer surface of a swelling mica: ^{23}Na, ^{111}Cd, and ^{133}Cs vermiculites, *J. Phys. Chem.*, 94, 8821, 1990.
163. Weiss, C. A., Kirkpatrick, R. J., and Altaner, S. P., The structural environments of cations adsorbed onto clays: cesium-133 variable temperature MAS NMR spectroscopy of hectorite, *Geochim. Cosmochim. Acta*, 54, 1655, 1990.

164. Altaner, S. P., Weiss, C. A., and Kirkpatrick, R. J., Evidence from ^{29}Si NMR for the structure of mixed-layer illite/smectite clay minerals, *Nature*, 331, 669, 1988.
165. Herrero, C. P., Sanz, J., and Serratosa, J. M., Dispersion of charge deficits in the tetrahedral sheet of phyllosilicates. Analysis from ^{29}Si NMR spectra, *J. Phys. Chem.*, 93, 4311, 1989.
166 Woessner, D. E., Characterization of clay minerals by ^{27}Al nuclear magnetic resonance spectroscopy, *Am. Mineral.*, 74, 203, 1989.
167. Brown, G. E., Jr., Parks, G. A., and Chisholm-Brause, C. J., In situ x-ray absorption spectroscopic studies of ions at oxide-water interfaces, *Chimia*, 43, 248, 1989.
168. Schulze, D. G. and Bertsch, P. M., Synchrotron x-ray techniques in soil, plant, and environmental research, *Adv. Agron.*, 55, 1, 1995.
169. Bidoglio, G., Gibson, P. N., O'Gorman, M. O., and Roberts, K. S., X-ray absorption spectroscopy investigation of surface redox transformation of thallium and chromium on colloidal mineral oxides, *Geochim. Cosmochim. Acta*, 57, 2389, 1993.
170. Manceau, A., Gorshkov, A. I., and Drits, V., Structural chemistry of Mn, Fe, Co and Ni in Mn hydrous oxides. I. Inforamtion from XANES spectroscopy, *Am. Mineral.*, 77, 1133, 1992.
171. Manceau, A. Gorshkov, A. I., and Drits, V., Structural chemistry of Mn, Fe, Co and Ni in Mn hydrous oxides. II. Information from XANES spectroscopy, electron and x-ray diffraction, *Am. Mineral.*, 77, 1144, 1992.
172. Lytle, C. M., Lytle, F. W., and Smith, B. N., Use of XAS to determine the chemical speciation of bioaccumulated manganese in Ptamogeton pectinatus, *J. Environ. Qual.*, 25, 311, 1996.
173. Pickering, I. J., Brown, G. E., Jr., and Tokunaga, T. K., Quantitative speciation of selenium in soils using x-ray absorption spectroscopy, *Environ. Sci. Technol.*, 29, 2456, 1995.
174. Bidoglio, G., Gibson, P. N., Haltier, E., Omenetto, N., and Lipponen, M., XANES and laser fluorescence spectroscopy for rare earth speciation at mineral water interfaces, *Radiochim. Acta*, 59, 191, 1992.
175. Bajt, S., Sutton, S. R., and Delaney, J. S., X-ray microprobe analysis of iron oxidation states in silicates and oxides using X-ray absorption near edge structure (XANES), *Geochim. Cosmochim. Acta*, 58, 5209, 1994.
176. Bertsch, P. M., Hunter, D. B., Sutton, S. R., Bajt, S., and Rivers, M. L., In situ chemical speciation of uranium in soils and sediments by micro x-ray absorption spectroscopy, *Environ. Sci. Technol.*, 28, 980, 1994.
177. Waychunas, G. A., Apted, M. J., and Brown, G. E., Jr., X-ray K-edge absorption spectra of Fe minerals and model compounds: near-edge structure, *Phys. Chem. Miner.*, 10, 1, 1983.
178. Petiau, J., Calas, G., and Sainctavit, P., Recent developments in the experimental studies of XANES, *J. Phys. Colloq.*, 48, 1987.
179. Waychunas, G. A., Synchotron radiation XANES spectroscopy of Ti minerals: effects of Ti bonding distances, Ti valence, and site geometry on absorption edge structure, *Am. Mineral.*, 72, 89, 1987.
180. Manceau, A., Boisset, M. C., Sarbet, G., Hazemann, J., Mench, M., Cambier, P., and Prost, R., Direct determination of lead speciation in contaminated soils by EXAFS spectroscopy, *Environ. Sci. Technol.*, 30, 1540, 1996.
181. Sayers, D. E., Stern, E. A., and Lytle, F. W., New technique for investigating noncrystalline structures: Fourier analysis of the extended x-ray absorption fine structure, *Phys. Rev. B: Solid State*, 27, 1204, 1971.
182. Calas, G. and Petiau, J., Structure of oxide glasses: spectroscopic studies of local order and crystal-lochemistry: geo-chemical implications, *Bull. Mineral.*, 196, 33, 1983.
183. Petiau, J. and Calas, G., EXAFS and edge structure; application to nucleation in oxide glasses, *J. Phys. Colloq.*, 46, 41, 1985.
184. Hayes, K. F., Roe, A. L., Brown, G. E., Jr., Hodgson, K. O., Leckie, J. O., and Parks, G. A., In situ x-ray absorption study of surface complexes: selenium oxyanions on α-FeOOH, *Science*, 238, 783, 1987.
185. Manceau, A. and Charlet, L., The mechanism of selenate adsorption on goethite and hydrous ferric oxide, *J. Colloid Interface Sci.*, 164, 87, 1994.
186. Smart, P. and Tovey, N. K., *Electron Microscopy of Soils and Sediments*, Oxford University Press, New York, 1981.
187. Bullock, P. and Murphy, C. P., *Soil Micromorphology*, Vol. 1, A. B. Academic, Berkhamsted, UK, 1983.
188. Douglas, L. A., *Soil Micromorphology. A Basic and Applied Science*, Elsevier, Amsterdam, 1990.

189. Whalley, W. B., Scanning electron microscopy and the sedimentological characterization of soils, in *Geomorphology of Soils*, Richards, K. S., Arnett, R. R., and Ellis, S., Eds., Elsevier, Amssterdam, 1985, 183.
190. Bisdom, E. B. A., Tessier, D., and Schoute, J. F. T., Micromorphological techniques in research and teaching (submicroscopy), in *Soil Micromorphology: A Basic and Applied Science*, Douglas, L. A., Ed., Elsevier, Amsterdam, 1990, 581.
191. Tovey, N. K., Krinsley, D. H., Dent, D. L, and Corbett, W. M., Techniques to quantitatively study the microfabric of soils, *Geoderma*, 53, 217, 1992.
192. Chen, Y., Electron microscopy techniques applied to soil organic matter and soil structure studies, in *15th World Congr. Soil Science*, ISSS, Acapulco, Mexico. Transactions, Vol. 3a, Commission II, 1994.
193. Hochella, M. F., Eggleston, C. M., Elings, V. B., Parks, G. A., Brown, G. E., Jr., Wu, C. M., and Kjoller, K. K., Mineralogy in two dimensions: scanning tunneling microscopy of semiconducting minerals with implications for geochemical reactivity, *Am. Mineral.*, 74, 1233, 1989.
194. Eggleston, C. M. and Hochella, M. F., Scanning tunneling microscopy of sulfide surfaces, *Geochim. Cosmochim. Acta*, 54, 1511, 1990.
195. Maurice, P. A. Scanning probe microscopy of mineral surfaces in *Structure and Surface Reactions of Soil Particles*, Huang, P. M., Senesi, N., and Buffle, J., Eds., John Wiley & Sons, New York, 1998.
196. Johnsson, P. A., Eggleston, C. M., and Hochella, M. F., Imaging molecular-scale structure and microtopography of hematite with atomic force microscope, *Am. Mineral.*, 76, 1442, 1991.
197. Ohnesorge, F. and Binnig, G., True atomic resolution by atomic force microscopy through repulsive and attractive forces, *Science*, 260, 1451, 1993.
198. Ducker, W. A., Senden, T. J., and Pashley, R. M., Direct measurement of forces using an atomic force microscope, *Nature*, 353, 239, 1991.
199. Ducker, W. A., Senden, T. J., and Pashley, R. M., Measurement of forces in liquids using a force microscope, *Langmuir*, 8, 1831, 1992.
200. Manne, S., Cleveland, J. P., Gaub, H. E., Stucky, G. D., and Hansma, P. K., Direct visualization of surfactant hemimicelles by force microscopy of the electrical double layer, *Langmiur*, 10, 4409, 1994.
201. Hartman, H. G. S., Yang, A., Manne, S., Gould, A. A. C., and Hansma, P. K., Molecular-scale imaging of clay mineral surfaces with atomic force microscope, *Clays Clay Miner.*, 38, 337, 1990.
202. Friedbacher, G., Hansma, P. K., Ramli, E., and Stucky, G. D., Imaging powders with atomic force microscope: from biominerals to commercial materials, *Science*, 253, 1261, 1991.
203. Lindgreen, H., Garnaes, J., Hansen, P. L., Besenbach, F., Laegsgaard, E.,. Stensgaard, I., Gould, S. A., and Hansma, P. K., Ultrafine particles of North Sea illite/smectite clay minerals investigated by STM and AFM, *Am. Mineral.*, 76, 1218, 1991.
204. Blum, A. E. and Eberl, D. D., Determination of clay thicknesses and morphology using scanning force microscopy, in *7th Int. Symp. Water-Rock Interaction*, Rotterdam, Park City, Utah, 1992.
205. Maurice, P. A., Hochella, M. F., Jr., Parks, G. A., Sposito, G., and Schwertmann, U., Evolution of hematite surface microtopography upon dissolution by simple organic acids, *Clays Clay Miner.*, 43, 29, 1995.
206. Grantham, H. C. and Dove, P. M., Investigation of bacterial-mineral interactions using fluid tapping mode atomic force microscopy, *Geochim. Cosmochim. Acta*, 60, 2473, 1996.
207. Hochella, M. F., Atomic structure, microtopography, composition, and reactivity of mineral surfaces in *Reviews in Mineralogy, Vol. 23, Mineral-Water Interface Geochemistry*, Hochella, M. F. and White, A. F., Eds., Mineralogical Society of America, Washington, D.C., 1990, 87.
208. Vempati, R. K. and Cocke, D. L., Applications of scanning force microscopy to soil minerals, in *15th World Congr. Soil Science*, ISSS, Acapulco, Mexico, Transactions, Vol. 3a, Commission II, 1994.
209. Fendorf, S. E., Eick, M. J., Grossl, P. R., and Sparks, D. L., Arsensate and chromate retention mechanisms on goethite. I. Surface structure, *Environ. Sci. Technol.*, 31, 315, 1997.
210. Scheidegger, A. M., Lamble, G. M., and Sparks, D. L., The kinetics of nickel sorption on pyrophyllite as monitored by x-ray absorption fine structure (XAFS) spectroscopy, *J. Phys. IV*, 7, C2-773, 1997.
211. McBride, M. B., *Environmental Chemistry of Soils*, Oxford University Press, New York, 1994.
212. Frahm, R., Quick XAFS: potentials and practical applications in materials science, in *X-ray Absorption Fine Structure*, Hasnain, S. S., Ed., Ellis Harwood, New York, 1991, 731.
213. Lytle, F. W. and Greegar, R. B., New developments in XAS experiments in *X-ray Absorption Fine Structure*, Hasnain, S. S., Ed., Ellis Harwood, New York, 1991, 625.

214. Dobson, B. R., Quick scanning EXAFS facilities at Daresbury, *SRS Synchrotron Radiat. News*, 7 (1), 21, 1994.
215. Baker, G., Dent, A. J., Derbyshire, G., Greaves, G. N., Catlow, C. R. A., Couves, J. W., and Thomas, J. M., Time resolved structural studies of nickel exchanged zeolite and nickel oxide using energy dispersive EXAFS, in *X-ray Absorption Fine Structure*, Hasnain, S. S., Ed., Ellis Harwood, New York, 1991, 738.
216. Hunter, D. B. and Bertsch, P. M., *In situ* measurements of tetraphenylboron degradation kinetics on clay mineral surfaces by FTIR, *Environ. Sci. Technol.*, 28, 686, 1994.
217. Dove, P. M. and Hochella, M. F. Jr., Calcite precipitation mechanisms and inhibition by orthophosphate: *in situ* observations by scanning force microscopy, *Geochim. Cosmochim. Acta*, 57, 705, 1993.
218. Gratz, A. J. and Hillner, P. E., Poisoning of calcite growth viewed in the atomic force microscope (AFM), *J. Cryst. Growth*, 129, 789, 1993.
219. Bosbach, D. and Rammensee, W., In situ investigation of growth and dissolution on the (010) surface of gypsum by scanning force microscopy, *Geochim. Cosmochim. Acta*, 58, 843, 1994.
220. Stipp, S. L., Eggleston, C. M., and Nielsen, B. S., Calcite surface structure observed at microtopographic and molecular scales with atomic force microscopy (AFM), *Geochim. Cosmochim, Acta*, 58, 3032, 1994.
221. Fendorf, S. E., Li, G., and Gunter, M.E., Micromorphologies and stabilities of chromium (III) surface precipitates elucidated by scanning force microscopy, *Soil Sci. Soc. Am. J.*, 60, 99, 1996.
222. Dove, P. M., Hochella, M.F., Jr., and Reeder, R. J., In situ investigation of near-equilibrium calcite precipitation by atomic force microscopy, in *Water-Rock Interaction, Vol. 7*, Kharaka, Y. K. and Maest, A. S., Eds., A. A. Balkema, Rotterdam, 1992, 141.
223. Hellman, R., Drake, B., and Kjoller, K., Using atomic force microscopy to study the structure, topography and dissolution of albite surfaces, in *Water-Rock Interaction, Vol. 7*, Kharaka, Y. K. and Maest, A. S., Eds., A. A. Balkema, Rotterdam, 1992, 149.
224. Hillner, P. E., Gratz, A. J., Manne, S., and Hansma, P. K., Atomic-scale imaging of calcite growth and dissolution in real-time, *Geology*, 20, 359, 1992.
225. Hillner, P. E., Manne, S., Gratz, A. J., and Hansma, P. K., AFM images of dissolution and growth on a calcite crystal, *Ultramicroscopy*, 44, 1387, 1992.
226. Johnsson, P. A., Hochella, M. F., Jr., Parks. G. A., Blum, A. E., and Sposito, G., Direct observation of muscovite basal-plane dissolution and secondary phase formation: an XPS, LEED, and SFM study, in *Water-Rock Interaction, Vol. 7*, Kharaka, Y. K. and Maest, A. S., Eds., A. A. Balkema, Rotterdam, 1992, 159.
227. Hochella, M. F., Jr., The changing face of mineral-fluid interface chemistry, in *Water-Rock Interaction, Vol. 7*, Kharaka, Y. K. and Maest, A. S., Eds., A. A. Balkema, Rotterdam, 1992. 7.
228. Knight, R. and Dvorkin, J., Seismic and electrical properties of sandstones at low saturation, *J. Geophys. Res.*, 12, 17425, 1992.
229. Somorjai, G. A. and van Hove, M. A., Adsorbate-induced restructuring of surfaces, *Prog. Surface Sci.*, 30, 201, 1989.
230. Somorjai, G. A., Modern concepts in surface science and heterogeneous catalysis, *J. Phys. Chem.*, 94, 1013, 1990.